Complexes of Palladium and Copper with Bicyclic (alkyl)(amino) Carbene (BICAAC)

Soumyadeep Chakrabortty

A dissertation submitted for the partial fulfilment of
Master of Science (MS)

in

Chemical Sciences

Department of Chemical Sciences

Indian Institute of Science Education and Research Mohali

April 2019

Dedicated to my family

Certificate of Examination

This is to certify that the dissertation "***Complexes of Palladium and Copper with Bicyclic (alkyl)(amino) Carbene (BICAAC)***" submitted by Mr. Soumyadeep Chakrabortty (MP16002) for the partial fulfilment of MS by thesis programme of the Institute, has been examined by the thesis committee duly appointed by the Institute. The committee finds the work done by the candidate satisfactory and recommends that the report be accepted.

Dr. Debashis Adhikari	**Dr. R Vijaya Anand**	**Dr. Sanjay Singh**
Assistant Professor	*Associate Professor*	*Associate Professor*
IISER Mohali	IISER Mohali	IISER Mohali
		(Supervisor)

Date:

Declaration

The work presented in this dissertation has been carried out by me under the guidance of Dr. Sanjay Singh at the Department of Chemical Sciences, Indian Institute of Science Education and Research Mohali.

This work has not been submitted in part or in full for a degree, a diploma, or a fellowship to any other University or Institute. Whenever contributions of others are involved, every effort is made to indicate this clearly, with due acknowledgment of collaborative research and discussions. The thesis is a bonafide record of original work done by me and all sources listed within have been detailed in the bibliographic section.

Soumyadeep Chakrabortty

Date:
Place:

In my capacity as the supervisor of the candidate's project work, I certify that the above statements by the candidate are true to the best of my knowledge.

Dr. Sanjay Singh
Associate Professor
Department of Chemical Sciences
Indian Institute of Science Education and Research Mohali

Date:
Place:

Acknowledgement

First and foremost, I would like to thank my advisor, Dr. Sanjay Singh, for his encouragement and supervision throughout my master's study. His valuable scientific advice, suggestions, and discussions, and his sincere never-ending care make my graduation project successful. The strong scientific foundation that he has given me will continue to guide and inspire me in my future career.

I also express my gratitude to Dr. R Vijaya Anand and Dr. Debashis Adhikari for their fruitful and enjoyable suggestions and discussions during the research work and hope we will continue with such projects in the future. I also thank Dr. Sanchita Sengupta for her kind guidance in the cyclic voltammetry measurements, Dr. Yogesh Singh, and Mr. Anjar Ali for generous support in magnetic measurements and Dr. Ananth Venkatesan for providing the SEM and EDX facilities. I also thank all the non-teaching staff of IISER Mohali for their assistance on various occasions. I especially acknowledge Mr. Triveni Sankar and Mr. Balbir for their valuable support given to me all the time. I thank Dr. Angshuman Roy Choudhury, Dr. Deependra Bawari and Mr. Mayank Joshi for their valuable suggestions and help in measurement and handling of XRD instrument. I would like to acknowledge IISER Mohali for providing the basic requirements like SCXRD facility, NMR, HRMS, IR, UV-Vis and fluorescence facilities.

I am thankful for pleasant company, friendly counselling, cooperation, practical help and patronage of my lab mates, Mr. Sandeep Rawat, Ms. Mamta Bhandari, Mr. Sandeep Kumar Thakur, Ms. Chandrakala Negi, Mr. Manu Adhikari, Ms. Tanuja Tiwari, Mr. Nitish Garg, Mr. Vishal Porwal, Mr. Rohit Kamte, Ms. Darsana Prakash, Ms. Navneet Kaur. I am thankful to all the faculty members of IISER Mohali for their help, cooperation and encouragement at various stages. I would like to express my special gratitude to Dr. Krishna Kumar Manar for his generous help and support throughout the tenure of my research work.

I would like to mention my appreciation to all of my previous teachers who educated me with great effort and patience to prepare me for the future. Particularly, I am very grateful to Dr. Chandrakanta Bannerjee, Dr. Subhabrata Bannerjee and Dr. Chandan Kumar Saha my teachers during my bachelor's studies (Ramakrishna Mission VCC, Rahara) for their trust, support and encouragement that stimulated my interest in chemistry more.

I am grateful to all my family member and friends for their support and encouragements. Particularly, my deepest and most sincere gratitude goes to my parents, Mr. Bisweswar Chakrabortty and Mrs. Putul Chakrabortty, my elder brother Dr. Sabyasachi Chakrabortty and my sister-in-law Mrs. Amrita Chakrabortty and my little niece Prisha Chakrabortty for their constant encouragement, unconditional support and endless love. I feel like I have been blessed with the best family that anyone ever had and I owe anything good that I have done for their support.

I would like to thank IISER Mohali for providing the fellowship during my master's studies.

Soumyadeep Chakrabortty

List of Figures

List of Schemes

List of Tables

Notations and Abbreviations

$\tilde{\nu}$	Wave number
μ_β	Magnetic moment
AP	Atmospheric solids analysis probe
Ar	Aryl
av	Average
BICAAC	Bicyclic (alkyl)(amino)carbene
calcd.	Calculated
cAAC	Cyclic (alkyl)(amino)carbene
CV	Cyclic Voltammetry
^{0}C	Degree Celsius
d	Doublet
dd	Doublet of doublets
decomp.	Decomposition
Dipp	Diisopropylphenyl
EDX	Energy-dispersive X-ray spectroscopy
ESI	Electron spray ionization
eq.	Equivalents
eV	Electron volt
FMO	Frontier Molecular Orbital
g	Grams
HOMO	Highest Occupied Molecular Orbital
h	Hours
Hz	Hertz
^{i}Pr	*i*so-propyl
J	Coupling constant
K	Kelvin
L	Ligand
LUMO	Lowest Unoccupied Molecular orbital
M	Metal

m	Multiplet
m/z	Mass/Charge
M^+	Molecular ion
Me	Methyl
min.	Minutes
MP	Melting point
MS	Mass spectrometry
NHC	N-heterocyclic carbene
NMR	Nuclear magnetic resonance
ppm	Parts per million
R, R’	Organic substituents
s	Singlet
SEM	Scanning Electron Microscope
Sept	Septet
T	Tesla
t	Triplet
THF	Tetrahydrofuran
TMS	Tetramethylsilane
V	Volt
Z	Number of molecules in the unit cell
δ	Chemical shift

Abstract

Carbenes, neutral compounds containing divalent carbon atom with six electrons in valance shell, are the intriguing class of organic compound and possess potential to a new area of research particularly in organic transformations. After the successful isolation of N-heterocyclic carbene by Arduengo the major application of NHCs are found when they coordinate with transition metals. However, I have developed my interest on the advanced version of six-membered N-heterocyclic carbene namely bicyclic (alkyl)(amino) carbene, reported by Bertrand *et al.* which is more electrophilic (π-accepting) and nucleophilic (σ-donating) in comparison to NHCs.

In the first chapter, the synthesis of a palladium complex stabilized by two bicyclic (alkyl)(amino) carbene units is demonstrated well [$(BICAAC)_2PdCl_2$]. The complex was synthesized starting from $PdCl_2$ reacting with the free carbene under inert conditions. The complex was fully characterized by M.P., NMR, single crystal and powder X-ray diffraction and high-resolution mass spectrometry. The [$(BICAAC)_2PdCl_2$] complex has been investigated as a potential pre-catalyst towards different C-C coupling reactions (Heck-Mizoroki and Suzuki-Miyaura coupling) under the ambient condition with low catalyst loading.

In the second chapter, the syntheses and photophysical studies of bicyclic (alkyl)(amino) carbene copper complex as [(BICAAC)CuX] are demonstrated. The complexes were synthesized starting from CuX (X = Cl, I) with BICAAC. The mono and bis coordinated Cu(I) complexes, [(BICAAC)CuCl] and $[(BICAAC)_2Cu]^+[CuI_2]^-$, were characterized by NMR, single crystal X-ray diffraction and high-resolution mass spectrometry. The photophysical studies were also done in the solution phase. Then the neutral mononuclear copper complex $[(BICAAC)_2Cu]^0$ stabilized by two units of bicyclic (alkyl)(amino) carbene was attempted to synthesize starting from their carbene coordinated monohalide salt by potassium graphite (KC_8) reduction method and was characterized by magnetic properties, absorption spectroscopy and HRMS of the complex.

CONTENTS

Supporting information

1. Carbenes: Properties, Metal Complexes and Applications

1.1 Introduction

Defined as neutral compounds containing divalent carbon with six electrons in valance shell, carbene is one of the functional groups in the area of chemistry that entertains the idiosyncratic properties in bonding, nature of interactions and reactivities. Depending upon the nature of hybridization at the carbon centre, carbene can have linear or bent geometry. It can also be classified as singlet or triplet based on the spin multiplicity of the nonbonding pair of electrons.

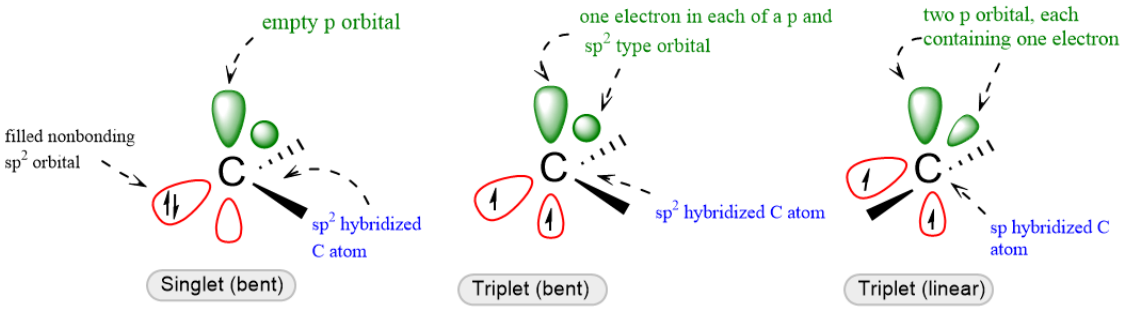

Fig. 1.1 Electronic states of divalent carbenes along with possible geometries (adapted from *Fundamental Concepts* of *Inorganic Chemistry, by* Asim K. Das, Vol-2).

Singlet carbene has empty *p orbital* and filled sp^2 type of orbital, which allow it to behave like a nucleophile as well as electrophile i.e. ambiphilic while triplet carbene has two unpaired electrons thereby shows biradicaloid character (Fig. 1.1).

The linear geometry of *sp*-hybridized carbene can be easily explained by the MO diagram where two p-orbitals are degenerate in nature (non-bonding). On bending the angle at the carbene carbon, the degeneracy breaks and the hybridization changes to sp^2 from *sp*. This linear geometry is the extreme case but generally, it is hardly observed. The molecular orbital energy diagram of simple carbenes ($:CH_2$) are depicted (Scheme 1.1).

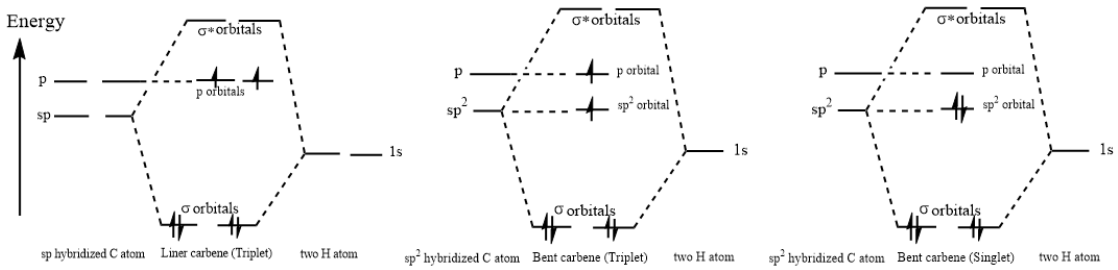

Scheme 1.1 Molecular orbital energy diagram of simple carbene ($:CH_2$) (adapted from *Organic Chemistry* by Jonathan Clayden, Nick Greeves, Stuart Warren, 2nd Edition).

Carbenes are highly desperate to find another pair of an electron to complete their valance shell in the octet. They can readily undergo insertion reactions, among which insertion to C=C is the well-studied one.

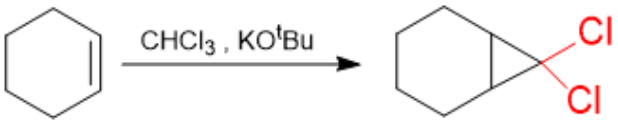

Scheme 1.2 Insertion reaction of cyclohexene by di-chlorocarbene (adapted from *Advanced Organic Chemistry* by Jerry March, 3rd Edition).

Cyclopropane derivatives can easily be formed by the insertion reaction of carbene to C=C bond (Scheme 1.2). The mechanism of the reaction depends on the nature of the carbene whether it is singlet or triplet and the outcome also. As the process is concerted, the geometry of the alkene should be conserved in the product i.e. the reaction ought to be *stereospecific* (Scheme 1.3).

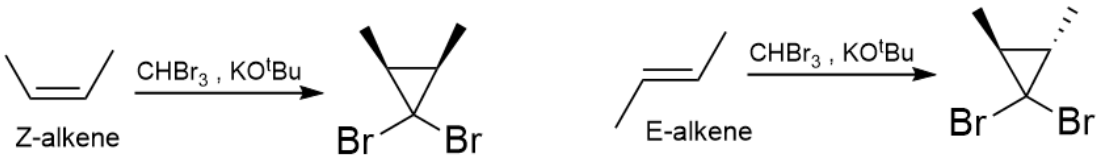

Scheme 1.3 Stereo-specificity of singlet carbene towards olefins (*Advanced Organic Chemistry*: Part A: Francis A. Carey and Richard J. Sundberg).

However, the olefin insertion reaction is *stereospecific* for singlet carbene only. Triplet carbene reacts in a different way towards olefins.

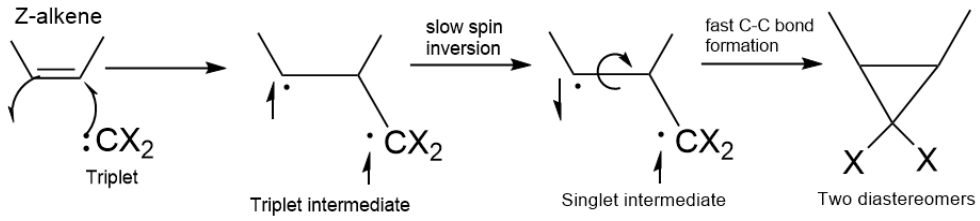

Scheme 1.4 Reactivity of triplet carbene towards olefins (*Advanced Organic Chemistry*: Part A: Francis A. Carey and Richard J. Sundberg).

It first attacks to the π* of the olefin to make a triplet intermediate followed by slow spin inversion (following *Möbius strip*) to form the singlet intermediate. Then it has two possibilities – it can easily form the C-C bond or it can form the other diastereomer following the C-C bond rotation (Scheme 1.4).

Now, the ground state spin multiplicity of carbenes depends on the relative energy of the σ and $p\pi$ orbitals. Larger σ-$p\pi$ separation ($\geq$2 eV) makes the carbene singlet as a ground state whereas σ-$p\pi$ separation ($\leq$1.5 eV) impose to be in triplet ground state. This σ-$p\pi$ separation largely depends on the substituents of the adjacent atoms to the carbene. Inductive effect or mesomeric effect can alter the ground state configuration of the carbene. If the substituents are, *σ-electron* withdrawing then it can stabilize the *non-bonding* orbital by increasing the *s-character* leaving the $p\pi$ orbital remaining same. Thus σ-$p\pi$ energy separation leading to singlet state of the carbene. In contrast, *σ-electron* donating substituents favours the triplet ground state.[1]

After the discovery of cyclopentadienyl derivatives as a new type of ligand, chemists have captured their imagination and extended into the horizon of *N-heterocyclic carbenes* (NHCs) and other *divalent* carbon species.

In tetravalent carbon, all the four electrons are engaged in bonding whereas species involving two electrons in *bonding* and rest remaining *nonbonding* at carbon centre are rare. These divalent species comprise carbon monoxide, isocyanides and carbenes. Now, carbon monoxide (CO_2) and isocyanides (-NC) are stable enough and have been known for more than one century, but carbenes have been found to be stable only in metal complexes[2-4] reported first in the *1970s*. Wanzlick first proposed the synthesis of an *imidazolidin-2-ylidene* in 1960 but it was not isolated as a single entity.[5] However, the breakthrough came when Bertrand's and co-workers reported the stable *[bis- (diisopropylamino)phosphino](trimethylsilyl)* carbene, stabilized by phosphorus and silicon substituents adjacent to the carbene centre in 1988.[6] Three years later, the first example of a free and stable "bottle-able" carbene (N-heterocyclic carbene) was reported by Arduengo *et al*. which unfastened the door of this area of research, which now has lasted more than 25 years.[7]

Now, NHCs are defined to be the first heterocyclic species in the carbene family with at least one nitrogen atom within the ring structure (Fig. 1.2). They are considered as superior ligand other than conventional two-electron donors such as phosphines, amines or ethers and can be considered as better alternatives to phosphines in the area of organometallic as well as organic chemistry.

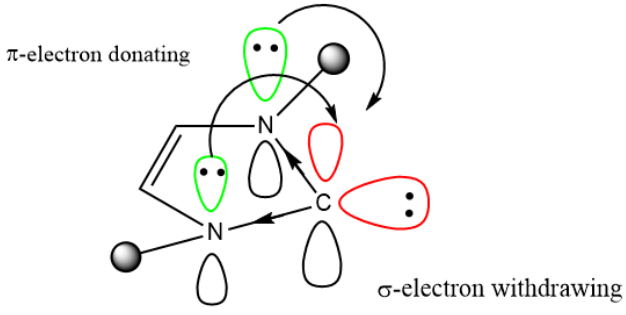

Fig. 1.2 Structural and electronic features of classical NHCs.[8]

The better *σ-donation* along with *π-acceptance* are inherently linked to the ligand's frontier molecular orbitals (FMOs). These electronic and steric properties are well utilized in different aspects as depicted in Fig. 1.3.[8]

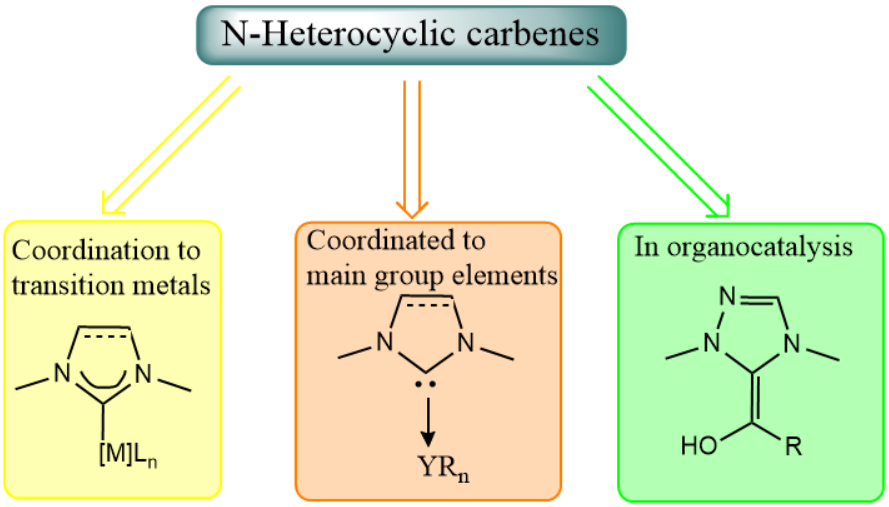

Fig. 1.3 Major applications of NHCs (an overview).[8]

The major applications of N-heterocyclic carbenes have been found when they coordinate with transition metals. Diez-Gonzalez and Nolan have reviewed the electronic properties and nature of bonding of NHC complexes with base metals[9] that made the track easy for the synthetic chemist to investigate the further application of the carbene-complexes across the chemical sciences. They are also important in material chemistry[10-11] and metallopharmaceuticals.[12] However, the largest applications are indeed in the area of catalysis towards organic transformations, which was demonstrated first by Herrmann and co-workers in Mizoroki-Heck reaction catalyzed by Pd-NHC complex.[13] Ruthenium complexes bearing unsymmetrical *imidazolin-2-ylidene* have been found with high Z-selectivity in cross-metathesis reactions.[14a] Copper (I)-catalyzed *azide alkyne cycloaddition* (CuAAC) reaction[14b], hydrogenation reaction[14c] catalyzed by NHC-Ir complex are also reported. Extensive studies have been done on NHC-Au complexes as they are found to be a good catalyst in alkyne isomerization, enyne cycloisomerization, and hydroamination.[15]

Most recently, NHCs are found to have great application in the area of organocatalysis as it readily attacks as a nucleophile to the carbonyl group in any organic moiety. Taton and co-workers have reported metal free polymerization by NHCs.[16] Several reports are demonstrated NHC catalyzed Morita-Baylis-Hilman reactions in an efficient way.[17] NHCs help a lot to understand and improve the fundamental chemistry. They have been used as a better electron donor as compared to phosphine to stabilize the low valent transition metals. Arduengo *et al.* reported $[(NHC)_2]M^0$ [M = Ni, Pt][18], two coordinated metal(0) complexes. After that, many transition metal complexes have been reported with NHCs in variable oxidation state even with modified ligand backbone. In 2008, Robinson *et al* showed diatomic allotropes L_2E_2 [E = B, Si, P in formal oxidation state zero, L= NHC ligand] which has increased tremendous research attention towards low coordinated main group compounds.[19-21]

Though NHCs have been in the front line of this area of research, several other singlet carbenes have also been isolated (Fig 1.4.) since the discovery of NHCs, which includes *cyclopropylidines, imidazolin-2-ylidines, imidazole-2-ylidines, 1,2,4-triazol-5-ylidnies etc*.[22]

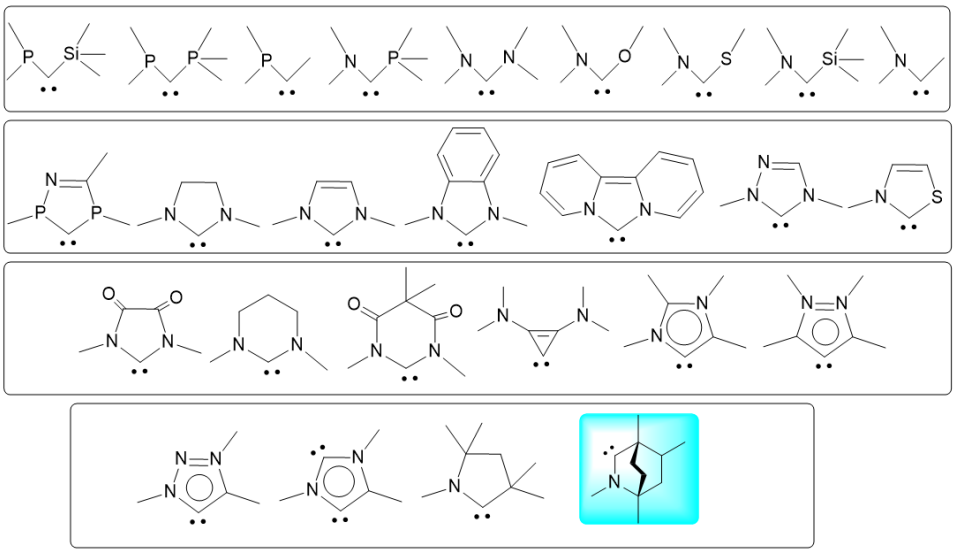

Fig 1.4 Different types of isolable singlet carbenes.[22]

In 2005, Bertrand *et al.* reported on the first synthesis of cyclic (alkyl)(amino) carbene[23] in which one of the nitrogen atom is replaced by one σ-donating quaternary carbon atom. As a result, the HOMO-LUMO gap is smaller in comparison to NHC (Fig. 1.5).[24] As a consequent, cAAC became better σ-donor and π-acceptor, which has been experimentally established by ^{31}P NMR studies of carbene-phophinidine, adducts.[25] This energy difference was further investigated by computational studies. Bertrand *et al.* showed that the HOMO of cAACs is slightly higher, and the singlet-triplet gap slightly smaller, than NHCs (HOMO: -4.9 *vs.* -5.2 eV; $\Delta E_{\text{singlet/triplet}} \sim 45$ *vs.* 68 kcal mol^{-1}).[26-27]

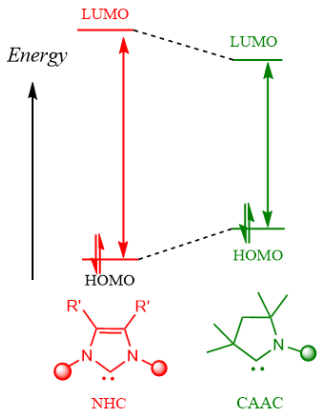

Fig. 1.5 Qualitative FMO comparison between NHC and cAAC.

cAACs have been very efficient towards low coordinate metal complexes which are not isolable with other neutral donor ligands. cAACs stabilize a board area of elements starting from transition metals to main group elements in a different mode which makes them even much more interesting than NHCs. cAAC can stabilize many transition metals in their different oxidation states which play an important role in various organic transformations.[28] [(Ad-cAAC)Au] complex efficiently mediates the catalysis coupling of enamines and terminal alkyne to yield allenes,[29] intramolecular hydroamination of alkyne to form imine and enamine.[30] (Scheme 1.5).[31]

The better σ-donating ability of cAAC makes them as a good ligand for palladium-catalyzed α-arylation of carbonyl compound and for ruthenium-catalyzed olefin metathesis Due to stronger electrophilicity and smaller singlet-triplet gap, cAAC have been shown to activate small molecules and even enthalpically stronger bonds under mild conditions (Scheme 1.6).

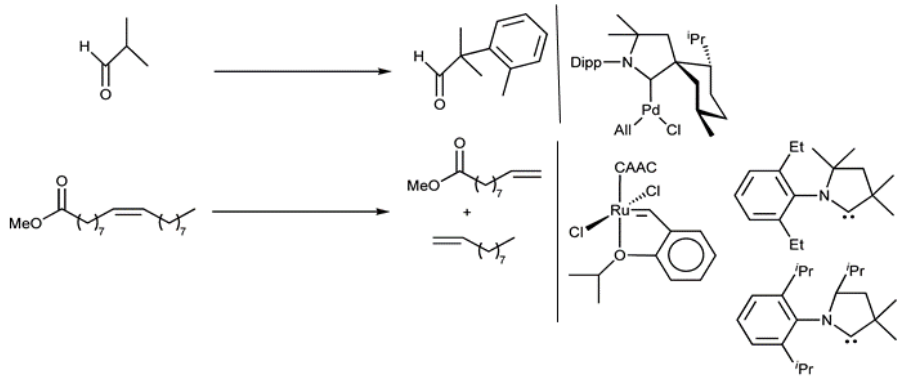

Scheme 1.5 cAAC as ligand for Pd and Ru based catalysis.[31]

cAAC could activate H_2[32], B-H bond[33-34], Si-H bond[35], P-H bond[33], and even NH_3[32] which is thought to be a difficult task even for transition metals.[36] More interestingly, Turner et al have recently shown that cAAC can also activate sp^3-, sp^2- and sp- hybridized C-H bond at room temperature[37] as shown in Scheme 1.7. These outcomes can easily demonstrate that cAACs can readily undergo oxidative addition just like the transition metals.

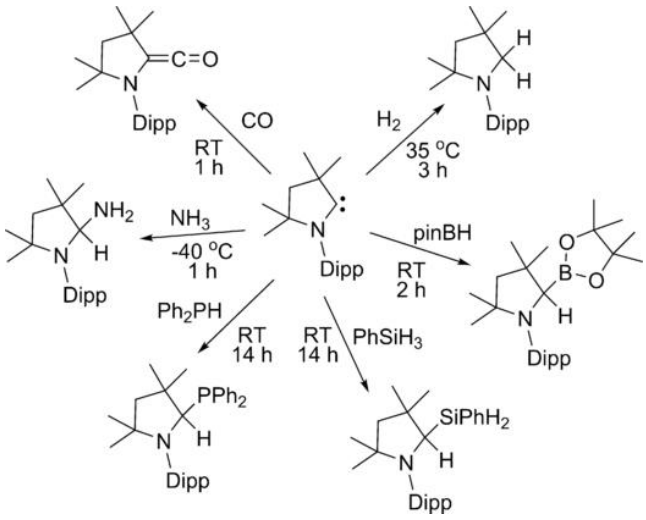

Scheme 1.6 Small molecules activation by cAAC.[32-36]

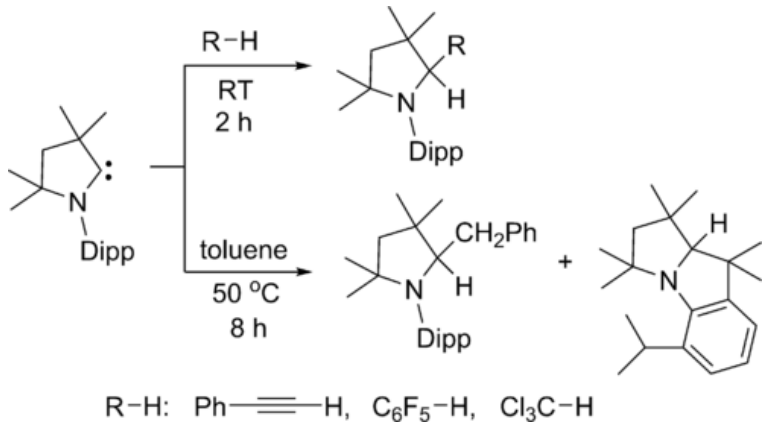

Scheme 1.7 sp^3-, sp^2- and sp- hybridized C-H bond activation by cAACs.[37]

Very few cAAC-complexes of group 1 and group 2 have been reported so far. Recently, Schuster *et al.* reported zero valent beryllium compound [$(cAAC)_2Be$] following the standard KC_8 reduction route.[38] cAAC has been used for preparing nucleophilic organoborons[39], tricoordinated boron anions[40] and many low valent boron derivatives.

Following the pioneering work by Robinson *et al.* who demonstrated the utility of NHCs towards the stabilization of Si species in different oxidation state, Roesky *et al.* have also reported cAAC supported [$(Si)_n$, n =1 & 2].[41-42]

Until 2015, most of the transition metal complexes were prepared from the carbene itself or when the carbene was not isolable, by the deprotonation of iminium salt. In 2015, [(cAAC) CuCl] complex was reported by the treatment of iminium salt (chloride) with Cu_2O.[43] Then Pd, Au and Ir cAAC complexes were synthesized by transferring the cAAC ligand from the previously reported Cu complex.[44] Transition metals with formal zero oxidation state have also been demonstrated for example, [$(cAAC)_2M$] where M = Mn,[45] Zn,[46] Au,[47], Co & Fe,[48] Ni[49]. In 2015, Roesky *et al.* reported the two coordinated palladium(0) and platinum(0) complexes starting from their phosphine salt.[50]

Now, among the transition metals, group 10 and group 11 elements have served a lot in the aspect of fundamental chemistry as well as in different application purpose.

The work in this thesis deals with another advance version of cyclic (alkyl)(amino) carbene named bicyclic (alkyl)(amino) carbene (BICAAC)[51] which is recently reported by Bertrand and co-workers in 2017. By the modification of cAAC skeleton, they have successfully synthesized this six-membered bicyclic carbene, which leads to a geometry somewhat similar to NHCs (Fig. 1.6).

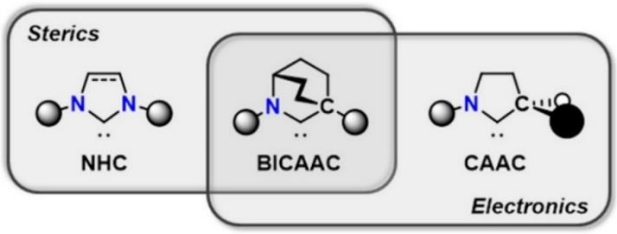

Fig. 1.6 Schematic resemblance among NHC, cAAC and BICAAC (adapted from *J. Am. Chem. Soc*., **2017**, *139*, 7753–7756).

This novel carbene shows enhanced *σ donating* and *π-accepting* properties compared to cAACs and as well as NHCs (Fig. 1.7). The better ambiphilicity can also be supported by the experimental evidence (such as ligand exchanges and ^{31}P, ^{77}Se NMR) as they have reported. There is a significant decrease in the singlet-triplet gap from 49.2 kcal mol^{-1} to 45.7 kcal mol^{-1} , which can be easily correlated to the wider carbene bond angle (110.2^0 *vs.* 106.9^0).

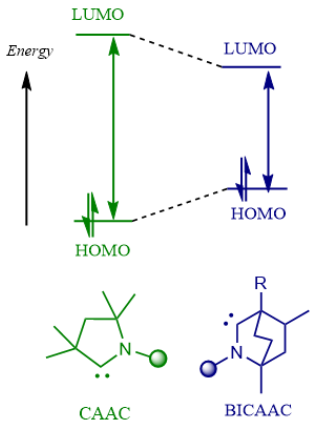

Fig. 1.7 Qualitative FMO comparison between cAAC and BICAAC (adapted from *J. Am. Chem. Soc*. **2017**, *139*, 7753–7756).

Now, several compounds of palladium and copper have been made with NHCs and cAACs and found to have applications in different directions.[13, 14b, 31]

Following those ideas in mind, we were able to synthesize, during the work of this dissertation, the first [$(BICAAC)_2PdCl_2$] complex. We have discussed the preparation, isolation and characterization of the palladium complex and investigated the catalytic activity of the complex in C-C coupling reactions under ambient conditions. We have also synthesized, characterized and isolated BICAAC-copper complexes as mono as well as bis carbene coordination fashion. The neutral mononuclear copper complex [$(BICAAC)_2Cu(0)$] stabilized by two units of bicyclic (alkyl)(amino) carbene was attempted to synthesize starting from their carbene coordinated monohalide salt by potassium graphite (KC_8) reduction route and was characterized by different analytical techniques.

1.2 References

1. Bourissou, D.; Guerret, O.; Gabbai, F. P.; Bertrand, G. *Chem. Rev*. **2000**, *100*, 39–91.
2. Wanzlick, H.-W.; Schoenherr, H.-J. *Angew. Chem., Int. Ed.* **1968**, *7*, 141-142.
3. Ofele, K. *J. Organomet. Chem*. **1968**, *12*, 42-43.
4. Cardin, D. J.; Cetinkaya, B.; Lappert, M. F.; Manojlovic-Muir, L.; Muir, K. W. *Chem. Commun*. **1971**, 400-401.
5. Wanzlick, H.-W.; Schikora, E. E. *Angew. Chem.* **1960**, *72*, 494.
6. Gau, A.; Grutzmacher, H.; Baceiredo, A.; Bertrand, G. *J. Am. Chem. Soc.* **1988**, *110*, 6463-6466.
7. Arduengo, A. J. III; Harlow, R. L.; Kline, M. *J. Am. Chem. Soc*. **1991**, *113*, 361-363.
8. Hopkinson M. H.; Richter C.; Schedler M.; Glorius F. *Nature chemistry* **2014**, *510*, 485.
9. Diez-Gonzalez, S.; Nolan, S. P.; *Coord. Chem. Rev.* **2007**, *251*, 874-883.
10. Mercs, L.; Albrecht, M. *Chem. Soc. Rev.* **2010**, *39*, 1903-1912.
11. Oisaki, K.; Li, Q.; Furukawa, H.; Czaja, A. U.; Yaghi, O. M. *J. Am. Chem. Soc*. **2010**, *132*, 9262-9264.
12. Hickey A. M.; Ruhayel R. A.; Barnard P. J.; Baker M. V.; Berners-Price S. J.; Filipovska A. *J. Am. Chem. Soc.* **2008**, *130* (38), 12570-12571.
13. Herrmann, W. A.; Elison, M.; Fischer, J.; Kocher, C.; Artus, G. R. J. *Angew. Chem. Int. Ed.* **1995,** *34*, 2371-2374.
14. a) Endo, K.; Grubbs, R. H. *J. Am. Chem. Soc*. 2011. *133*, 8525-8527. b) Heina, J. E.; Fokin, V. V. *Chem. Soc. Rev.* **2010**, *39*, 1302-1315. c) Jimenez, M. V.; Fernandez-Tornos, J.; Perez-Torrente, J. J.; Modrego, F. J.; Garcia-Orduna, P.; Oro, L. A. *Organometallics* **2015**, *34* (5), 926–940.
15. Mariona, N.; Nolan, S. P. *Chem. Soc. Rev*. **2008**, *37*, 1776-1782.
16. Feivre, M.; Pinaud, J.; Gnanou, Y.; Vignolle, J.; Taton, D. *Chem. Soc. Rev.* **2013,** *42*, 2142-2172.
17. Chen, X.Y.; Ye, S. *Org. Biomol. Chem*. **2013,** *11*, 7991–7998.
18. Arduengo, A. J.; Gamper, S. F.; Calabrese, J. C.; Davidson, *J. Am. Chem. Soc.* **1994**, *116*, 4391-439.
19. Wang, Y.; Robinson, G. H. *Inorg. Chem*. **2011**, *50*, 12326-12337.
20. Wang, Y.; Xie, Y.; Wei, P.; King, R. B.; Schaefer, H. F. III; Schleyer, P. v. R.; Robinson, G. H. *Science* **2008**, *321*, 1069-1071.
21. Wang, Y.; Robinson, G. H. *Chem. Commun*. **2009**, 5201-5213.

22. Malaimi, M.; Jazzar, R.; Soleihavoup, M.; Bertrand, G. *Angew. Chem. Int. Ed.* **2017**, *56*, 10046-10068.
23. Lavallo, V.; Canac, Y.; Prasang, C.; Donnadieu, B.; Bertrand, G. *Angew. Chem., Int. Ed.* **2005**, *44*, 5705-5709.
24. Martin, D.; Melaimi, M.; Soleilhavoup, M.; Bertrand, G. *Organometallics* **2011**, *30*, 5304-5313.
25. Back, O.; Henry-Ellinger, M.; Martin, C. D.; Martin, D.; Bertrand, G. *Angew. Chem., Int. Ed*. **2013**, *52*, 2939−2943.
26. Malaimi, M.; Jazzar, R.; Soleihavoup, M.; Bertrand, G. *Angew. Chem. Int. Ed.* **2017**, *56*, 10046-10068.
27. Singh, A. P.; Samuel, P. P.; Roesky, H. W.; Schwarzer, M. C.; Frenking, G.; Sidhu, N. S.; Dittrich, B. *J. Am. Chem. Soc*. **2013**, *135*, 7324-7329.
28. Roy, S.; Mondal, K. C.; Roesky, H. W. *Acc. Chem. Res*. **2016**, *49*, 357-369.
29. Lavallo, V.; Frey, G. D.; Kousar, S.; Donnadieu, B.; Bertrand, G. *Proc. Natl. Acad. Sci. U. S. A.* **2007**, *104*, 13569-13573.
30. Zeng, X.; Frey, G. D.; Kousar, S.; Bertrand, G. *Chem. Eur. J*. **2009**, *15*, 3056-3060.
31. Lavallo, V.; Canac, Y.; Prasang, C.; Donnadieu, B.; Bertrand, G. *Angew. Chem., Int. Ed.* **2005**, *44*, 5705-5709.
32. Frey, G. D.; Lavallo, V.; Donnadieu, B.; Schoeller, W. W.; Bertrand, G. *Science* **2007**, *316*, 439-441.
33. Frey, G. D.; Masuda, J. D.; Donnadieu, B.; Bertrand, G. *Angew. Chem. Int. Ed.* **2010**, *49*, 9444-9447.
34. Wgrtemberger-Pietsch, S.; Schneider, H.; Marder, T. B.; Radius, U. *Chem. Eur. J.* **2016**, *22*, 13032–13036.
35. Mohapatra, C.; Samuel, P. P.; Li, B.; Niepçtter, B.; Schgrmann, C. J.; Herbst-Irmer, R.; Stalke, D.; Maity, B.; Koley, D.; Roesky, H. W. *Inorg. Chem*. **2016**, *55*, 1953-1955.
36. Klinkenberg, J. L.; Hartwig, J. F. *Angew. Chem., Int. Ed*. **2011**, *50*, 86-95.
37. Turner, Z. R. *Chem. Eur. J.* **2016**, *22*, 11461-11468.
38. Arrowsmith, M.; Braunschweig, H.; Celik, M. A.; Dellermann, T.; Dewhurst, R.; Ewing, W. C.; Hammond, K.; Kramer, T.; Krummenacher, I.; Mies, J.; Radacki, K.; Schuster, K. *Nature Chemistry* **2016**, *8*, 890-894.
39. Kinjo, R.; Donnadieu, B.; Celik, M. A.; Frenking, G.; Bertrand, G. *Science* **2011**, *333*, 610-613.

40. Ruiz, D. A.; Ung, G.; Melaimi, M.; Bertrand, G. *Angew. Chem. Int. Ed*. **2013**, *52*, 7590-7592.
41. Mondal, K. C.; Roesky, H. W.; Stuckl, A. C.; Ihret, F.; Kaim, W.; Dittrich, B.; Maity, B.; Koley, D. *Angew. Chem. Int. Ed.* **2013**, *52*, 11804-11807.
42. Mondal, K. C.; Dittrich, B.; Maity, B.; Koley, D.; Roesky, H. W. *J. Am. Chem. Soc.* **2014**, *136*, 9568-9571.
43. Bidal, Y. D.; Lesieur, M.; Melaimi, M.; Nahra, F.; Cordes, D. B.; Arachchige, K. S. A.; Slawin, A. M. Z.; Bertrand, G.; Cazin, C. S. J. *Adv. Synth. Catal*. **2015**, *357*, 3155-3161.
44. Bidal, Y. D.; Santoro, O.; Melaimi, M.; Cordes, D. B.; Slawin, A. M. Z.; Bertrand, G. C.; Cazin, S. J. *Chem. Eur. J.* **2016**, *22*, 9404-9409.
45. Samuel, P. P.; Mondal, K. C.; Roesky, H. W.; Hermann, M.; Frenking, G.; Demeshko, S.; Meyer, F.; C. Stuckl, A.; Christian, J. H.; Dalal, N. S.; Ungur, L.; Chibotaru, L. F.; Propper, K.; Meents, A.; Dittrich, B. *Angew. Chem. Int. Ed.* **2013**, *52*, 11817-11812.
46. Singh, A. P.; Samuel, P. P.; Roesky, H. W.; Schwarzer, M .C.; Sidhu, N. S.; Dittrich, B. *J. Am. Chem. Soc.* **2013**, *135*, 7324-7329.
47. Weinberger, D. S.; Melaimi, M.; Moore, C. E.; Rheingold, A. L.; Frenking, G.; Jerabek, P.; Bertrand, G. *Angew. Chem. Int. Ed*. **2013**, *52*, 8964-8967.
48. Ung, G.; Rittle, J.; Soleilhavoup, M.; Bertrand, G.; Peters, J. C. *Angew. Chem. Int. Ed*. **2014**, *53*, 8427-8433.
49. Mondal, K. C.; Samuel, P. P.; Li, Y.; Roesky, H. W.; Roy, S.; Ackermann, L.; Sidhu, N. S.; Sheldrick, G. M.; Carl, E.; Demeshko, S.; De, S.; Parameswaran, P.; Ungur, L.; Chibotaru, L. F.; Andrada, D. M. *Eur. J. Inorg. Chem.* **2014**, 818-823.
50. Roy, S.; Mondal, K. C.; J. Niepötter, B.; Köhler, C.; Irmer, R. H.; Stalke, D.; Dittrich, B.; Andrada, D. M.; Frenking, G.; Roesky, H. W. *Chem. Eur. J.* **2015**, *21*, 9312-9318.
51. Mendivil, E. T.; Hansmann, M. M.; Weinstein, C. M.; Jazzar, R.; Melaimi, M.; Bertrand, G. *J. Am. Chem. Soc.* **2017**, *139*, 7753-7756.

Chapter 1

Synthesis and characterization of palladium bicyclic (alkyl)(amino) carbene complex including its catalytic applications in C-C coupling reactions

Abstract: This chapter demonstrates the synthesis of a palladium complex stabilized by two *bicyclic (alkyl)(amino) carbene* units and the complex was synthesized starting from $PdCl_2$ reacting with the free carbene under inert conditions. The complex formation was further confirmed by following ^{1}H and ^{13}C NMR spectroscopic measurements. The complex was fully characterized by melting point, single crystal X-ray diffraction, high-resolution mass spectrometry, SEM and EDX. The single crystal X-ray structure of the *trans-[(BICAAC)$_2$PdCl$_2$]* was obtained. The *[(BICAAC)$_2$PdCl$_2$]* complex has been investigated as a potential pre-catalyst towards different C-C cross-coupling reactions (*Heck-Mizoroki* and *Suzuki-Miyaura* coupling) under ambient condition with low catalyst loading.

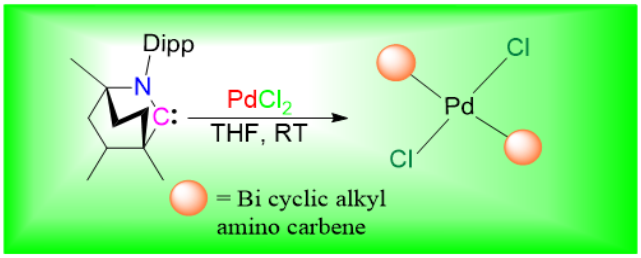

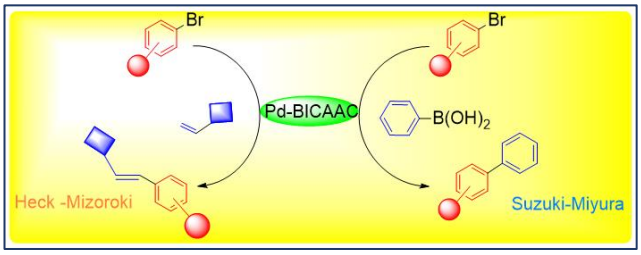

2.1 Introduction

Although some of the first attempts to synthesize complexes from stable N-heterocyclic carbene involved *3d* transition metals, most of the studies of the coordination and catalytic activities of NHC complexes focused on the heavier transition metals particularly group 10 metals. Possible reasons that may be responsible for this are their diamagnetic nature (d^{10} *electronic configuration* in +II oxidation state), air-stability and strong metal-$C_{carbene}$ bonds. The transmetallation reaction is commonly used to prepare M^{II}- NHC complexes from the parent Ag-NHC adducts.[1] Apart from that, metal plate electrolysis,[2] metal powder,[3] or thermolysis[4] routes have also been explored (Scheme 2.1). However, direct adducts formation have been achieved later by reacting the free carbene with the corresponding metal-salt with high yield.

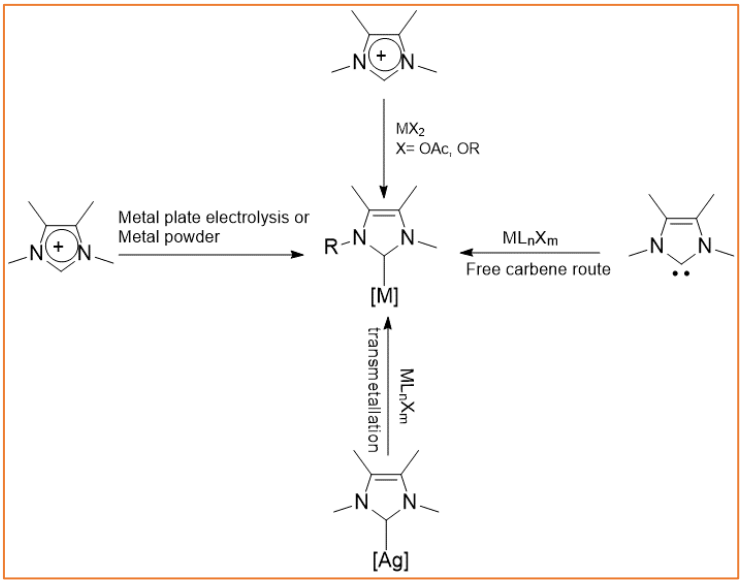

Scheme 2.1 Synthetic routes of metal-NHC complexes.[1-4]

N-heterocyclic carbene and cyclic (alkyl)(amino) carbene have been shown as supporting ligand to stabilize group 10 transition metals in variable oxidation states (Fig. 2.1). Among them, some important complexes with modified ligand backbone have shown good catalytic activity in various organic transformations.

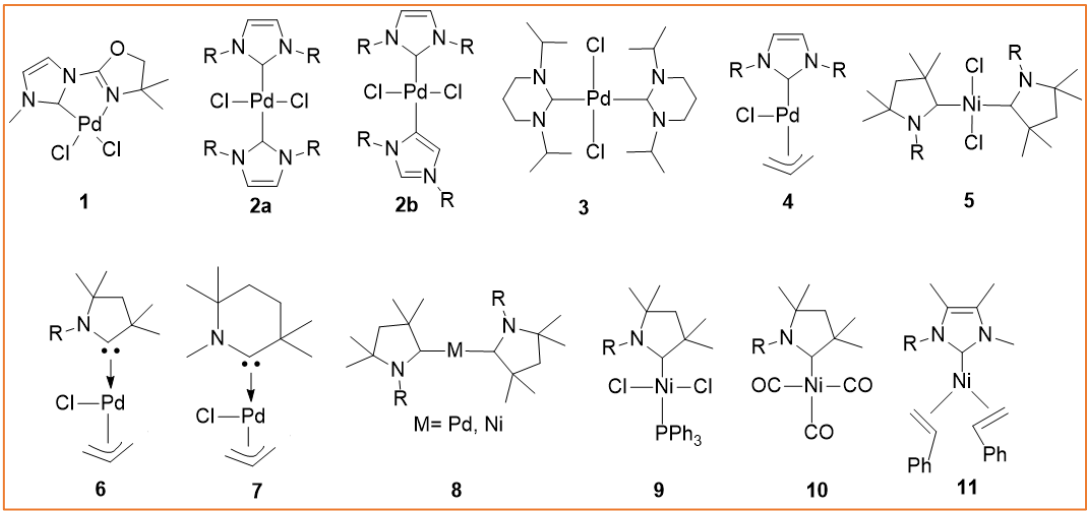

Fig. 2.1 Some well-known group 10 transition metal carbene complexes.

Transition metal catalyzed cross-coupling reaction is one of the most versatile and powerful methods that has led to a vast improvement in the synthesis of pharmaceuticals, agrochemicals and precursors for materials chemistry. The major advances are observed in the past 20 years by the use of well-defined, bench-stable *palladium* and *nickel* precatalyst.

Most recently, Shi and co-workers have reported regio- and enantio-selective cyclization of pyridine with olefin catalyzed by Ni-NHC complex[5] (Scheme 2.2). Apart from that, Ni-catalyzed cross-coupling between amines and aryl boronic ester under reductive condition has also been recently achieved.[6]

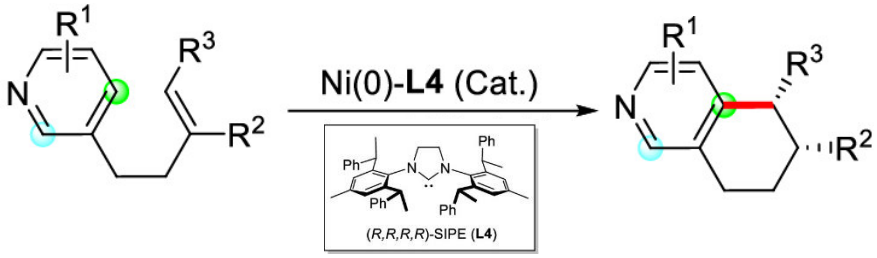

Scheme 2.2 Intramolecular cyclization of pyridine with olefin via C-H activation.

Over the past decade, the use of Pd-NHC complex has blossomed so much it diverted the attention of the chemist from a fundamental point of view towards more applicative. Palladium-catalyzed C-C and C-N bond formation are the most versatile and powerful

synthetic methods. NHCs have enjoyed increasing popularity as ligands in Pd-mediated coupling reactions. Typically, phosphine based ligands have been explored intensively in most of the cross-coupling reaction but recently, carbene has attracted much more recognition. The steric and electronic properties of N-heterocyclic carbene make the catalyst much more favourable towards the fundamental steps such as oxidative addition and reductive elimination forming relatively stronger *Pd-C* (carbene) bond (Fig. 2.2).[7] The strong binding of carbene ligand to the metal centre make the catalyst active and sustainable towards the end of the reaction. Furthermore, palladium complexes are generally tolerant towards a variety of functional groups and especially the +II oxidation state of palladium are not sensitive to air and moisture.

Fig. 2.2 Comparison of electronic environment between phosphine and carbene palladium complex.

In 2003, Gregory *et al.* first reported the Sonogashira reaction between alkyl electrophile and alkyl bromide under ambient condition supported by Pd-carbene complex[8] with 2.5 mol% loading. In 2004, Nolan and co-workers demonstrated the reactivity of "Unusual" N-heterocyclic carbene Palladium complex towards C-C coupling reaction with 2-mol% catalyst loading.[9]

Following the precedence from the literature, we also synthesized Pd(II) complex supported by two BICAAC units (Scheme 2.3).

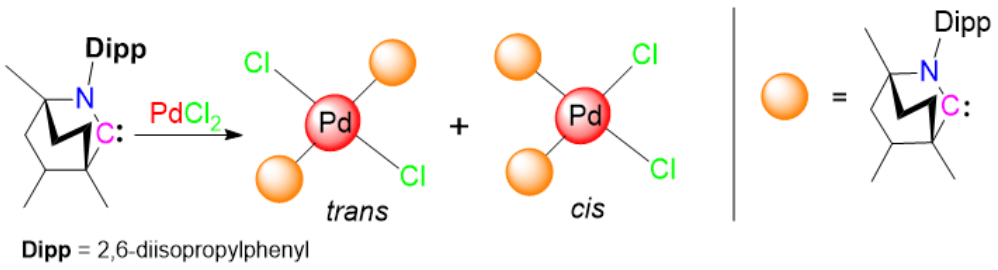

Scheme 2.3 Synthetic scheme of ***[(BICAAC)$_2$PdCl$_2$]*** **(1)** (our work).

Additionally, we also wanted to explore the catalytic activity of the newly synthesized [(*BICAAC*)$_2$PdCl$_2$] complex in suitable chemical transformations. The main aim was to investigate the catalytic activity of the complex as compared to the reported carbene complexes in literature. After several attempts, we finally found that the complex is catalytically active towards Heck-Mizoroki (Scheme 2.4) as well as Suzuki-Miyaura (Scheme 2.5) reaction under the optimized conditions as a pre-catalyst.

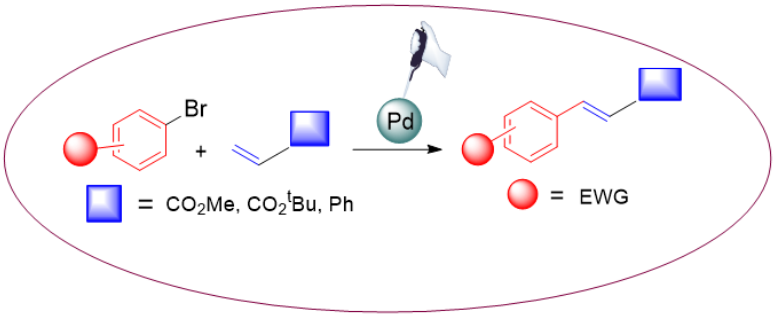

Scheme 2.4 ***[(BICAAC)$_2$PdCl$_2$]*** catalyzed Heck-Mizoroki reaction.

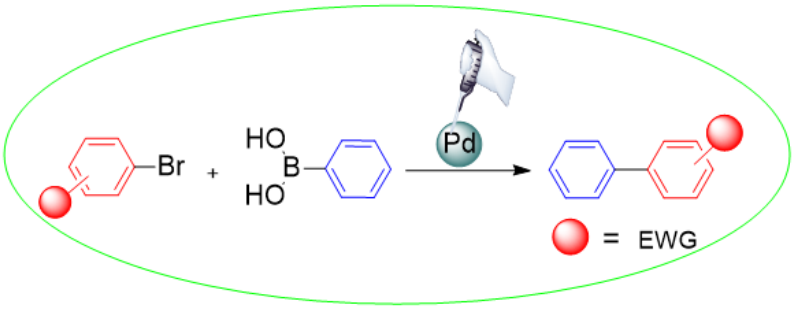

Scheme 2.5 ***[(BICAAC)$_2$PdCl$_2$]*** catalyzed Suzuki-Miyaura reaction.

2.2 Results and Discussion

2.2.1. Synthesis of $[(BICAAC)_2PdCl_2]$ (1)

Bicyclic (alkyl)(amino) carbene (BICAAC) was dissolved in THF and then $PdCl_2$ was added directly to the solution and stirred at room temperature for 10 h in the glove box (Scheme 2.6). The progress of the reaction was observed by the colour changes from light yellow to deep brown. All the volatiles were removed under vacuum and the residue was washed with hexane and dried properly to yield a deep brown solid in 78% yield.

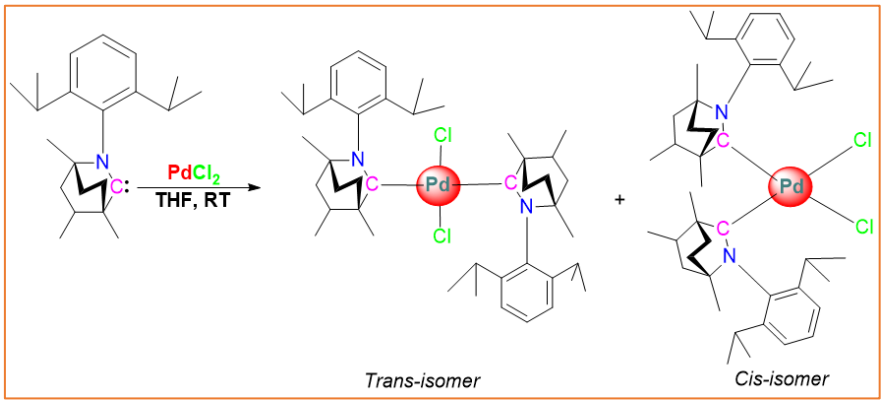

Scheme 2.6 Synthesis of ***[(BICAAC)$_2$PdCl$_2$]*** **(1).**

The ^{1}H NMR spectrum of **(1)** in $CDCl_3$ shows three septets and one merged doublet at 3.25, 3.12, 2.85 and 2.54 ppm respectively which can be attributed to the *cis* and *trans* isomers of the biscarbene $PdCl_2$ adduct. From the ^{1}H NMR spectrum of **(1)** we cannot predict the *cis/trans* relative quantitative ratio as all four signals were giving rise to only 1 H in each case. However, the peaks at 263.0 and 259.2 ppm in the ^{13}C NMR spectrum also suggest the formation of both *cis* and *trans* products. The HRMS data shows a signal at *m/z* = 763.3917 corresponding to $[M\text{-}Cl]^+$ of **(1)**.

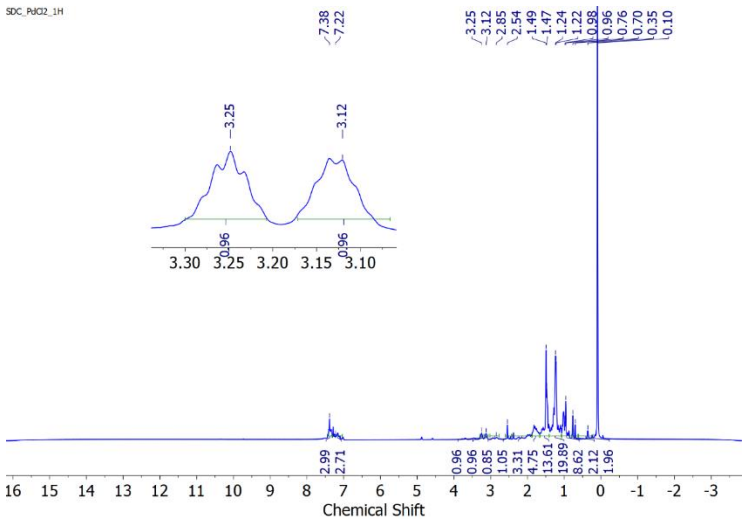

Fig. 2.3 ^{1}H NMR spectrum of ***[(BICAAC)$_2$PdCl$_2$]*** **(1)** (400 MHz, $CDCl_3$).

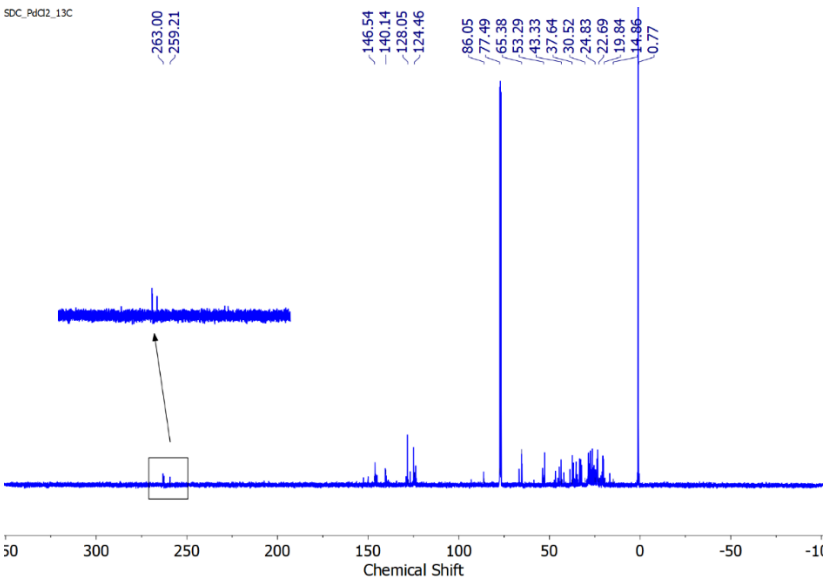

Fig. 2.4 ^{13}C NMR spectrum of ***[(BICAAC)$_2$PdCl$_2$]*** **(1)** (100 MHz, $CDCl_3$).

Further structural details of **(1)** was examined by single crystal X-ray diffraction study. We were able to isolate only the *trans* adduct which crystallized in *P2$_1$/n* space group in the monoclinic system. Then we also investigated whether the crystalline properties match with the crude product.

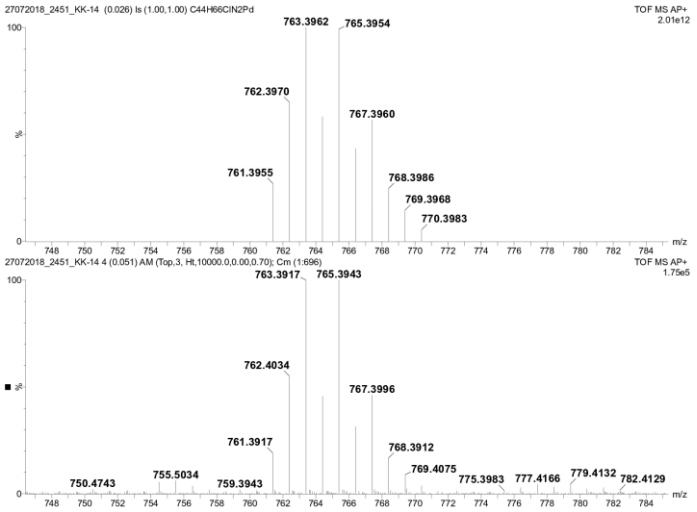

Fig. 2.5 HRMS of ***[(BICAAC)$_2$PdCl$_2$]*** (**1**).

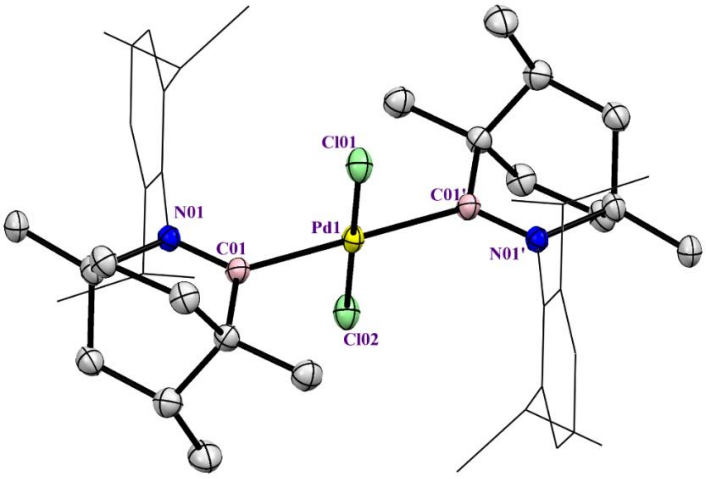

Fig. 2.6 *Single crystal X-ray structure of trans*-[(BICAAC)$_2$PdCl$_2$] **(1)**. Ellipsoids are shown at 50 % probability levels. All hydrogen atoms are omitted for clarity. Selected bond lengths [Å] and bond angles [°]: Pd-C01 2.0297(3), Pd-C01' 2.0297(3), Pd-Cl01 2.3247(8), Pd-Cl01' 2.3247(8), N01'-C01' 1.309(4), N01-C01 1.309(4); Cl01-Pd1-C01' 90.90(4), Cl01-Pd- Cl02 180.00(4), Cl01-Pd1-C01 89.10(5), C01'-Pd1-Cl02 89.10(5), C01'-Pd1-C01 180.0(4); Cl02-Pd1-C01 90.90(4).

We performed the powder X-ray diffraction studies of the crude sample and compared with the simulated pattern from the single crystal structure. However, we found that the two patterns are not exactly matching with each other (this is probably due to the mixture of *cis* and *trans*

products present in the crude sample) but they are quite similar in nature, which is clear from Fig. 2.7 and Fig. 2.8.

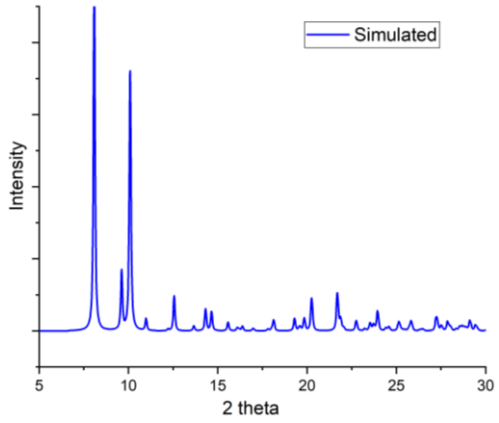

Fig. 2.7 PXRD pattern of the *trans-[(BICAAC)$_2$PdCl$_2$]* **(1)** simulated from single crystal data.

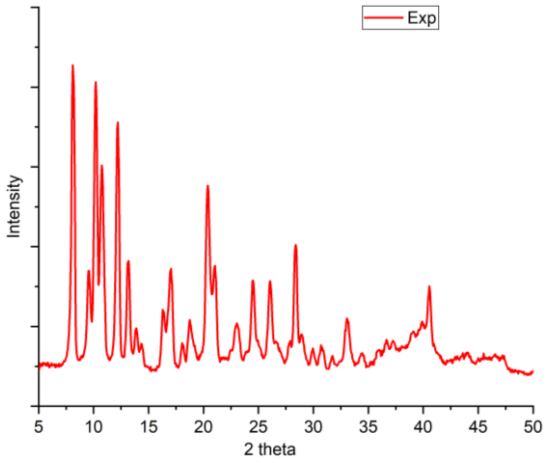

Fig. 2.8 PXRD pattern of the ***[(BICAAC)$_2$PdCl$_2$]*** **(1)** (crude product).

The UV-Vis spectrum shows peaks at 290 nm ($\varepsilon = 4*10^2$ *L mol^{-1}cm^{-1}*) and 435 nm ($\varepsilon = 1.9*10^2$ *L mol^{-1}cm^{-1}*) due to intra ligand charge transfer (ILCT) and Metal to ligand charge transfer (MLCT). No *d-d transition* has been observed in this case.

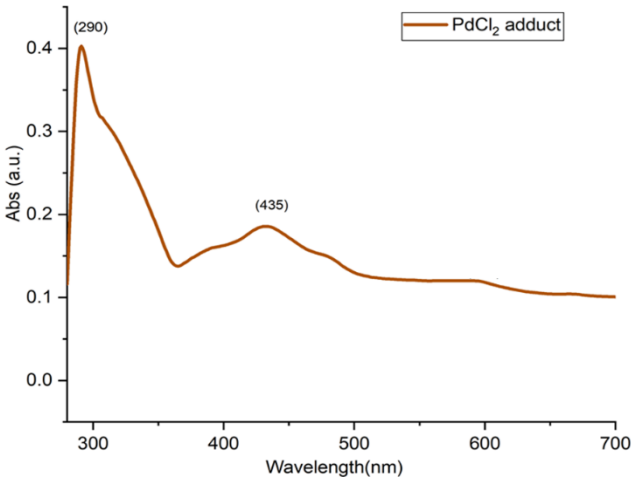

Fig. 2.9 UV-Vis. spectrum of ***[(BICAAC)$_2$PdCl$_2$]*** (**1**).

Then the complex **1** was investigated as a potential pre-catalyst in C-C coupling reactions with low catalyst loading. To check the surface topography and the composition of the pre-catalyst, Scanning Electron Microscopic (SEM) and Energy-dispersive X-ray spectroscopic (EDX) measurements have also been performed. From the SEM images (Fig. 2.10), we can clearly observe the crystalline nature of the material. The EDX analysis depicts the Pd: Cl ratio to be 1:2 as in the complex **1**. The SEM and EDX analysis were done just to compare the morphology of the pre-catalyst with the material recovered after the reactions (see below).

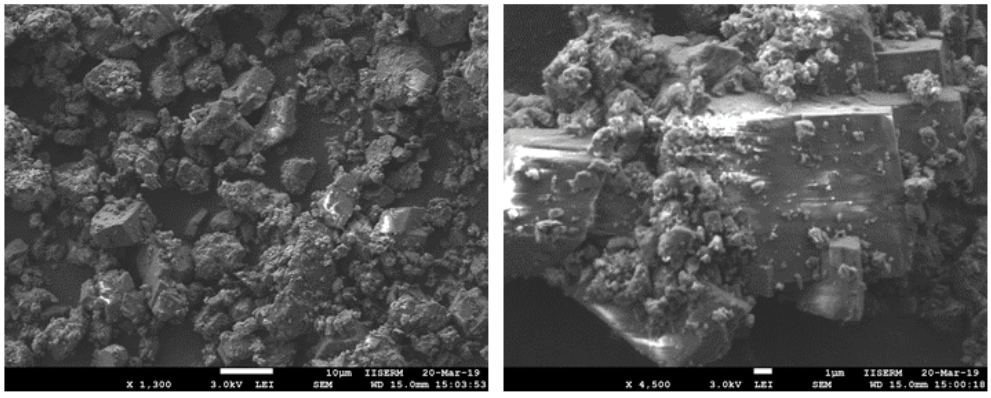

Fig. 2.10 SEM images of ***[(BICAAC)$_2$PdCl$_2$]*** (**1**).

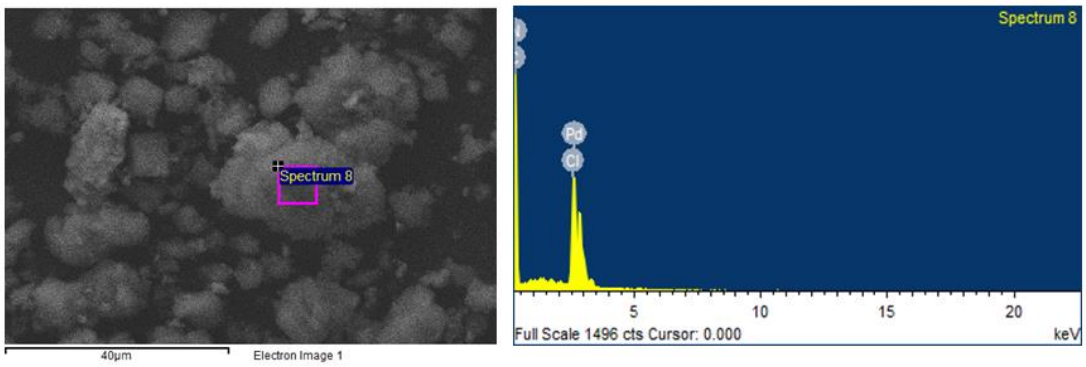

Fig. 2.11 EDX spectrum of ***[(BICAAC)$_2$PdCl$_2$]*** (**1**).

Element	Weight%	Atomic (%)
C K	57.19	65.49
N K	32.76	32.16
Cl K	4.03	1.56
Pd L	6.02	0.78
Total		100.0

Table 2.1 Percentage composition data from EDX analysis (precatalyst).

2.2.2. Synthesis of substituted aromatic derivatives of different olefins via Heck-Mizoroki reaction

Aryl halide (bromide) and activated olefin (methyl acrylate) were mixed in a reaction tube followed by the addition of base (potassium carbonate), additive (tetra-n-butyl ammonium bromide) and catalyst, complex (**1**) in dioxane. Very low conversion of the reaction was observed when dioxane was used as a solvent. Then the reaction was optimized in dimethylacetamide (DMA) solvent. The role of additive in Heck reaction is not fully understood but the plausible hypothesis is that it inhibits the formation of inactive palladium-black and deliver the active ligand to the free palladium(0) species into the catalytic cycle. Sometimes, it can also act as a phase transfer catalyst mostly in H_2O/DMF reaction medium.

The reaction mixture was heated up to 90 ^{o}C- 110 ^{o}C for about 10 h followed by workup in ether. The progress of the reaction was monitored by checking the TLC of the reaction mixture.

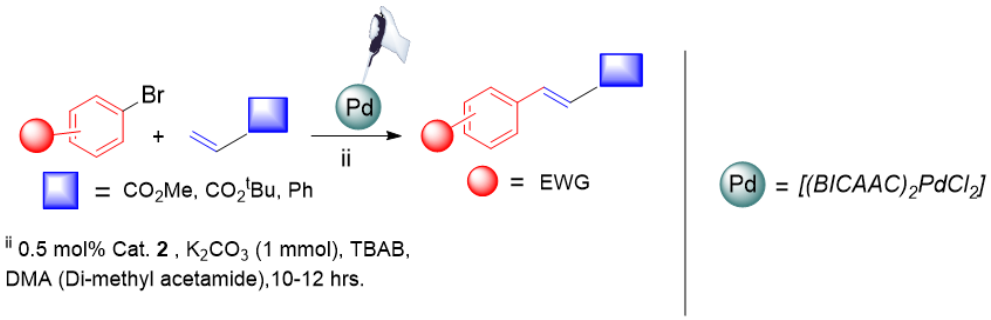

Scheme 2.7 Optimized reaction scheme of Heck-Mizoroki reaction.

Varieties of substrates were screened with different electron withdrawing moiety in the aryl part. The products were clearly characterized by the coupling constant value (*J*) of the *trans* hydrogen (*16 Hz)* of the coupled product at around 6.4-6.5 ppm region in ^{1}H NMR spectra. No *cis* product was observed at all. The feasibility of the reaction was extended to *ortho*, *meta* and *para* substituents in the aromatic part and found to be active in all the cases (Fig. 2.12).

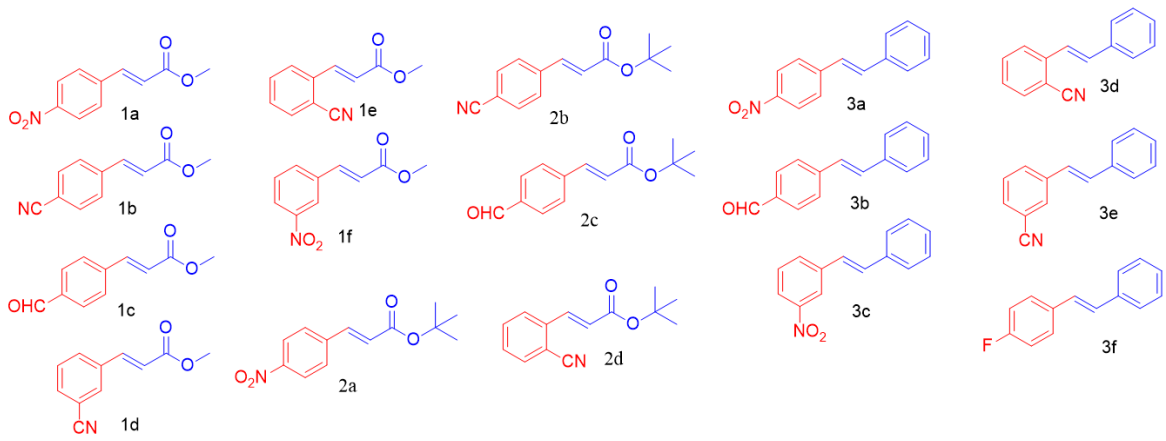

Fig. 2.12 Substrates scope of Heck-Mizoroki reaction.

Then the activated olefin was modified with different substituents to investigate whether there is any influence on the reaction rate or the yield but significant change was not observed. Good to moderate yield was observed in every case (Table 2.2).

Entry	[Pd]mol%	t (h)	Yield (%)
1a	0.5 mol%	12	78
1b	0.5 mol%	12	71
1c	0.5 mol%	12	81
1d	0.5 mol%	12	76
1e	0.5 mol%	12	78
1f	0.5 mol%	12	83
2a	0.5 mol%	12	81
2b	0.5 mol%	12	74
2c	0.5 mol%	12	82

Entry	[Pd]mol%	t (h)	Yield (%)
2d	0.5 mol%	12	75
3a	0.5 mol%	10	81
3b	0.5 mol%	10	83
3c	0.5 mol%	10	80
3d	0.5 mol%	10	75
3e	0.5 mol%	10	77
3f	0.5 mol%	10	73

Table 2.2 Substrate screening and catalytic performance of Pd-complex in Heck reaction.

Interestingly, once the reaction was over, we observed some material to be precipitated out at the bottom of the reaction mixture. We were curious to

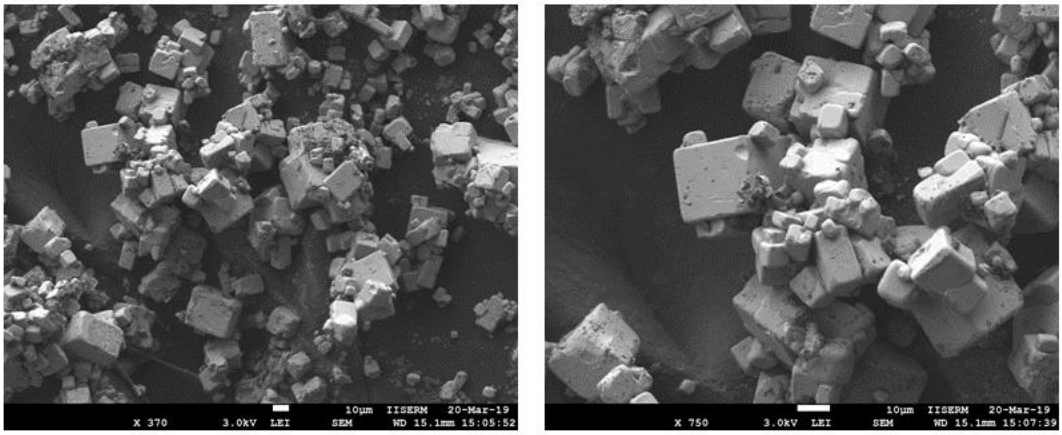

Fig. 2.13 SEM image of recovered material after catalysis (Heck reaction).

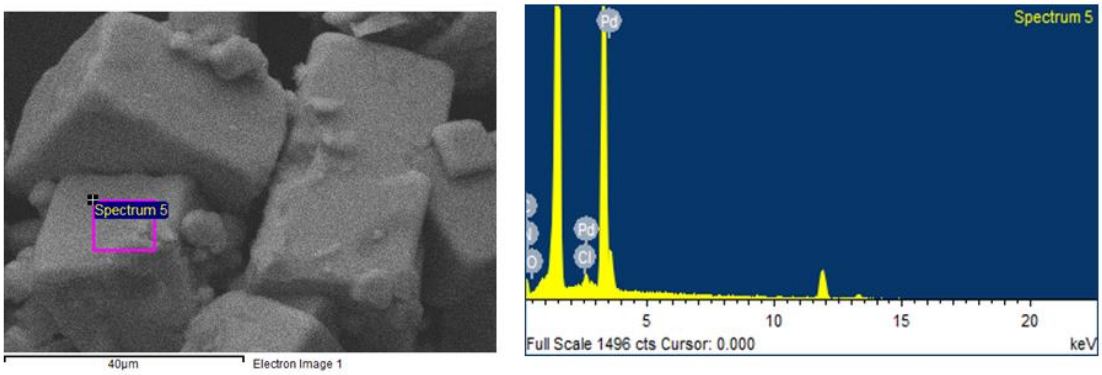

Fig. 2.14 EDX spectrum of recovered materials after the catalysis (Heck reaction).

Element	Weight %	Atomic (%)
C K	39.44	56.56
N K	28.88	35.51
OK	18.00	16.31
Cl L	4.05	1.66
Pd	6.58	0.90
Total	100.0	

Table 2.3 Percentage composition data from EDX analysis (Heck reaction).

investigate the nature of the ppt. and what would be the fate of the catalyst once the reaction is over. To probe these, the SEM and EDX measurements have also been performed after the catalysis where 4-bromo nitrobenzene and methyl acrylate were chosen as coupling partner, in a model reaction. The block shape morphology was observed from the SEM images. Since the recovered material exhibited no catalytic activity during the coupling reactions, it was concluded that Pd nanoparticle was not the active species, which catalyzes the reaction in this case. The Hg-drop test was performed following the literature.[11] The formation of the product in significant amount was observed by ^{1}H NMR spectroscopy, even in the presence of Hg.

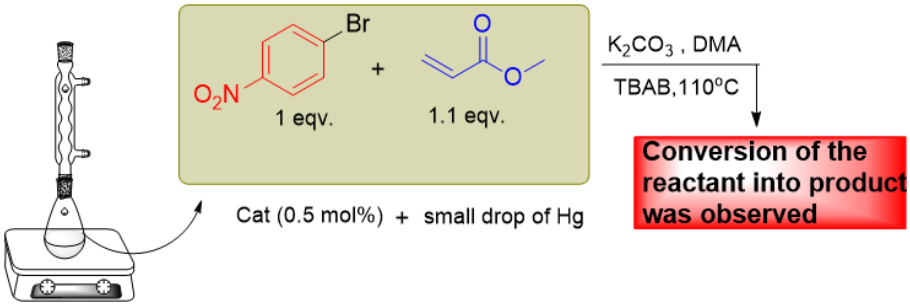

Fig. 2.15 Hg-drop test experiment.

2.2.3. Synthesis of biaryl derivatives via Suzuki-Miyura reaction

Aryl halide (bromide) and phenylboronic acid were mixed in a reaction tube followed by the addition of base K_2CO_3 (potassium carbonate) and catalyst (complex **1**). The reaction was optimized in dimethyl acetamide (DMA) solvent under refluxing condition. Then the reaction was stirred for about 10-11 h at 90-110 ^oC followed by the work up. The progress of the reaction was monitored by checking the TLC of the reaction mixture.

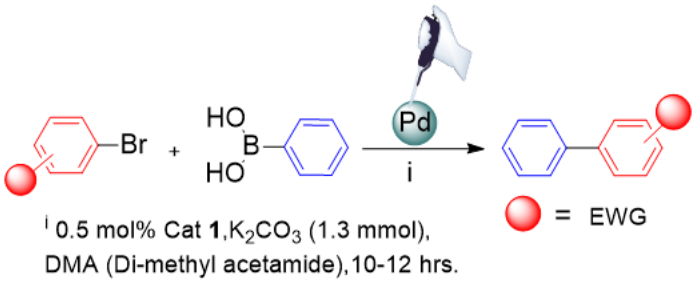

Scheme 2.8 Optimized reaction scheme of Suzuki-Miyaura reaction.

The feasibility of the reaction was extended to *ortho*, *meta* and *para* substituents in the aromatic part and found to be active in all the cases.

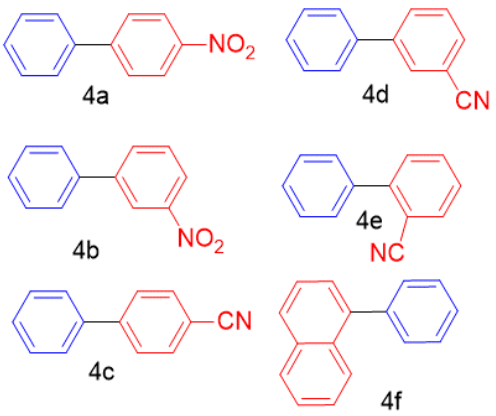

Fig. 2.16 Substrate scope of Suzuki-Miyaura reaction.

All the products have been characterized by the ^1H NMR spectroscopy and further matched with literature reports. Here also, we observed the precipitation material.

Entry	[Pd]	t (h)	Yield (%)
4a	0.5 mol%	10	85
4b	0.5 mol%	10	82
4c	0.5 mol%	10	88
4d	0.5 mol%	10	85
4e	0.5 mol%	10	82
4f	0.5 mol%	10	72

Table 2.4 Substrate screening and catalytic performance of Pd-complex in Suzuki reaction.

The material was recovered and analysed by SEM and EDX method where 4-bromo nitrobenzene and phenylboronic acid have been chosen as coupling partner, as a model reaction. The block shape morphology has been observed in a similar manner as we observed in the previous coupling reaction.

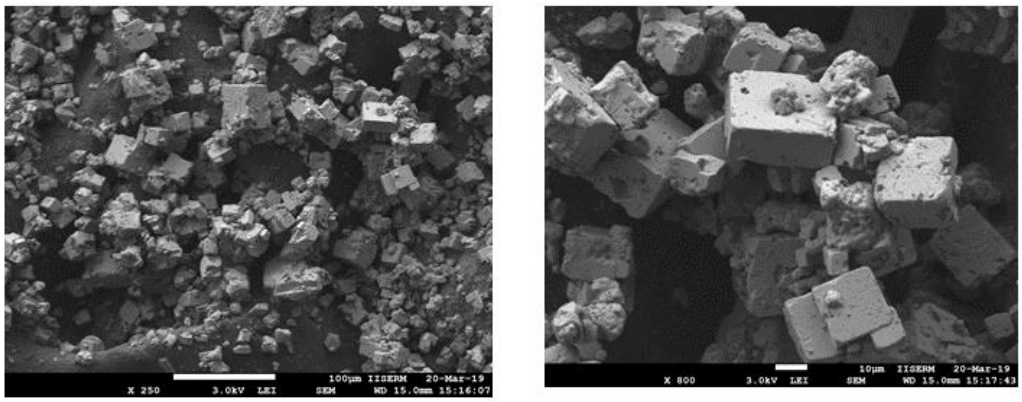

Fig. 2.17 SEM image of recovered materials after the catalysis (Suzuki reaction).

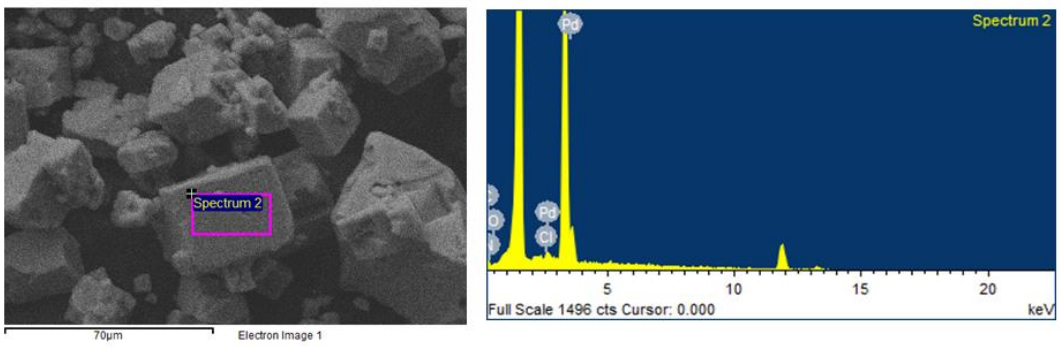

Fig. 2.18 EDX spectrum of the recovered materials after the catalysis (Suzuki reaction).

Element	Weight %	Atomic (%)
C K	42.41	51.18
N K	28.95	29.95
OK	18.00	16.31
Cl L	4.05	1.66
Pd	6.58	0.90
Total	100.0	

Table 2.5 Percentage composition data from EDX analysis (Suzuki reaction).

Here also, we can conclude that, this is not the same material that catalyzes the reaction and if it is Pd nanoparticle or clusters then it is not the active catalyst, which was further supported by Hg-drop test. The UV-Vis spectrum of the recovered material has been recorded to check the existence of Pd-carbene complex. From the UV-Vis., only the intra ligand charge transfer ILCT was observed which depicts that there is no carbene-metal complex once the catalysis is

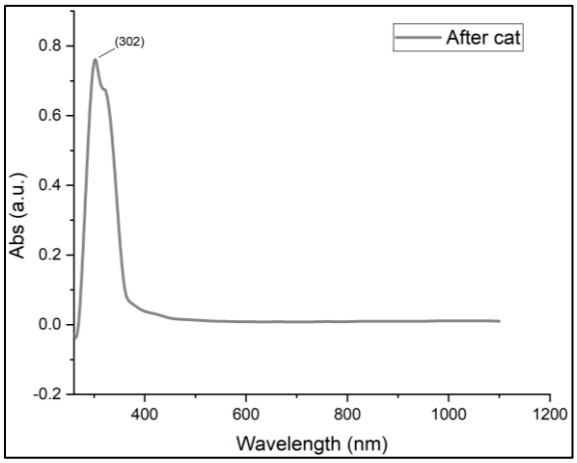

Fig. 2.19 UV-Vis spectrum of the recovered material after catalysis.

over, as there is no metal to ligand charge transfer (MLCT) observed. The ILCT observed in the spectrum might be due to the dissociated ligand recovered after the reaction. Therefore, from the above discussion, it may be concluded that the reactions happen in a homogeneous fashion.

2.3 Conclusions

In summary, we have synthesized and characterized the first bicyclic (alkyl)(amino) carbene palladium complex [*(BICAAC)$_2$PdCl$_2$*] by different spectroscopic and analytical techniques. Formation of *cis* and *trans* isomer of the palladium complex have been observed in ^{13}C NMR spectroscopy but only the *trans* isomer was isolated via single crystal X-ray diffraction. The [*(BICAAC)$_2$PdCl$_2$*] complex was investigated as a pre-catalyst for C-C coupling reactions. Heck-Mizoroki and Suzuki-Miyura reactions have been screened so far with broad substrate scope irrespective of the *ortho, meta* and *para* substituents in the aryl part with good to moderate yield. This [*(BICAAC)$_2$PdCl$_2$*] complex is found to have better catalytic activity with the low catalyst loading as compared to the previously reported carbene Pd(II)-chloride complexes.

2.4 Experimental Section

2.4.1 General procedure

All syntheses were carried out under an inert atmosphere of dry nitrogen in oven-dried glassware using standard Schlenk techniques or a glove box where O_2 and H_2O levels were maintained. All the glassware was dried at 150 °C in an oven for at least 12 h and assembled hot and cooled in vacuo prior to use. Solvents were purified by MBRAUN solvent purification system MB SPS-800 and were used directly from the SPS system. For NMR, $CDCl_3$ was purchased from Merck and CIL. High-resolution mass spectrometry was performed with a Waters SYNAPT G2–S instrument. The ^{1}H and ^{13}C NMR spectra were recorded with a Bruker 400 MHz spectrometer with TMS as an external reference; chemical shift values are reported in ppm. For absorption spectroscopy measurement, LABINDIA UV-Vis Spectrophotometer 3000+ was used. SEM and EDX analysis were performed with JEOL JSM 7600F Field Emission Electron Microscope.

2.4.2 Starting material

All chemicals were purchased from Merck and used without further purification. *2,6-Diisopropylaniline* was distilled before making the starting material. The bicyclic (alkyl)(amino) carbene was prepared following the literature procedure reported by G. Bertrand *et al.*[12]and was characterized well in each time by NMR and IR method.

2.4.3 Single crystal X-ray structural determination

Single crystal X-ray diffraction data for *trans-[(BICAAC)$_2$PdCl$_2$]* was collected using a RigakuXtaLAB mini diffractometer equipped with Mercury375M CCD detector. The data was collected with graphite monochromatic MoKα radiation (λ = 0.71073 Å) at 100.0(2) K using scans. During the data collection the detector distance was 50 mm (constant) and the detector was placed at 2θ = 29.85° (fixed) for all the data sets. The data collection and data reduction were done using Crystal Clear suite [10a]. The crystal structure was solved by using either OLEX2 [10b] and the structure was refined using SHELXL-97 2008[c]. All non-hydrogen atoms were refined anisotropically. The graphic was generated using Mercury 3.9.

2.4.4 Synthetic procedure

Synthesis of BICAAC: *[BICAACH]$^+$[BF$_4$]$^-$* salt (0.80 g, 2.00 mmol) was dissolved in THF (15 mL) and cooled to -20 ºC for 5-10 minutes in a glove-box. This was followed by the addition of potassium bis(trimethylsilyl)amide, KHMDS (0.42 g, 2.10 mmol) to this solution and stirred for about 2-3 h. Subsequently, all volatiles were removed under vacuum and hexane (30 mL) was added to this residue to extract the carbene formed. Removal of hexane under vacuum (5-6 h) afforded free carbene as a white crystalline powder in 65% yield.

Synthesis of [(BICAAC)$_2$PdCl$_2$] (1): BICAAC (0.15 g, 0.50 mmol) was dissolved in THF (10 mL) and subsequently solid palladium chloride (0.04 g, 0.25 mmol) was added to this solution. The resulting mixture was stirred for about 10-12 h (preferably overnight). This was followed

by removal of all volatiles under vacuum and washing of the resulting residue with hexane (15 mL). Drying of the residue under vacuum afforded the titled compound as a brown powder. Recrystallization from toluene gave the product in 78 % yield. **MP**: 240 ^{o}C. **^{1}H NMR** (400 MHz, $CDCl_3$): δ = 7.38 (t, 3H, pAr-H, $^{3}J_{H-H}$ = 8 Hz), 7.22 (d, 3H, mAr-H, $^{3}J_{H-H}$ = 8 Hz), 3.25(sept, 1H, $CH(CH_3)_2$, $^{3}J_{H-H}$ = 8Hz), 3.12 (sept, 1H, $CH(CH_3)_2$, $^{3}J_{H-H}$ = 8Hz), 2.85 (sept, 1H, $CH(CH_3)_2$, $^{3}J_{H-H}$ = 8Hz), 2.54 (br d, 1H, $CH(CH_3)_2$), 1.49 (m, 3H), 1.47 (m, 5H), 1.24 (m, 14H), 1.22 (br, 20H), 0.98 (m, 9H), 0.96(s, 2H), 0.76 (m, 2H) ppm. **^{13}C NMR** (100 MHz, $CDCl_3$) of **1**: δ = 263.0, 259.2, 146.5, 140.1, 128.0, 124.4, 86.0, 77.4, 65.3, 53.2, 43.3, 37.6, 30.5, 24.8, 22.6, 19.8 ppm. **HRMS (AP^{+})**: *m/z* calculated for $C_{44}H_{66}PdCl$: (763.3962); $[M-Cl]^{+}$: found : (763.3917).

General Method for Heck Mizoroki Reaction: In a typical reaction, a mixture of aryl bromide (2.0 mmol), substituted olefin (2.2 mmol), K_2CO_3 (1.0 mmol), TBAB (10 mol %), complex **1** (0.5 mol %) and solvent, DMA (4 mL) was added into microwave vials and heated up to 110 ^{o}C for about 10-12 h in silicon oil bath. Then the reaction mixture was dissolved in 20 mL of water and extracted in diethyl ether (10 mL × 3). The organic layer was dried over anhydrous $MgSO_4$. The solvent was removed in vacuum and the crude product was purified using column (silica 100-200) chromatography.

General Method for Suzuki Reaction: In a typical reaction, a mixture of aryl bromide (2.0 mmol), phenyl boronic acid (2.2 mmol), K_2CO_3 (1.0 mmol), complex **1** (0.5 mol %) and solvent, DMA (4 mL) was added into microwave vials and heated up to 110 ^{o}C for about 10-12 h in silicon oil bath. Then the reaction mixture was dissolved in 20 mL of water and extracted in diethyl ether (10 mL × 3). Organic layer was dried over anhydrous $MgSO_4$. The solvent was removed in vacuum and crude product was purified using column (silica 100-200) chromatography.

2.4.5 NMR data for Heck reaction:

***trans*-4-nitrocinnamic acid methyl ester 1a**

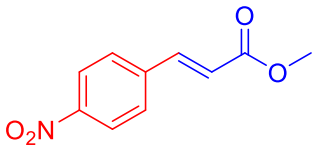

^{1}H NMR (400 MHz, $CDCl_3$), δ: 8.27 (d, 2H, $^{3}J_{H-H}$ = 8 Hz, Ar-H), 7.74 (d, 1H, $^{3}J_{H-H}$ = 16 Hz, alkene), 7.68 (d, 2H, $^{3}J_{H-H}$ = 8 Hz, Ar-H), 6.58 (d, 1H, $^{3}J_{H-H}$ = 16 Hz, alkene) , 3.84 (s, 3H, OCH_3) ppm.

^{13}C NMR (100 MHz, $CDCl_3$), δ: 165.4, 142.1, 132.9, 130.2, 128.9, 125.3, 124.4, 122.0, 52.0 ppm.

***trans*-4-cyanocinnamic acid methyl ester 1b**

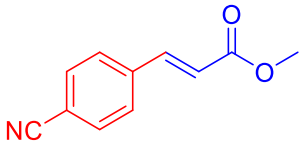

^{1}H NMR (400 MHz, $CDCl_3$), δ: 7.69- 7.60 (m, 5H, alkene & Ar-H), 6.54 (d, 1H, $^{3}J_{H-H}$ = 16 Hz, alkene), 3.83 (s, 3H, OCH_3) ppm.

^{13}C NMR (100 MHz, $CDCl_3$), δ: 166.6, 142.6, 138.7, 133.3, 133.1, 128.3, 121.6, 118.3, 52.2 ppm.

***trans*-4-formylcinnamic methyl ester 1c**

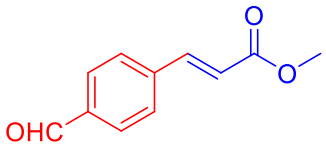

^{1}H NMR (400 MHz, $CDCl_3$), δ: 10.01(s, 1H, CHO), 7.90 (d, 2H, $^{3}J_{H-H}$ = 8 Hz, Ar-H), 7.72 (d, 1H, $^{3}J_{H-H}$ = 16 Hz, Alkene), 7.68 (d, 2H, $^{3}J_{H-H}$ = 8 Hz, Ar-H), 6.56 (d, 1H, $^{3}J_{H-H}$ = 16 Hz, Alkene) , 3.82 (s, 3H, OCH_3) ppm.

^{13}C NMR (100 MHz, $CDCl_3$) δ: 191.8, 167.2, 143.5, 140.4, 137.5, 130.5, 128.9, 121.3, 52.4 ppm.

***trans*-3-cyanocinnamic methyl ester 1d**

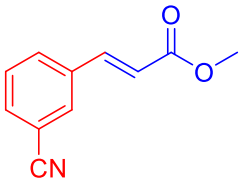

^{1}H NMR (400 MHz, $CDCl_3$), δ: 7.72 (d, 2H), 7.59 (d, 1H, $^{3}J_{H-H}$ = 16 Hz, Alkene), 7.51(d, 1H), 7.36 (m, 2H), 6.50 (d, 1H, $^{3}J_{H-H}$ = 16 Hz, Alkene), 3.81 (s, 3H, OCH_3) ppm.

^{13}C NMR (100 MHz, $CDCl_3$) δ: 166.7, 142.1, 136.2, 134.8, 130.8, 122.9, 120.5, 117.4, 114.2, 52.1 ppm.

***trans*-2-cyanocinnamic methyl ester 1e**

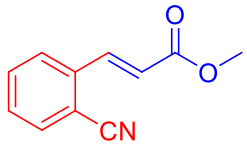

^{1}H NMR (400 MHz, $CDCl_3$) δ: 7.97(d, 1H, $^{3}J_{H-H}$ = 16 Hz, alkene), 7.71 (m, 2H), 7.44 ((m, 2H)), 6.57 d, 1H, $^{3}J_{H-H}$ = 16 Hz, alkene, 3.82 (s, 3H, OCH_3) ppm.

^{13}C NMR (100 MHz, $CDCl_3$) δ: 166.3, 139.6, 137.3, 134.3, 133.2, 130.2, 127.7, 125.3, 122.6, 117.2, 115.8, 112.7, 52.1 ppm.

***trans*-3-nitrocinnamic methyl ester 1f**

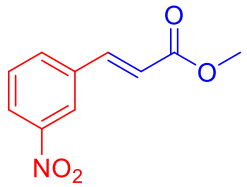

^{1}H NMR (400 MHz, $CDCl_3$) δ: 8.34(s, 1H), 8.16 (d, 2H), 7.57 (d, 1H, $^{3}J_{H-H}$ = 16 Hz, alkene), 6.52 (d, 1H, $^{3}J_{H-H}$ = 16 Hz, alkene), 3.81 (s, 3H, OCH_3) ppm.

^{13}C NMR (100 MHz, $CDCl_3$) δ: 166.6, 148.7, 142.0, 137.7, 133.7, 130.0, 126.7, 124.6, 122.4, 120.9, 52.1 ppm.

***trans*-4-nitrocinnamic ^{t}Butyl ester 2a**

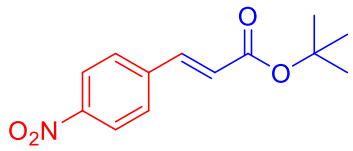

^{1}H NMR (400 MHz, $CDCl_3$) δ 8.25 (d, 2H, J= 8 Hz, ArH), 7.70-7.63 (m, 3H, ArH, =CH), 6.51 (d, 1H, 3*J* d, 1H, $^{3}J_{H-H}$ = 16 Hz, alkene), 1.54 (s, 9H, -O^{t}Bu) ppm.

^{13}C NMR (100 MHz, $CDCl_3$) δ 165.4, 140.7, 132.7, 130.4, 128.6, 125.1, 124.2, 81.5, 28.3 ppm.

***trans*-4-cyanolcinnamic ^{t}Butyl ester 2b**

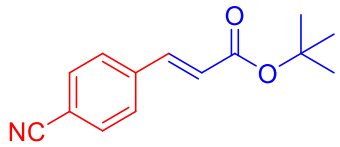

^{1}H NMR (400 MHz, $CDCl_3$) δ: 7.67-7.57 (m, 5H, Ar-H & =CH), 6.46 (d, 1H, $^{3}J_{H-H}$ = 16 Hz, alkene), 1.53 (s, 9H, -O^{t}Bu) ppm.

^{13}C NMR (100 MHz, $CDCl_3$) δ: 165.5, 141.2, 133.5, 132.7, 128.3, 123.9, 118.5, 81.3, 28.2 ppm.

***trans*-4-formylcinnamic ^{t}Butyl ester 2c**

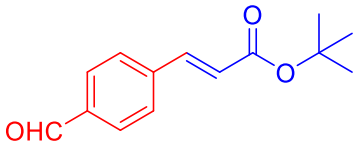

^{1}H NMR (400 MHz, $CDCl_3$) δ: 10.01 (s, 1H, CHO), 7.74 (s, 1H), 7.69 (m, 4H), 7.64 (d, 1H, $^{3}J_{H-H}$ = 16 Hz, alkene), 6.50 d, 1H, $^{3}J_{H-H}$ = 16 Hz, alkene), 1.54 (s, 9H, -O^{t}Bu) ppm.

^{13}C NMR (100 MHz, $CDCl_3$) δ: 191.2, 165.7, 141.9, 140.5, 132.5, 131.1, 128.5, 123.5, 81.2, 28.3 ppm.

***trans*-2-cyanocinnamic ^{t}Butyl ester 2d**

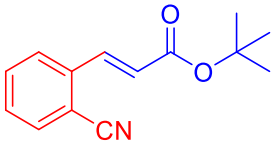

^{1}H NMR (400 MHz, $CDCl_3$) δ: 7.82 (t, 1H), 7.65 (m, 3H), 7.44 (d, 1H), 6.53 (d, 1H, $^{3}J_{H-H}$ = 16 Hz, alkene), 1.52 (s, 9H, -O^{t}Bu) ppm.

^{13}C NMR (100 MHz, $CDCl_3$) δ: 165.0, 138.3, 134.2, 133.1, 127.7, 117.1, 81.2, 28.0 ppm.

4-nitrostilbene 3a

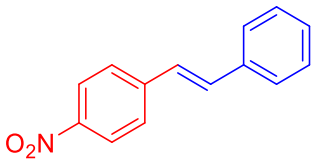

^{1}H NMR (400 MHz, $CDCl_3$) δ: 8.23 (d, 2H, J= 8 Hz, ArH), 7.70 (d, 2H, J= , ArH), 7.65 (d, 2H, ArH), 7.43(t, 2H, ArH), 7.31 (m, 1H, ArH), 7.29 (d, 1H, =CH), 7.16 (d, 1H, =CH) ppm.

^{13}C NMR (100 MHz, $CDCl_3$) δ: 144.3, 136.6, 133.7, 129.3, 127.5, 127.3, 126.7, 125.5, 124.6 ppm.

4-formylstilbene 3b

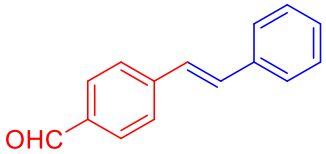

^{1}H NMR (400 MHz, $CDCl_3$) δ: 10.01 (s, 1H, CHO), 7.9 (d, 2H, J= 8 Hz, ArH), 7.75 (d, 2H, J= , ArH), 7.69 (d, 2H, ArH), 7.40(t, 2H, ArH), 7.31 (m, 1H, ArH), 7.33 (d, 1H, =CH), 7.17 (d, 1H, =CH) ppm.

^{13}C NMR (100 MHz, $CDCl_3$) δ: 191.4, 143.8, 136.9, 135.5, 132.8, 131.4, 130.6, 129.2, 127.3, 127.7, ppm.

3-nitrostilbene 3c

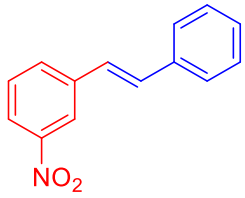

^{1}H NMR (400 MHz, $CDCl_3$) δ: 8.36 (s, 1H), 8.16 (d, 1H), 7.79 (d,1 H), 7.54-7.42 (m,5H), 6.78 (d, 1H, =CH), 6.74 (d, 1H, =CH) ppm.

^{13}C NMR (100 MHz, $CDCl_3$) δ: 148.7, 137.6, 136.9, 130.6, 128.5, 127.8, 126.7, 126.2, 122.1, 113.8 ppm.

2-cyanostilbene 3d

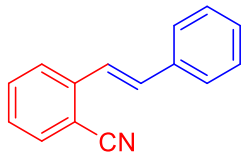

^{1}H NMR (400 MHz, $CDCl_3$) δ: 7.96 (d, 1H), 7.66 (m, 3H) , 7.59 (m, 4H), 7.34 (d, 2H) , 6.72 (d, 1H, =CH) ppm.

^{13}C NMR (100 MHz, $CDCl_3$) δ: 140.4, 136.9, 136.1, 134.3, 133.4, 128.9, 127.1, 126.2, 125.3, 123.9, 118.1, 113.8 ppm.

3-cyanostilbene 3e

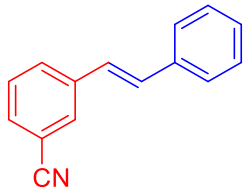

^{1}H NMR (400 MHz, $CDCl_3$) δ: 8.36 (s, 1H), 8.16 (d, 1H), 7.79-7.54 (m, 3H), 7.43 (d, 5H), 6.74 (d, 1H, =CH) ppm.

^{13}C NMR (100 MHz, $CDCl_3$) δ: 148.3, 137.6, 136.7, 135.9, 134.5, 130.5, 128.7, 128.3, 126.6, 126.0, 122.6, 117.1, 113.8 ppm.

4-flurostilbene 3f

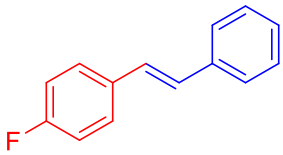

^{1}H NMR (400 MHz, $CDCl_3$) δ: 7.73 (d, 1H), 7.42-7.51 (m, 3H), 7.33 (m, 2H), 7.05 (m, 4H), 6.67 (d, 1H, =CH) ppm.

^{13}C NMR (100 MHz, $CDCl_3$) δ: 163.6, 161.2, 137.2, 133.6, 128.8, 128.0, 127.5, 126.5, 115.8, 115.6 ppm.

2.4.9 NMR data for Suzuki reaction:

4-nitrobiphenyl 4a

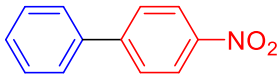

^{1}H NMR (400 MHz, $CDCl_3$) δ: 8.30 (d, J = 8.8 Hz, 2H, ArH), 7.75 (d, J = 8.8 Hz, 2H, ArH) , 7.62 (t, 2H, ArH), 7.52 (m, 3H, ArH) ppm.

^{13}C NMR (100 MHz, $CDCl_3$) δ: 147.6, 138.9, 135.6, 129.1, 128.9, 127.8, 125.0, 124.1 ppm.

3-nitrobiphenyl 4b

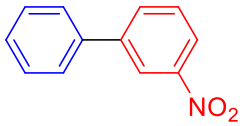

^{1}H NMR (400 MHz, $CDCl_3$) δ: 8.39 (s, 1H), 8.26 (d, 2H), 8.19 (t, 1H), 7.84 (d, 1H), 7.61 (m, 3H), 7.52 (dd, 2H), 7.44 (dd, 2H).

^{13}C NMR (100 MHz, $CDCl_3$) δ: 148.8, 142.9, 137.7, 135.7, 132.8, 130.7, 129.2, 128.1, 126.8, 122.2 ppm.

4-cyanobiphenyl 4c

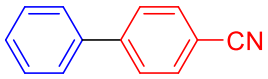

^{1}H NMR (400 MHz, $CDCl_3$) δ: 8.26 (d, 2H, ArH), 7.72 (d, 2H, ArH), 7.62(m, 1H, ArH), 7.53 (d, 2H, ArH), 7.43 (d, 2H, ArH).

^{13}C NMR (100 MHz, $CDCl_3$) δ: 145.8, 139.3, 133.5, 132.7, 129.2, 128.7, 127.8, 127.3, 118.1 ppm.

3-cyanobiphenyl 4d

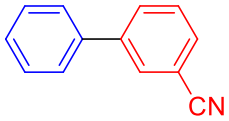

^{1}H NMR (400 MHz, $CDCl_3$) δ: 7.76 (s, 1H), 7.66 (2H, d), 7.51-7.42 (m, 4H), 7.30 (m, 2H) ppm.

^{13}C NMR (100 MHz, $CDCl_3$) δ: 141.8, 138.3, 135.8, 134.3, 130.4, 128.8, 126.7, 122.5, 117.0, 113.7, 112.4 ppm.

2-cyanobiphenyl 4e

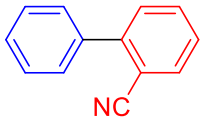

^{1}H NMR (400 MHz, $CDCl_3$) δ: 8.26 (d, 2H), 7.67 (d, 2H), 7.52 (m, 2H), 7.44 (m, 3H) ppm.

^{13}C NMR (100 MHz, $CDCl_3$) δ: 145.5, 138.1, 135.7, 134.4, 133.2, 132.7, 130.1, 128.0, 125.3, 117.2, 111.2 ppm.

4-phenylbiphenyl 4f

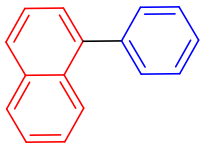

^{1}H NMR (400 MHz, $CDCl_3$) δ: 8.28 (d, 2H), 7.94-7.84 (m, 4H), 7.81 (d, 2H), 7.61-7.54 (m, 3H), 7.33 (d, 1H) ppm.

^{13}C NMR (100 MHz, $CDCl_3$) δ: 140.8, 140.3, 135.7, 134.7, 132.8, 130.0, 128.3, 128.0, 127.2, 126.8, 126.3, 125.8, 125.5, 122.9 ppm.

2.5 Crystallographic data for *trans-[(BICAAC)$_2$PdCl$_2$]* (1)

Compound[a]	*trans*-[(BICAAC)$_2$PdCl$_2$] **(1)**
Chemical formula	$C_{44}H_{66}Cl_2N_2Pd$
Molar mass	800.28
Crystal system	monoclinic
Space group	$P2_1/n$
T [K]	100.0(10)
a [Å]	13.292(3)
b [Å]	11.9062(14)
c [Å]	14.850(2)
α [°]	90.00
β [°]	102.791(8)
γ [°]	90.00
V [Å^3]	2291.9(6)
Z	4
D(calcd.) [g·cm^{-3}]	1.160
μ(Mo-K_α) [mm^{-1}]	0.550
Reflections collected	24334
Independent reflections	5261
Data/restraints/parameters	5261/0/114
$R1$,$wR_2[I>2\sigma(I)]$[a]	0.1022, 0.2701
R1, wR$_2$ (all data)[a]	0.1211, 0.2921
GOF	1.11

[a] $R1 = \Sigma||Fo| - |Fc||/\Sigma|Fo|$. $wR_2 = [\Sigma w(|Fo^2| - |Fc^2|)^2/\Sigma w|Fo^2|^2]^{1/2}$

2.6 References

1. Smith, J. M.; Long, J. R. *Inorg. Chem*, **2010**, *49*, 11223-11230.
2. Liu, B.; Zhang, Y.; Xua, D.; Chen, W. *Chem. Commun*. **2011**, *47*, 2883-2285.
3. Liu, B.; Xia, Q.; Chen, W. *Angew. Chem., Int. Ed*. **2009**, *48*, 5513-5516.
4. Enders, D.; Breuer, K.; Raabe, G.; Runsink, J.; Teles, J. H.; Melder, J. P.; Ebel, K.; Brode, S. *Angew. Chem., Int. Ed. Engl.* **1995**, *34*, 1021-1023.
5. Zhang, W. B.; Yang, X. T.; Ma, J. B.; Su, Z. M.; Shi. S. L; *J. Am. Chem. Soc*. **2019**, *141* (14), 5628–5634.
6. Cao, Z. C.; Xie, S. J.; Fang, H.; Shi, Z. J. *J. Am. Chem. Soc*., **2018**, *140* (42), 13575-13579.
7. Eckhardt M.; Gregory C. Fu. *J. Am. Chem. Soc*. **2003**, *125*, 13642-13643.
8. Marion, N.; Nolan, S. P. *Acc. Chem. Res.* **2008**, *41*, 1440–1449.
9. Lebel, H.; Janes, M. K.; Charette, A. B.; Nolan, S. P. *J. Am. Chem. Soc.* **2004**, *126*, 5046-5047.
10. (a) *CrystalClear 2.0*; Rigaku Corporation: Tokyo, Japan, 2013. (b) Dolomanov, O. V.; Bourhis, L. J.; Gildea, R. J.; Howard, J. A. K.; Puschmann, H. *J. Appl. Crystallogr*. **2009**, *42*, 339-341. (c) Sheldrick, G. M. *Acta Cryst. A* **2015**, *71*, 3-8.
11. Rishu,; Prashanth, B.; Bawari, D.; Mandal, U.; Verma, A.; Choudhury, A. R.; Singh, S. *Dalton Trans.* **2017**, *46*, 6291-6302.
12. Mendivil, E. T.; Hansmann, M. M.; Weinstein, C. M.; Jazzar, R.; Melaimi, M.; Bertrand, G. *J. Am. Chem. Soc.* **2017**, *139 (23)*, 7753-7756.

Chapter 2

Complexes of mono and bis carbene copper in their different oxidation states: Syntheses and Characterization

Abstract: The syntheses and some photo-physical studies of bicyclic (alkyl)(amino) carbene- copper complex [(BICAAC)CuX] have been demonstrated in this chapter. The complexes were synthesized starting from CuX (X = Cl, I). The complex formation was further confirmed by following ^{1}H, ^{13}C NMR and HRMS. The neutral Cu(I) and cationic Cu(I) complexes have been structurally confirmed by single crystal X-ray diffraction technique. The neutral mononuclear copper complex stabilized by two unit of bicyclic (alkyl)(amino) carbene was attempted to synthesize starting from their carbene coordinated monohalide salt followed by *in situ* reduction with potassium graphite (KC_8) reduction and was characterized by magnetic properties, absorption spectroscopy and HRMS of the complex.

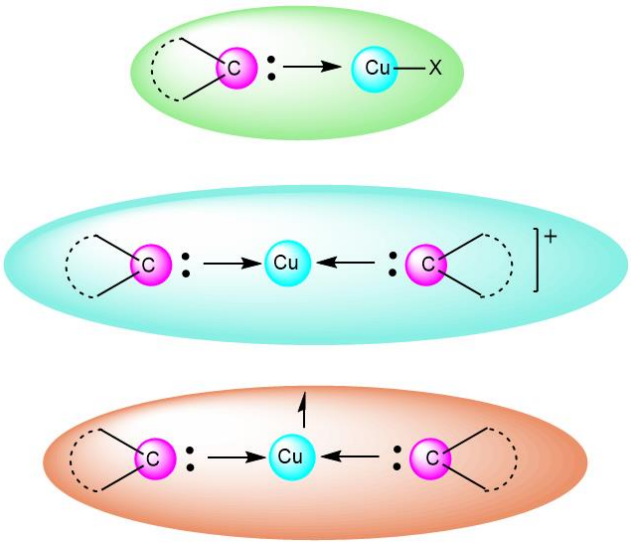

3.1 Introduction

Copper has a long history in chemistry particularly in coordination chemistry. It is one of the transition metals frequently found at the active site of different proteins. Copper is the main constituent of some of the biologically active compounds such as catechol oxidase, tyrosinase superoxide dismutase etc. The functions of these copper compounds involve oxidation, reduction, disproportionation, electron transfer, dioxygen transport and oxygenation in biological systems.

Nevertheless, N-heterocyclic carbene (NHC)-copper complexes have been known and studied well only last 20 years since Arduengo *et al.* first reported NHC-copper system in 1993[1] soon after the isolation of a free NHC (IAd) and opened up the a very promising field of catalytic chemistry. Raubenheimer *et al.* reported a neutral copper complex just one year later.[2] After that, NHC-copper chemistry has not attracted much attention for several years. It was only the beginning of the 2000s when the chemistry of copper with carbenes gained new recognition in organometallic chemistry. Eastham and co-workers reported the first use of Cu_2O for the synthesis of NHC-copper complex.[3] Then Fraser and Woodward reported the first catalytic application of NHC-copper complex in the conjugate addition of $ZnEt_2$ to enones.[4] Then, in 2003, the first well-defined NHC-copper catalysis was published by Buchwald and co-workers.[5] The first example of NHC-copper complexes in catalysis were analogues of the phosphine bearing species.

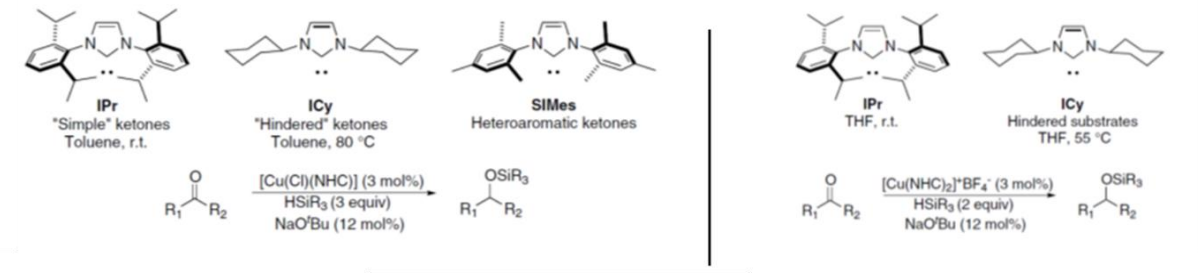

Fig. 3.1 Catalytic activity comparison of NHC-Copper complexes.[6]

It was also established that the bis-NHC-copper complexes are more efficient than the neutral analogues under the same reaction condition (Fig. 3.1). The bis-NHC complex can catalyze the reaction even at lower temperature, reduced catalyst loading and shorter reaction time.[6] The electronic and steric properties of NHCs are easily tuneable (abnormal, chiral, unsymmetrical etc.) which made them an ideal candidates for various applications. The properties, stability and low cost of copper also make it a proper choice for catalysis. Based on that several systems have been developed which show the high stability towards moisture, air and temperature.

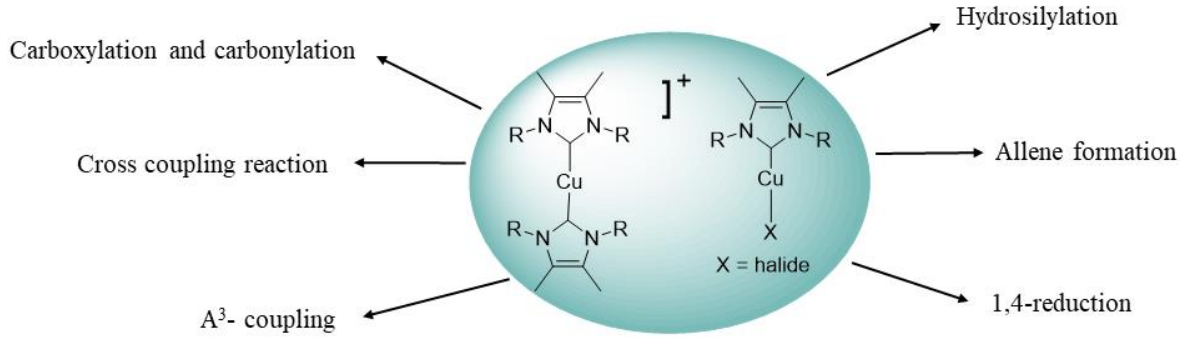

Fig. 3.2 Some important catalysis by NHC-copper complexes.

All copper-complexes were efficiently used opening new possibilities in the catalytic process in the area organometallic chemistry (Fig. 3.2).

Now, replacement of NHCs by cyclic (alkyl)(amino) carbene has shown improvement in catalysis as well as stabilization of transition metals in their different oxidation states low valent as well as high valent. Roesky *et al.* have reported a dimeric Cu^{I} and Cu^{0} complexes stabilized by cAAC ligand (Scheme 3.1).[7] Owing to the unusual electronic properties of cAACs as compared to NHCs, they appear to be a very attractive ligand for photoactive Cu(I) materials. Luminescent Cu(I) complexes have received great attention for their use in the application as organic light emitting diodes (OLEDs), solar energy conversion and in biological

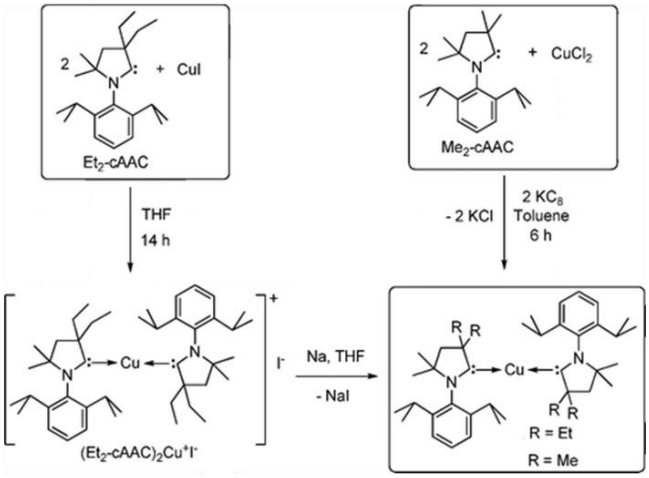

Scheme 3.1 Synthetic strategy for cAAC- copper complexes.[7]

systems. Due to low cost relative to heavier transition metals like platinum and iridium, Cu(I) complexes have been considered as a better alternative in the case of OLEDs.[8,9]

Following the intention, we also synthesized mono and bis bicyclic (alkyl)(amino) carbene coordinated copper(I) complex with different halides (Scheme 3.2). Now, copper halide can react with carbenes in a different mode, either it can form the neutral mono carbene adduct or the cationic Cu complex by the disproportionation reaction (mostly in polar solvent), which have been observed and studied well with NHC and cAAC.[10]

In continuation of our efforts in Cu-BICAAC chemistry, we also attempted to make the zero valent copper complex stabilized by bicyclic (alkyl)(amino) carbene. Starting from the Cu(I) complex and *in situ* reduction by KC_8 was adopted to obtain the [$(BICAAC)_2Cu$] complex (Scheme 3.3). Formation of this copper(0) complex was further confirmed by HRMS, magnetic properties and absorption spectroscopy.

3.2. Results and Discussion

3.2.1 Synthesis of [(BICAAC)CuCl] (1)

Bicyclic (alkyl)(amino) carbene (BICAAC) was dissolved in THF followed by the addition of solid copper(I) chloride (CuCl) (white powder) and the reaction mixture was stirred at room temperature for 12 h in the glove box (Scheme 3.4). The progress of the reaction was observed by the colour changes from light yellow to greenish. Then all the volatiles were removed under vacuum and the reaction mixture was washed with hexane and further characterized by different analytical techniques.

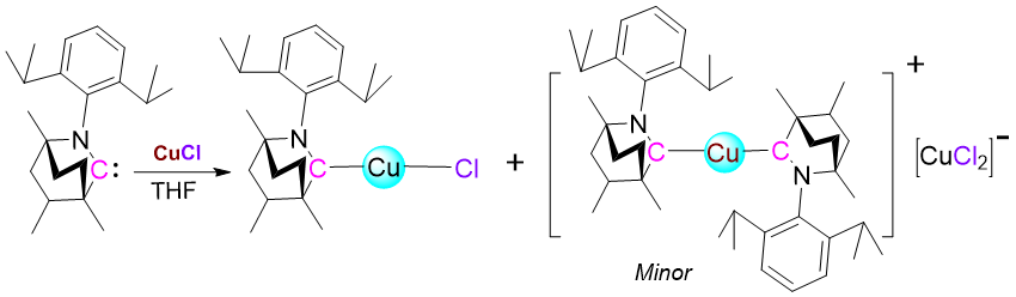

Scheme 3.2 Synthesis of ***[BICAAC-CuCl]*** **(1)**.

The shifting of the two septets in ^{1}H NMR (Fig. 3.3) spectrum, from 3.27 and 2.95 ppm (in case of free carbene) to 2.96 and 2.63 ppm respectively could be the effect of the adduct formation. Along with that, we also observed a sharp signal at 257.2 ppm in the ^{13}C NMR spectrum, which clearly depicts the M-$C_{carbene}$ bond formation. The solid product was dissolved in dichloromethane and left for crystallization. The HRMS spectrum is also in accordance with the complex [(BICAAC)CuCl] shown in Fig. 3.6. Surprisingly, along with the expected signal, another signal was also observed at *m/z* = 820.3124 that corresponds to the bis adduct of the Cu(I) complex, $[M+2H]^{+}$ where M= $[(BICAAC)CuCl]_2$ likely by the disproportionation reaction. This type of symmetric metathesis product formation was previously observed with NHC and cAAC also.[10]

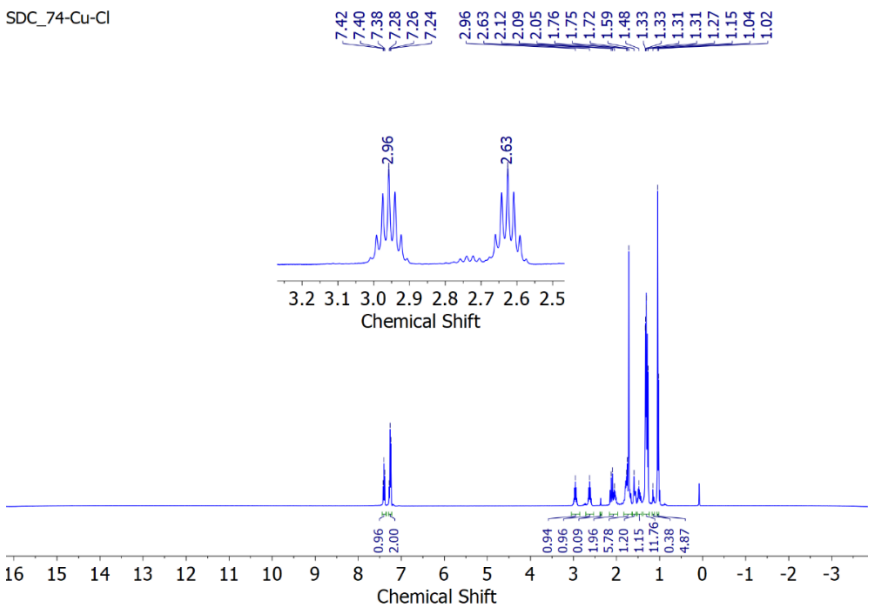

Fig. 3.3 ^{1}H NMR spectrum of ***[BICAAC-CuCl]*** **(1)** (400 MHz, $CDCl_3$).

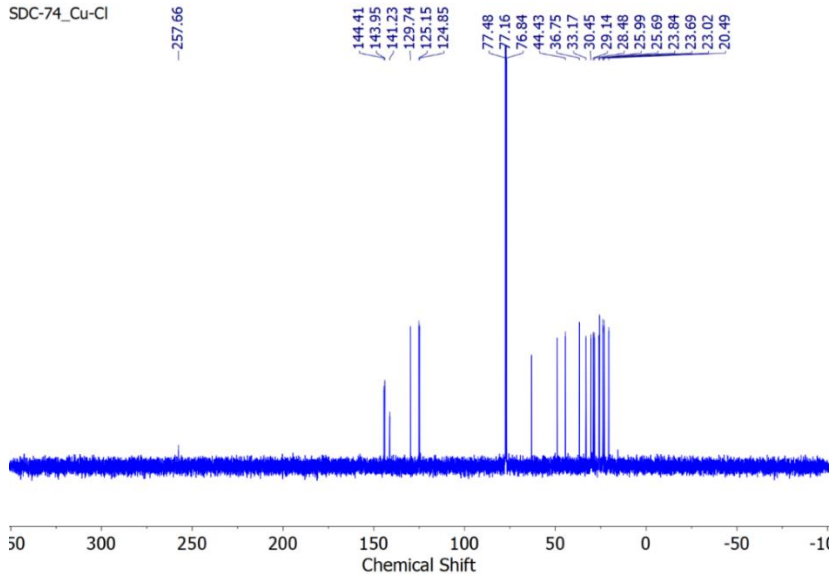

Fig. 3.4 ^{13}C NMR spectrum of ***[BICAAC-CuCl]*** **(1)** (100 MHz, $CDCl_3$).

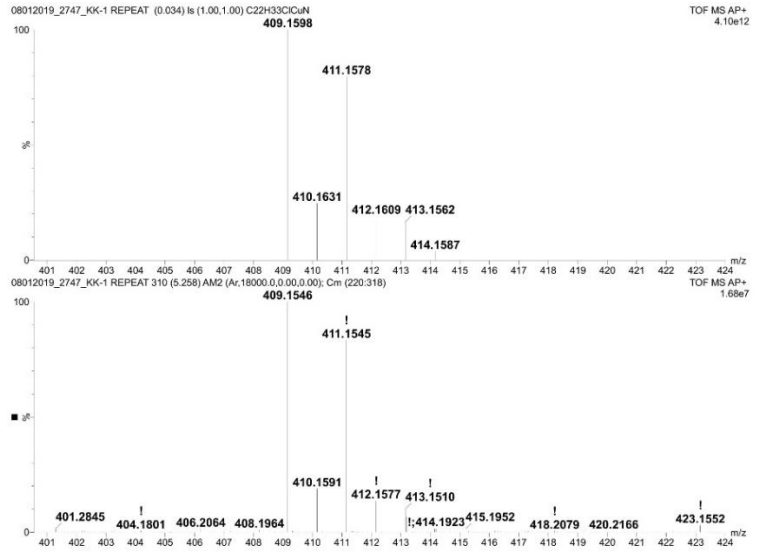

Fig. 3.5 HRMS of ***[BICAAC-CuCl]*** **(1).**

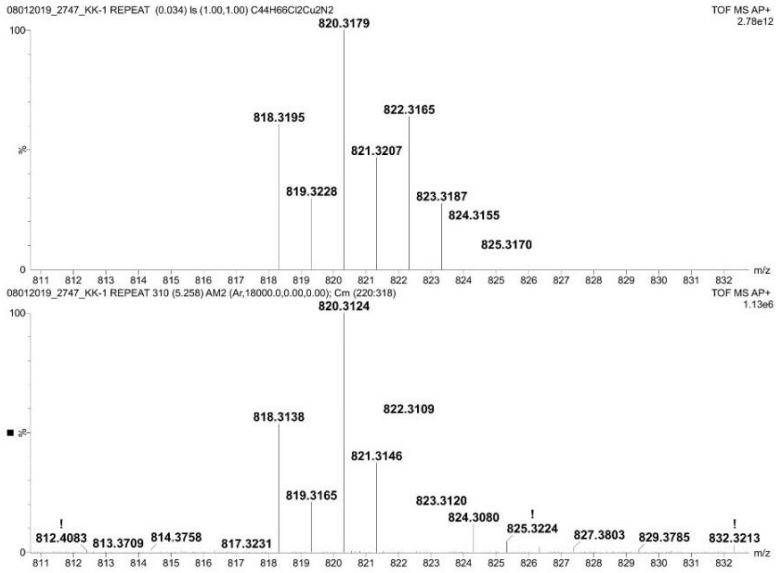

Fig. 3.6 HRMS of ***[(BICAAC)$_2$Cu]$^+$[CuCl$_2$]$^-$***.

But, here, in this case the mono carbene Cu(I) adduct has been isolated via single crystal X-ray diffraction. It could be possible the disproportionation product was present in minor quantities.

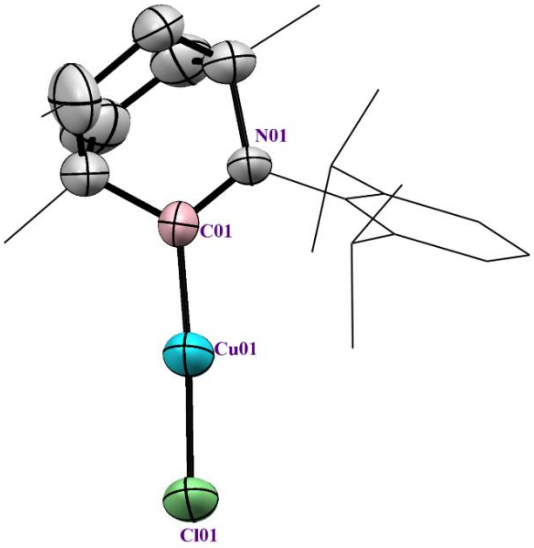

Fig. 3.7 Single crystal X-ray structure of ***[(BICAAC)CuCl]*** **(1)**. Ellipsoids are shown at 50 % probability levels. All hydrogen atoms are omitted for clarity. Selected bond lengths [Å] and bond angles [°]: Cu01-Cl01 2.104(2), Cu01-C01 1.894(6), N01-C01 1.302(7); Cl01-Cu01-C01 176.4(2), Cu01-C01-N01 124.2(4).

The UV-Vis., and fluorescence spectra of complex **(1)** were recorded in the solution phase. The signal at 293 ($\varepsilon = 7.9*10^3$ *L mol^{-1}cm^{-1}*) nm and 369 ($\varepsilon = 1.2*10^3$ *L mol^{-1}cm^{-1}*) nm, due to charge transfer (ILCT and MLCT). The compound shows a large Stokes shift at 423 nm in the emission spectrum in acetonitrile (10^{-4} M).

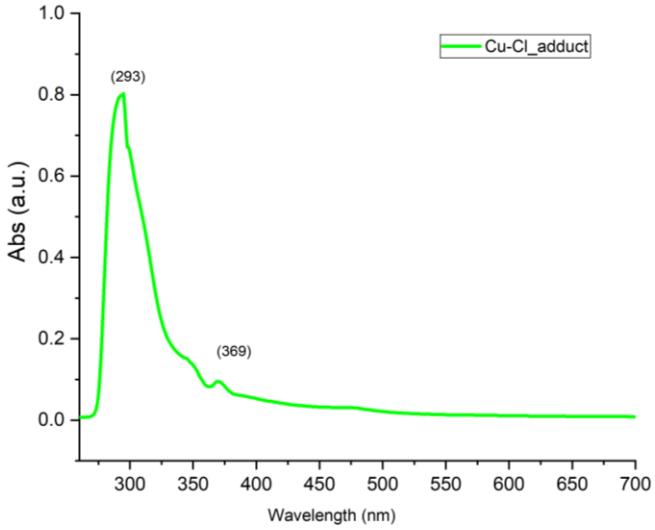

Fig. 3.8 UV-Vis of ***[(BICAAC)CuCl] (1)*****.**

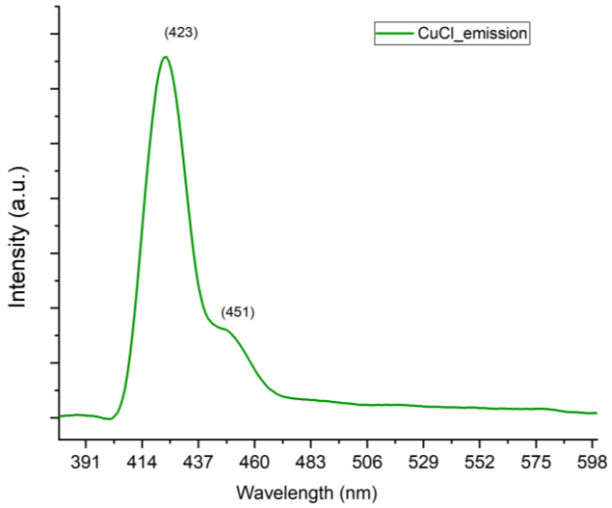

Fig. 3.9 Emission spectrum of ***[(BICAAC)CuCl] (1)***.

3.2.2 Synthesis of *[(BICAAC)CuI]* (2)

Bicyclic (alkyl)(amino) carbene (BICAAC) was dissolved in THF followed by the addition of solid copper(I) iodide (CuI) (white powder) and the reaction mixture was stirred at room temperature for 12 h in the glove box (Scheme 3.5). The progress of the reaction was observed by the colour changes from light yellow to greenish. Then all the volatiles were removed under vacuum for about 5-6 h and washed with hexane.

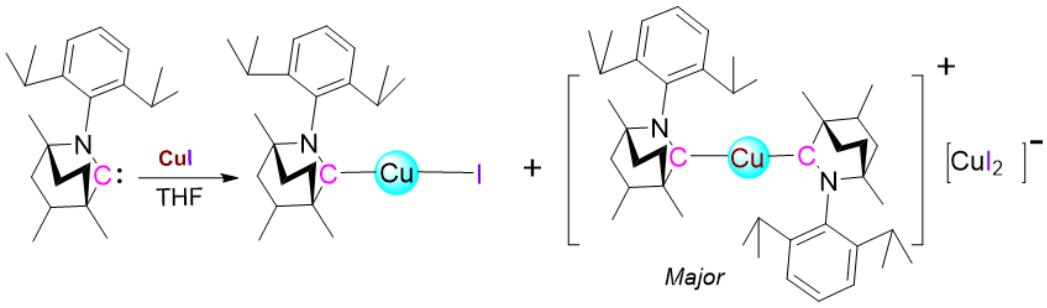

(2a) **(2b)**

Scheme 3.3 Synthesis of [(***BICAAC)CuI]*** (**2**).

The shifting of the two septets from 3.27 and 2.95 ppm (in case of free carbene) to 2.87 and 2.56 ppm in respectively ^{1}H NMR spectrum (Fig. 3.10) could be due to the complex formation. The ^{13}C NMR was not satisfactory due to solubility nature of the compound (sparingly soluble).

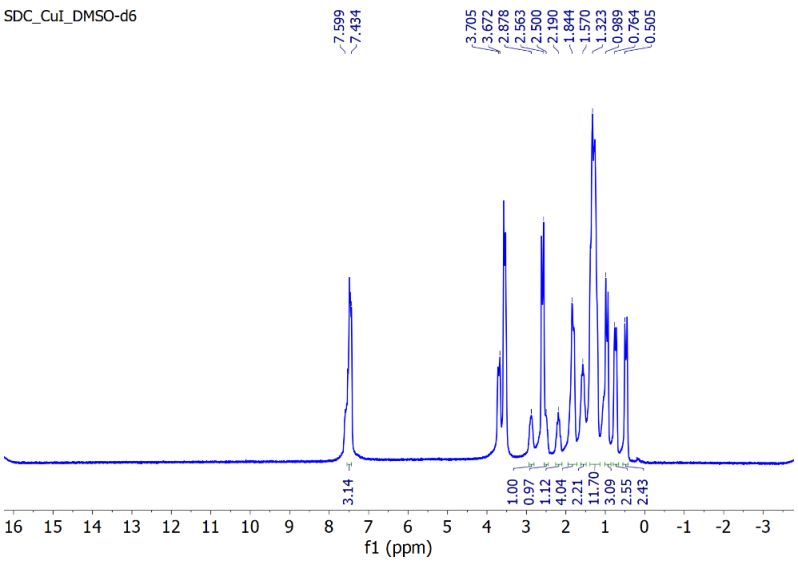

Fig. 3.10 ^{1}H NMR spectrum of [(***BICAAC)CuI]*** (**2**) (400 MHz, DMSO-d_6).

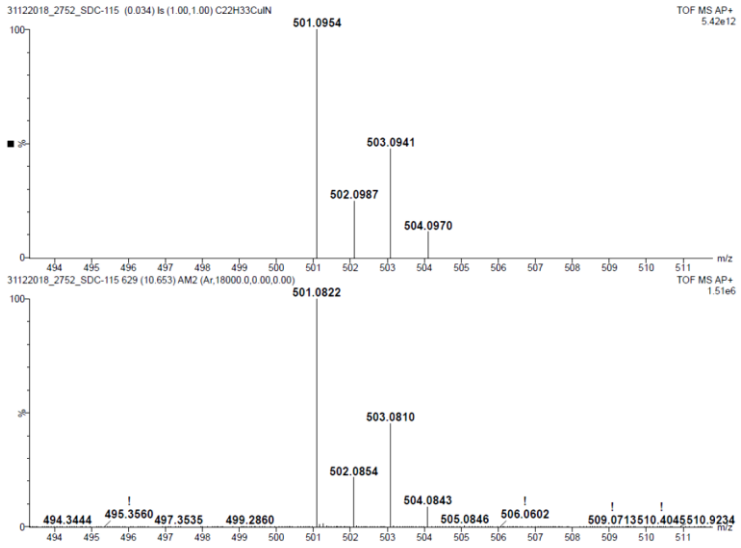

Fig. 3.11 HRMS spectrum of [(***BICAAC)CuI]*** (**2a**).

The HRMS spectrum shows the signal at *m/z* = 409.1546 which corresponds to carbene-CuI adduct and also *m/z* = 875.2638 corresponds to $[M\text{-}I]^+$ i.e. $[(BICAAC)_2Cu]^+[CuI]$ as we observed in the earlier case. We structurally confirmed the compound (**2b)** via SCXRD where we found that two units of carbene are coordinated with one Cu centre giving rise to the cationic copper complex and $[CuI_2]^-$ as a counter anion (Fig. 3.11).

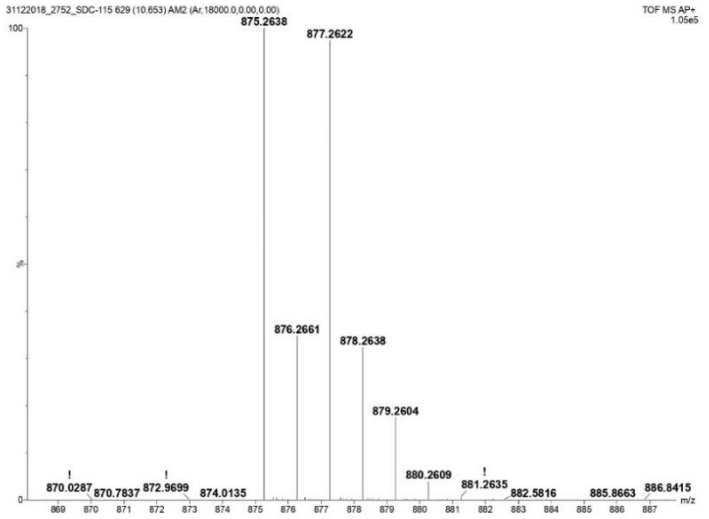

Fig. 3.12 HRMS of ***[(BICAAC)Cu]$^{+}$[CuI$_2$]$^{-}$ (2b)***.

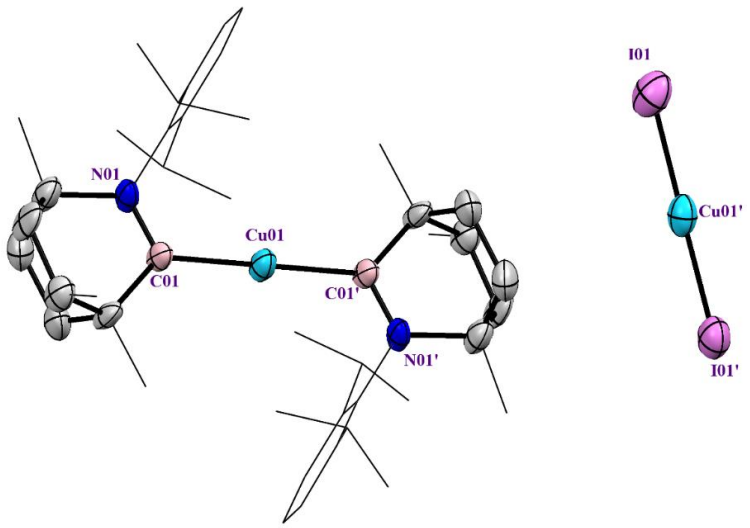

Fig. 3.13 Single crystal structure of ***[(BICAAC)Cu]$^{+}$[CuI$_2$]$^{-}$ (2b)***. Ellipsoids are shown at 50 % probability levels. All hydrogen atoms are omitted for clarity Selected bond lengths [Å] and bond angles [°]: C01-Cu01 1.948(1), C01-N01 1.313(1), Cu01-C01' 1.948(1), C01'-N01' 1.313(1), Cu01'-I01 2.351(5), Cu01'-I01' 2.369(5) ; N01-C01-Cu01 121.95 (1), C01 -Cu0-C01' 180.0(2), Cu01-C01'-N01' 121.95(1), I01-Cu01'-I01' 180.0(1).

Based on the observation and solubility behaviour, we believe that disproportionation to be more facile leading to the formation of bis carbene cationic complex as a major component and the neutral copper iodide complex as the minor fraction.

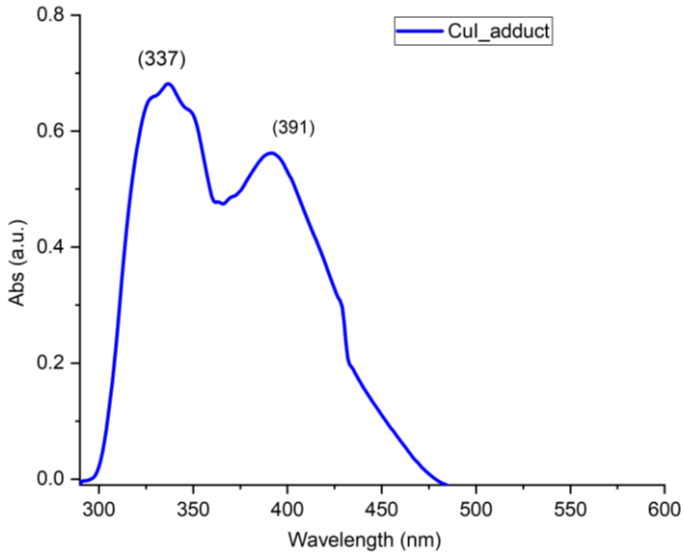

Fig. 3.14 UV-Vis spectrum of ***[(BICAAC)Cu]$^{+}$[CuI$_2$]$^{-}$ (2b)***.

Then the cationic BICAAC-copper(I) iodide complex shows good absorption at 337 nm (ε 7.5*10^3 L mol^{-1} cm $^{-1}$) and 391 nm (ε 5.9*10^3 L mol^{-1} cm $^{-1}$) due to MLCT and good emission at 450 nm in acetonitrile.

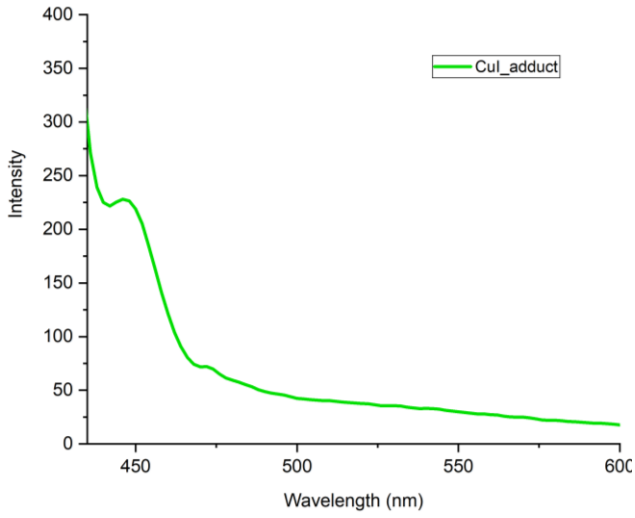

Fig. 3.15 Emission spectrum of ***[(BICAAC)Cu]$^{+}$[CuI$_2$]$^{-}$ (2b)***.

Then the complex was subjected to cyclic voltammetry measurement. The cyclic voltammogram of cationic Cu complex in CH_3CN containing nBu_4NPF_6 as electrolyte shows quasi-reversible one electron reduction $\boldsymbol{E_{1/2}}$ *= -1.175 V* versus Cp^*_2Fe+/ Cp^*_2Fe where,

Cp^*_2Fe = decamethyl ferrocene (as reference), whereas in the case of the cAAC-copper cationic complex the reported value is -1.36 V (with respect to same electrodes).[7]

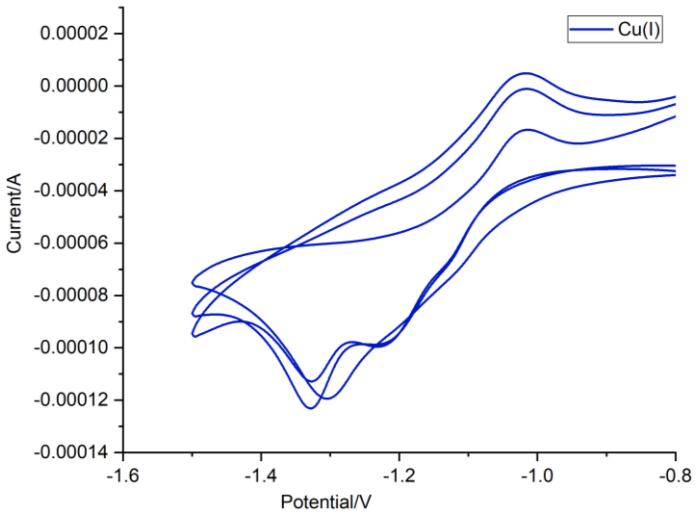

Fig. 3.16 Cyclic voltammogram of ***[(BICAAC)Cu]$^+$[CuI$_2$]$^-$ (2b)***.

3.2.3 Synthesis of *[(BICAAC)$_2$Cu]* (3)

Bicyclic (alkyl)(amino) carbene (BICAAC) was dissolved in THF and copper(I) chloride (CuCl) (white powder) was added to it and was stirred at room temperature for 12 hrs (preferably overnight) in the glove box. Then 1 eqv. of free carbene added to the reaction mixture followed by the addition of 1.1 eqv. of KC_8 and suddenly the colour of the reaction changed to deep green (Scheme 3.6).

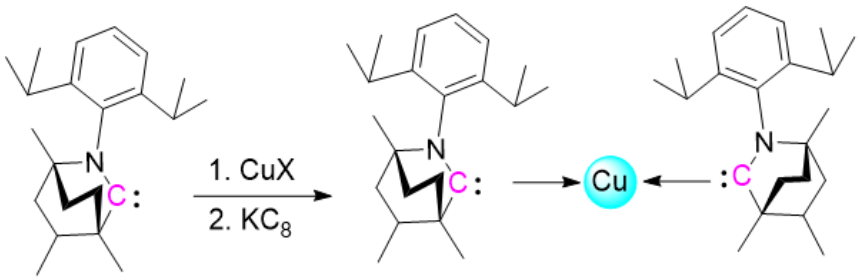

Scheme 3.4 Synthetic scheme for ***[(BICAAC)$_2$Cu]*** **(3)**.

The sudden change in colour was the indication of the formation of the expected compound as mentioned in the literature and the same observation was noticed in the case of copper iodide

also. Then the solution was stirred for about 2-3 h and dried well and the compound is extracted in hexane by filtration. Assuming the formation of zero valent copper complex, the magnetic moment of the compound was measured and was found to be in the range of ***1.2-1.3*** μ_β (Fig. 3.19) ranging from 300-2 K at 1 Tesla (constant magnetic field), whereas for one unpaired electron, the theoretical value of magnetic moment is **1.73** μ_β, which can be calculated via the following equation (Fig. 3.17).

$$\begin{aligned}\mu_{eff} &= \sqrt{n(n+2)}\,\mu_\beta \\ &= \sqrt{1(1+2)}\,\mu_\beta \\ &= \sqrt{3}\,\mu_\beta \\ &= 1.73\,\mu_\beta\end{aligned}$$

Fig. 3.17 Spin only magnetic moment calculation for one unpaired electron.

This drop of the magnetic moment from the theoretical value of one unpaired electron containing mononuclear Cu(0) centre plausibly hints the existence of strong anti-ferromagnetic coupling between the one unpaired electron of copper and two units of BICAACs as described in the Fig. 3.18.

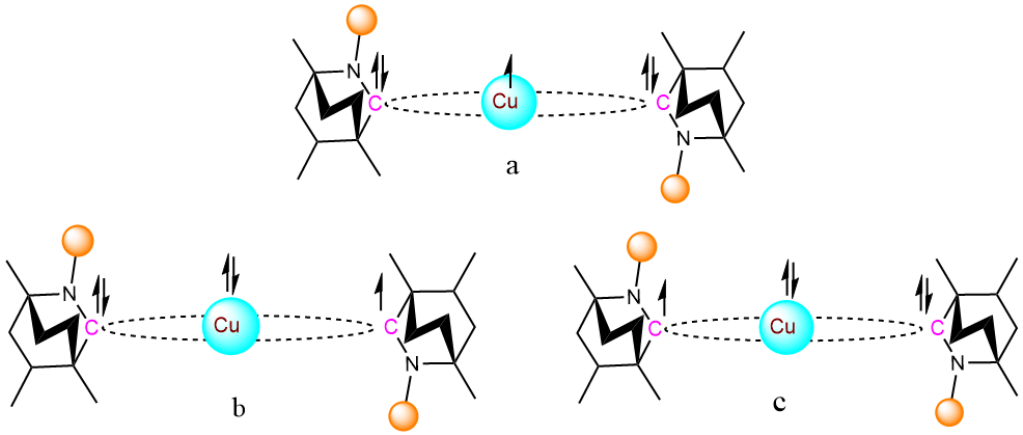

Fig. 3.18 Schematic diagram of antiferromagnetic coupling of Cu(0) and two units of BICAACs.

Further the compound was analysed by HRMS where the signal at *m/z* = 685.4554 corresponds to the expected zero valent bis carbene copper compound (Fig. 3.20).

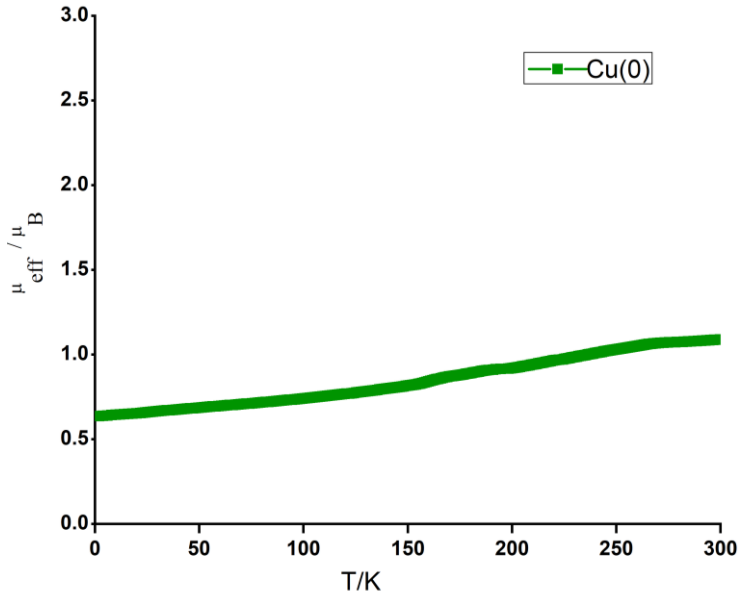

Fig. 3.19 Magnetic moment *vs.* temperature for ***[(BICAAC)$_2$Cu]*** **(3)**.

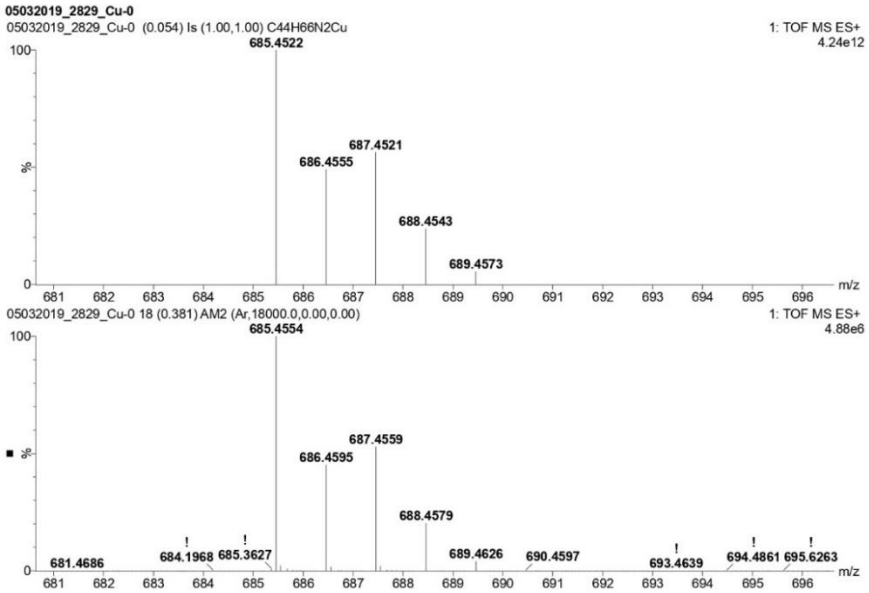

Fig. 3.20 HRMS of ***[(BICAAC)$_2$Cu]*** **(3).**

This type of zero valent complexes shows NIR absorption, which was reported earlier also in the case of cAAC. Here, the absorption spectra of the compound also showed a signal in the NIR region at 1143 nm, which further indicates the product formation.

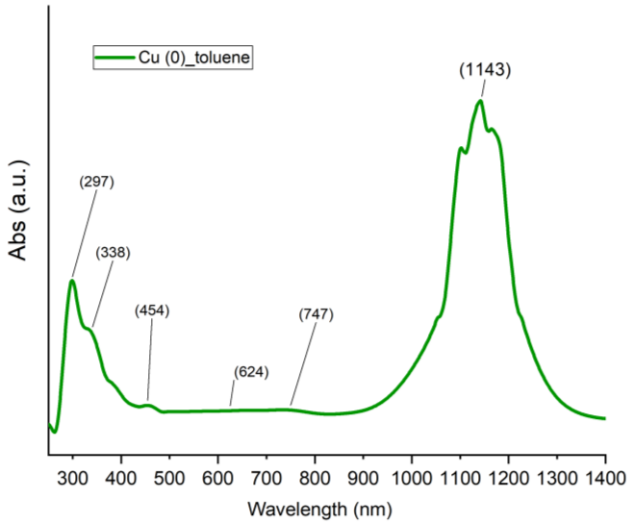

Fig. 3.21 UV-Vis spectrum of ***[(BICAAC)$_2$Cu]*** **(3)**.

3.3. Conclusion

In conclusion, we have synthesized new bicyclic (alkyl)(amino) carbene copper complexes in different coordination mode. We have investigated the reactivity of BICAAC with copper halide (CuCl, CuI) in the same reaction condition. We observed the mono as well as bis coordination of BICAAC with both the copper(I) halide which was confirmed by the high-resolution mass spectrometry also. Surprisingly, we were able to isolate the mono coordinated copper in the case of copper chloride whereas bis coordination in copper iodide via single crystal X-ray diffraction studies. Isolation of neutral bis coordinated copper(0) complex was also attempted via KC_8 reduction route. The magnetic property of $[(BICAAC)_2Cu]^0$ was also studied which indicates the existence of a strong antiferromagnetic coupling between the Cu and two units of BICAACs centre (plausibly). The NIR absorption at the range of 1150 nm also indicates the formation of zero valent Cu species.

3.4. Experimental Section

3.4.1 General Procedure

All syntheses were carried out under an inert atmosphere of dry nitrogen in oven-dried glassware using standard Schlenk techniques or a glove box where O_2 and H_2O levels were maintained. All the glassware was dried at 150 °C in an oven for at least 12 h and assembled hot and cooled in vacuo prior to use. Solvents were purified by MBRAUN solvent purification system MB SPS-800 and were used directly from the SPS system. For NMR, $CDCl_3$ and DMSO-d_6 were purchased from Merck and CIL and were used without further purification. High-resolution mass spectrometry was performed with a Waters SYNAPT G2–S instrument. The ^{1}H and ^{13}C NMR spectra were recorded with a Bruker 400 MHz spectrometer with TMS as an external reference; chemical shift values are reported in ppm. For absorption measurement, LABINDIA UV-Vis Spectrophotometer 3000+ was used. Steady-state fluorescence spectra were recorded using Shimadzu RF-6000 spectrofluorimeter. The excitation wavelength was chosen accordingly and emission was collected in the range of 375-700 nm. The magnetic moment measurement has been recorded in SQUID at 1T ranging from 300 K to 2 K. The cyclic voltammogram of cationic copper iodide complex was studied with a potentiostat using a three-electrode arrangement with a glassy carbon working electrode (2 mm diameter), an Ag/0.01 M $AgNO_3$ reference electrode and a Pt wire counter electrode. Decamethyl Ferrocene was added as an internal standard after the measurements and all potentials are referenced relative to the $(Cp^*)_2Fe/(Cp^*)_2Fe^+$ couple.

3.4.2 Starting material

All chemicals were purchased from Merck and used without further purification. *2,6-Diisopropylaniline* was distilled off before making the starting material. The bicyclic

(alkyl)(amino) carbene was prepared following the literature procedure reported by G. Bertrand *et al.*[12] and was characterized well in each time by NMR and IR method.

3.4.3 Single crystal X-ray structural determination

Single crystal X-ray diffraction data were collected using a RigakuXtaLAB mini diffractometer equipped with Mercury375M CCD detector. The data were collected with graphite monochromatic MoKα radiation (λ = 0.71073 Å) at 100.0(2) K using scans. During the data collection the detector distance was 50 mm (constant) and the detector was placed at 2θ = 29.85° (fixed) for all the data sets. The data collection and data reduction were done using Crystal Clear suite [10a]. The crystal structures were solved by using either OLEX2 [10b] and the structure were refined using SHELXL-97 2008[c]. All non-hydrogen atoms were refined anisotropically. All the graphics were generated using Mercury 3.9.

3.4.4 Synthetic procedure

Synthesis of [(BICAAC)CuCl] (1): BICAAC (0.31g, 1.00 mmol) was dissolved in THF (20 mL) and subsequently copper chloride (CuCl) (0.10 g, 1.00 mmol) was added to this solution. Then the reaction mixture was stirred for about 10-12 h (preferably overnight) and then all the solution was filtered off to remove the THF and the residue was washed with hexane and dried well to afford the greenish-white powder. Recrystallization from DCM gave the product in 74% yield. **MP**: 210-213 ºC. **^{1}H NMR** (400 MHz, $CDCl_3$): δ = 7.42 (t, 1H, pAr-H, $^{3}J_{H-H}$ = 8 Hz), 7.28 (d, 2H, mAr-H, $^{3}J_{H-H}$ = 8 Hz), , 2.96 (sept, ^{1}H, $CH(CH_3)_2$, $^{3}J_{H-H}$ = 8 Hz) , 2.63 (sept, 1H, $CH(CH_3)_2$, $^{3}J_{H-H}$ = 8 Hz), 2.12 (d, 2H), 2.05 (m, 6H), 1.76 (s, 1H), 1.59 (s, 1H), 1.48-1.27 (m, 12 H), 1.15 (s, 1H), 1.04 (m, 5H) ppm. **^{13}C NMR** (100 MHz, $CDCl_3$): δ = 257.6, 144.4, 143.9, 141.2, 129.7, 125.1, 124.8, 77.4, 77.1, 76.8, 44.4, 36.7, 33.1, 30.4, 29.1, 28.4, 25.9, 25.6, 23.8, 23.6, 23.0, 20.4 ppm. **HRMS (AP^{+})**: *m/z* calculated for $C_{22}H_{33}CuClN$: (409.1598): [M];

found: (409.1546) & *m/z* calculated for $C_{44}H_{68}Cu_2Cl_2N_2$: (820.3179): $[M+2H]^+$; found : (820.3124).

Synthesis of [(BICAAC)CuI] (2): BICAAC (0.31 g, 1.00 mmol) was dissolved in THF (20 mL) and subsequently solid copper iodide (CuI) (0.19 g, 1.00 mmol) was added to this solution. Then the reaction mixture was stirred for about 10-12 h (preferably overnight) and then the solution was filtered to remove the THF and the residue was washed with hexane and dried well to afford the light greenish powder. Recrystallization from DCM gave the product in 77% yield. **MP**: 231-234 °C. **^{1}H NMR** (400 MHz, DMSO) δ 7.60-7.43 (br, 3 H), 3.70*, 2.88 (merged septet, 1H) , 2.56 (sept, ^{1}H, $CH(CH_3)_2$, $^3J_{H-H}$ = 8 Hz), 2.50 (s, 1H), 2.19 (m, 4H), 1.84 (d, 2H), 1.57 (br, 12 H), 1.32 (m, 3H), 0.99 (d, 2H), 0.76 (d, 2H) ppm. **HRMS (AP^+)**: *m/z* calculated for $C_{22}H_{33}CuIN$: (501.0854): [M]; found: (501.0822) & *m/z* calculated for $C_{44}H_{66}Cu_2IN$, $[M-I]^+$; found: (875.2638)

* solvent impurity (residue THF)

Synthesis of [$(BICAAC)_2Cu$] (3): BICAAC (0.311 g, 1.00 mmol,) was dissolved in THF (20 mL) and subsequently solid copper halide (CuX) (1.00 mmol) was added into carbene containing THF solution. Then the reaction mixture was stirred for about 10-12 h (preferably overnight) and then free BICAAC (1 eqv.) was added in the reaction mixture followed by the addition of potassium graphite (KC_8), (1.2 eqv.) in situ in the reaction. Then the reaction mixture was stirred well for about two hrs, filtered and dried well to afford deep green solid and left for crystallization in toluene. **HRMS (ESI^+)**: *m/z* calculated for $C_{44}H_{66}Cu$: (685.4522): [M]; found: (685.4554).

3.5. Crystallographic data

Compound[a]	**1**	**2b**
Chemical formula	$C_{22}H_{33}ClCuN$	$C_{22}H_{33}CuIN$
Molar mass	410.48	501.93
Crystal system	monoclinic	triclinic
Space group	*I 2/a*	$P\bar{1}$
T [K]	149.98	100.00
a [Å]	20.7079(16)	10.4996(8)
b [Å]	11.525(3)	12.1852(9)
c [Å]	18.160(2)	19.2293(14)
α [°]	90.00	102.320(6)
β [°]	94.444(9)	92.333(6)
γ [°]	90.00	113.281(7)
V [Å^3]	4320.8(11)	2186.3(3)
Z	8	2
D(calcd.) [g·cm^{-3}]	2.997	0.762
μ(Mo-K_α) [mm^{-1}]	2.705	1.208
Reflections collected	26106	48814
Independent reflections	7506	15076
Data/restraints/parameters	7506/0/233	15076/0/454
$R1, wR_2[I>2\sigma(I)]$[a]	0.0995, 0.2235	0.1172, 0.2697
R1, wR_2 (all data)[a]	0.2956, 0.3193	0.2320, 0.3364
GOF	0.991	0.925

[a] $R1 = \Sigma||Fo| - |Fc||/\Sigma|Fo|$. $wR_2 = [\Sigma w(|Fo^2| - |Fc^2|)^2/\Sigma w|Fo^2|^2]^{1/2}$

3.6. References

1. Ardeungo, A. J. III; Dias, H. V. R.; Calabrese, J. C.; Davidson, F. *Organometallics* **1993** *12*, 3405-3409.
2. Raubenheimer, H. G.; Cronje, S.; Olivier, P. J.; Toerien, J. G.; Van R. P. H. *Angew. Chem., Int. Ed. Engl.*, **1994**, *33*, 672-673.
3. Tulloch, A. A. D.; Danopoulos, A. A.; Kleinheinz, S.; Light, M. E.; Hursthouse, M. B.; Eastham, G. *Organometallics* **2001**, *20*, 2027-2031.
4. Fraser, P. K.; Woodward, S. *Tetrahedron Lett.* **2001,** *42*, 2747-2749.
5. Jurkauskas, V.; Sadighi, J. P.; Buchwald, S. L. *Org. Lett.* **2003**, *5*, 2417-2420.
6. Kaur, H.; Zinn, F. K.; Stevens, E. D.; Nolan, S. P. *Organometallics* **2004,** *23*, 1157-1160.
7. Weinberger, D. S.; Nurul Amin, S. K.; Mondal, K. C.; Melaimi, M.; Bertrand, G.; Stückl, A. C.; Roesky, H. W.; Dittrich, B.; Demeshko, S.; Schwederski, B.; Kaim, W.; Jerabek, P.; Frenking, G. *J. Am. Chem. Soc*. **2014**, *136 (17)*, 6235-6238.
8. Hamze, R.; Peltier, J. L.; Sylvinson, D; Jung, M.; Cardenas, J.; Haiges, R.; Soleilhavoup, M.; Jazzar, R.; Djurovich, P. I.; Bertrand, G.; Thompson, M. E. *Science*, **2019,** *363*, 601-606.
9. Shuyang, S. S.; Moon C. J. M. C.; Caleb C. C.; Abegail T. A.; Sylvinson M. R. D.; Djurovich P. I.; Forrest S. R.; Thompson M. E. *J. Am. Chem. Soc.* **2019**, *141* (8), 3576–3588.
10. Hamze, R.; Jazzar, R.; Soleilhavoup, M.; Djurovich, P. I.; Bertrand, G.; Thompson M. E. *Chem. Commun*. **2017**, *53*, 9008-9011.
11. (a) *CrystalClear 2.0*; Rigaku Corporation: Tokyo, Japan, **2013**. (b) Dolomanov, O. V.; Bourhis, L. J.; Gildea, R. J.; Howard, J. A. K.; Puschmann, H. *J. Appl. Crystallogr*. **2009**, *42*, 339-341 (c) Sheldrick, G. M. *Acta Cryst. A* **2015**, *71*, 3-8.
12. Mendivil, E. T.; Hansmann, M. M.; Weinstein, C. M.; Jazzar, R.; Melaimi, M.; Bertrand, G. *J. Am. Chem. Soc.* **2017**, *139 (23)*, 7753-7756.

Supporting Information

Heteronuclear NMR (^{1}H and ^{13}C NMR spectra) of the catalysis part

(Heck-Mizoroki and Suzuki-Miyaura reaction)

1. Heck-Mizoroki Reaction

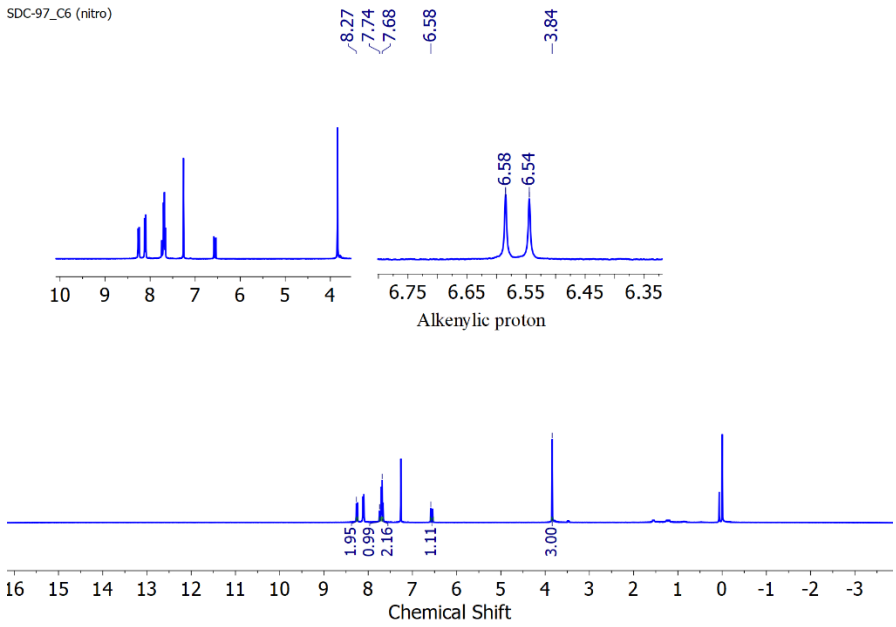

Fig. S1 ^{1}H NMR spectrum of **1a** (400 MHz, $CDCl_3$).

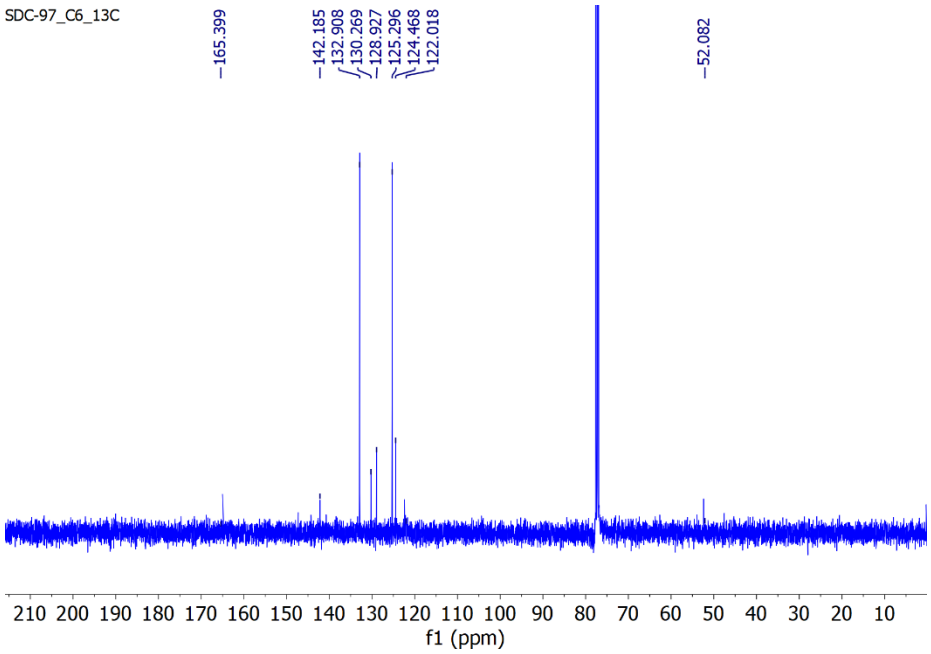

Fig. S2 ^{13}C NMR spectrum of **1a** (100 MHz, $CDCl_3$).

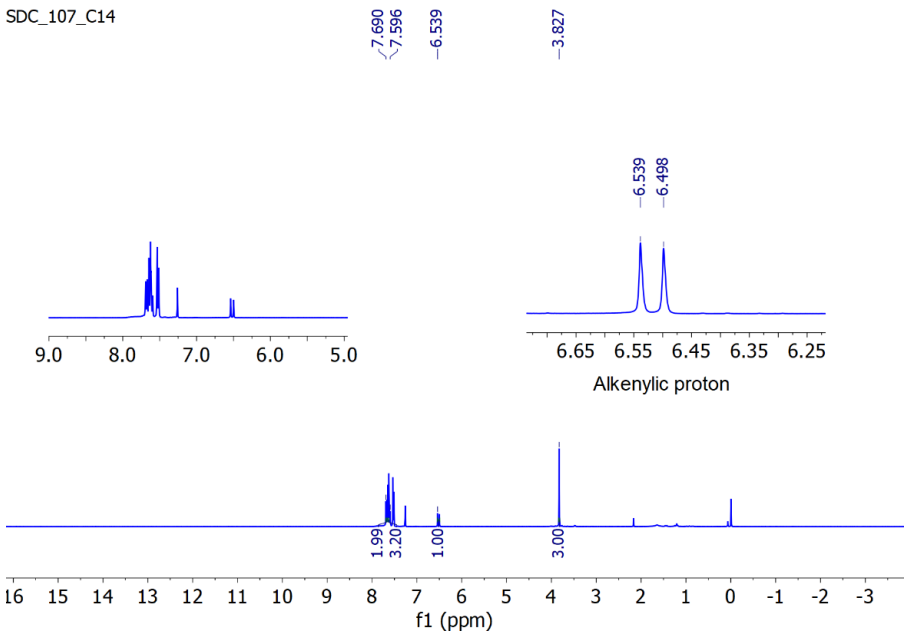

Fig. S3 ^{1}H NMR spectrum of **1b** (400 MHz, $CDCl_3$).

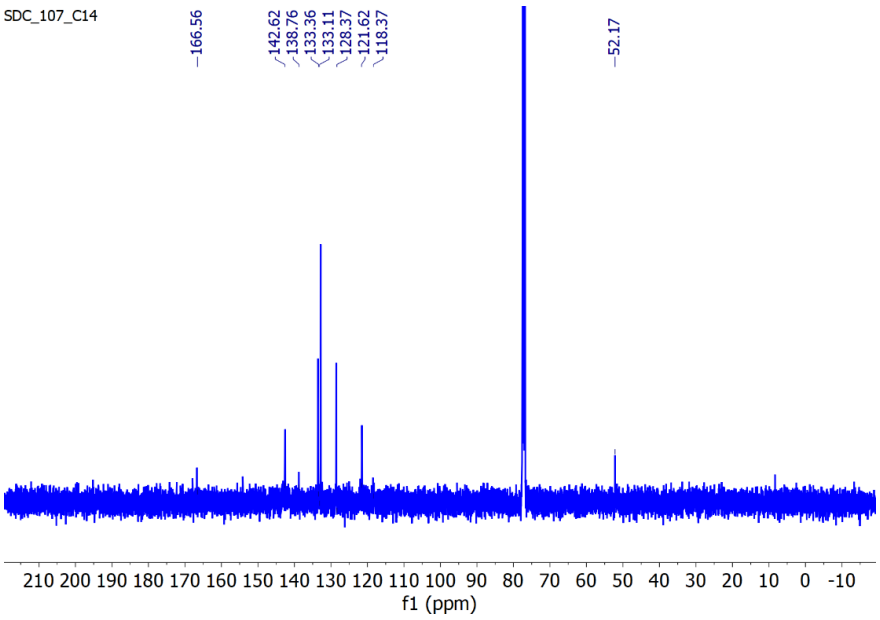

Fig. S4 ^{13}C NMR spectrum of **1b** (100 MHz, $CDCl_3$).

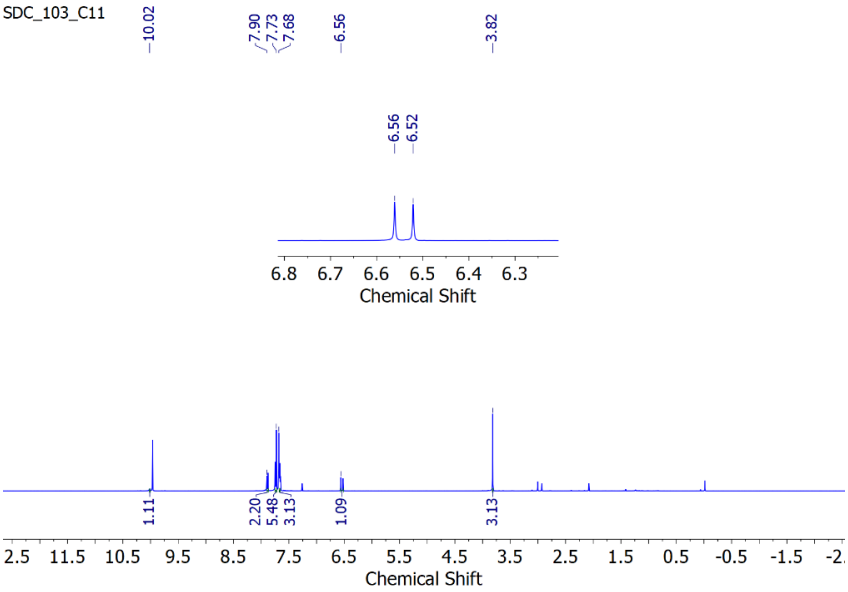

Fig. S5 ^{1}H NMR spectrum of **1c** (400 MHz, $CDCl_3$).

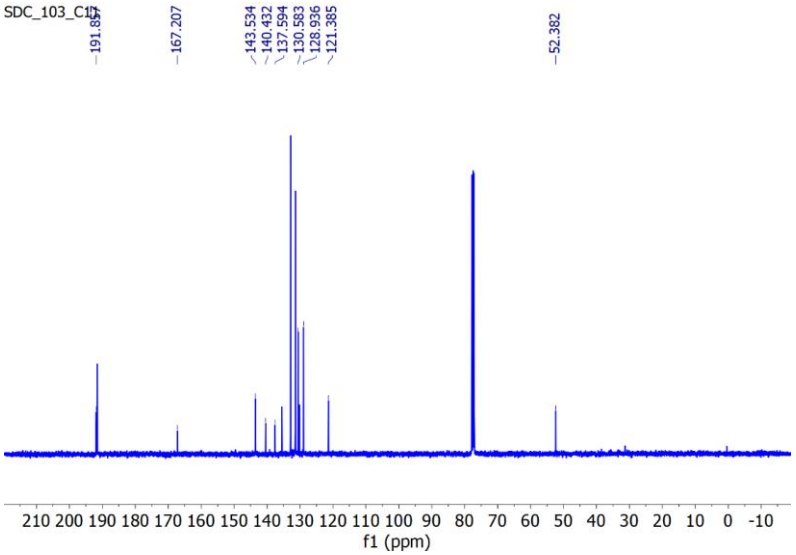

Fig. S6 ^{13}C NMR spectrum of **1c** (100 MHz, $CDCl_3$).

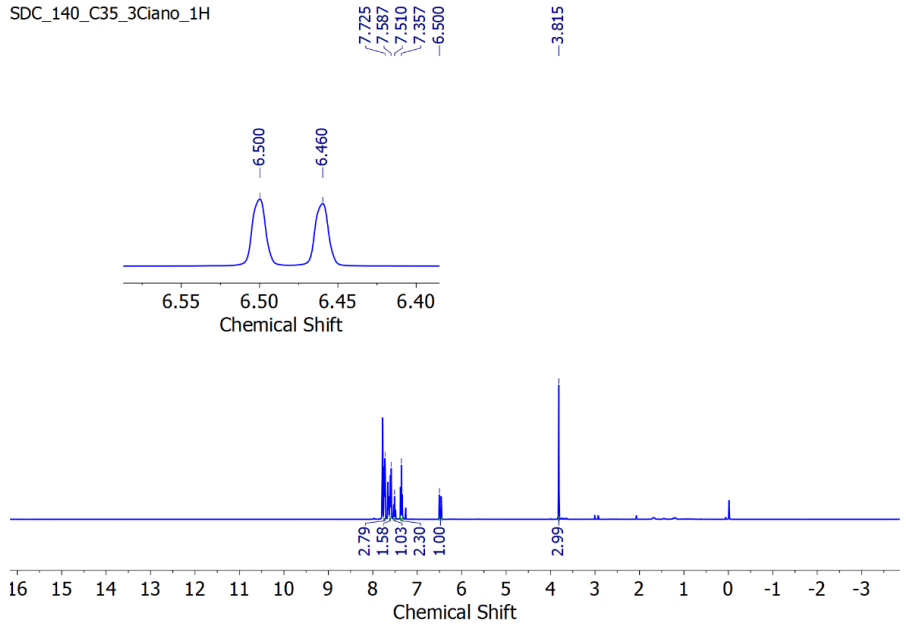

Fig. S7 ^{1}H NMR spectrum of **1d** (400 MHz, $CDCl_3$).

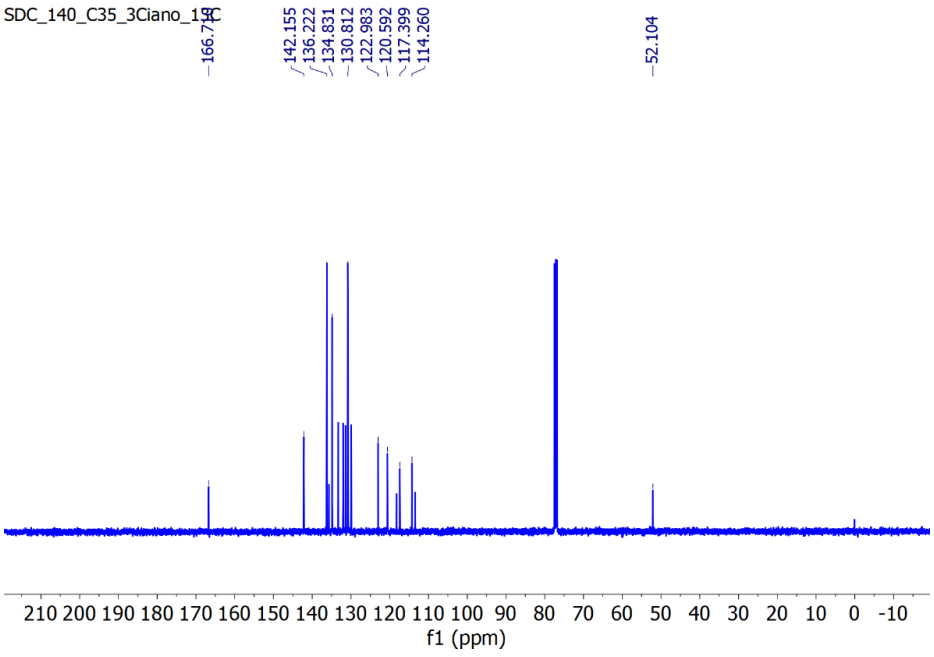

Fig. S8 ^{13}C NMR spectrum of **1d** (100 MHz, $CDCl_3$).

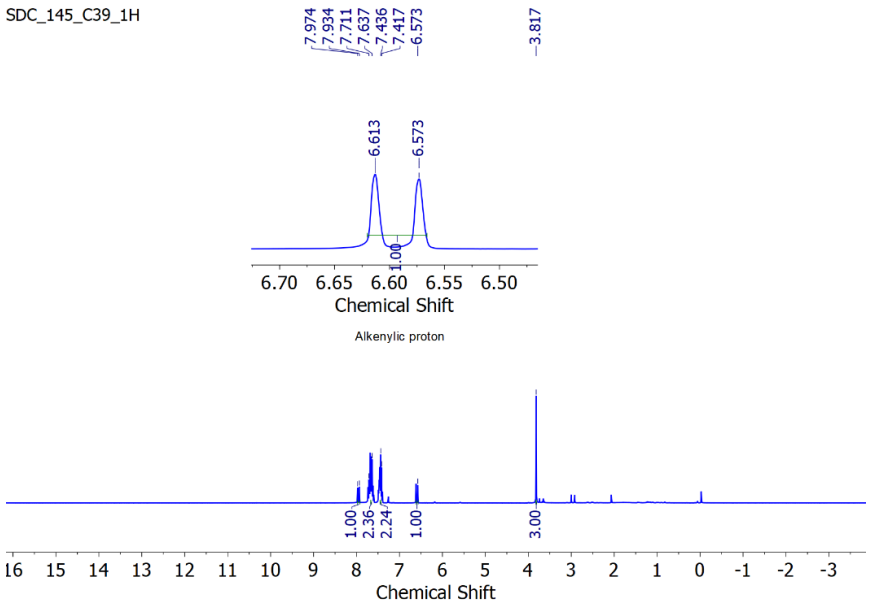

Fig. S9 ^{1}H NMR spectrum of **1e** (400 MHz, $CDCl_3$).

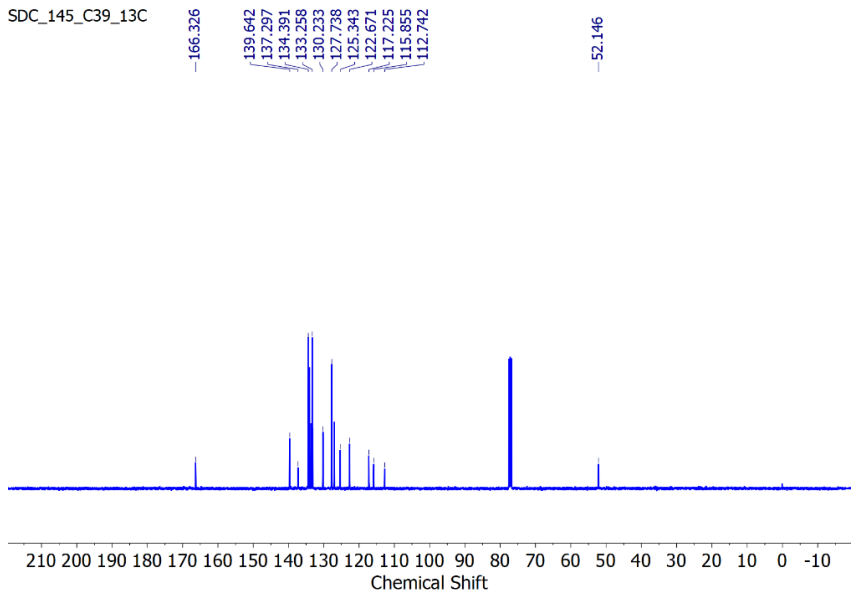

Fig. S10 ^{13}C NMR spectrum of **1e** (100 MHz, $CDCl_3$).

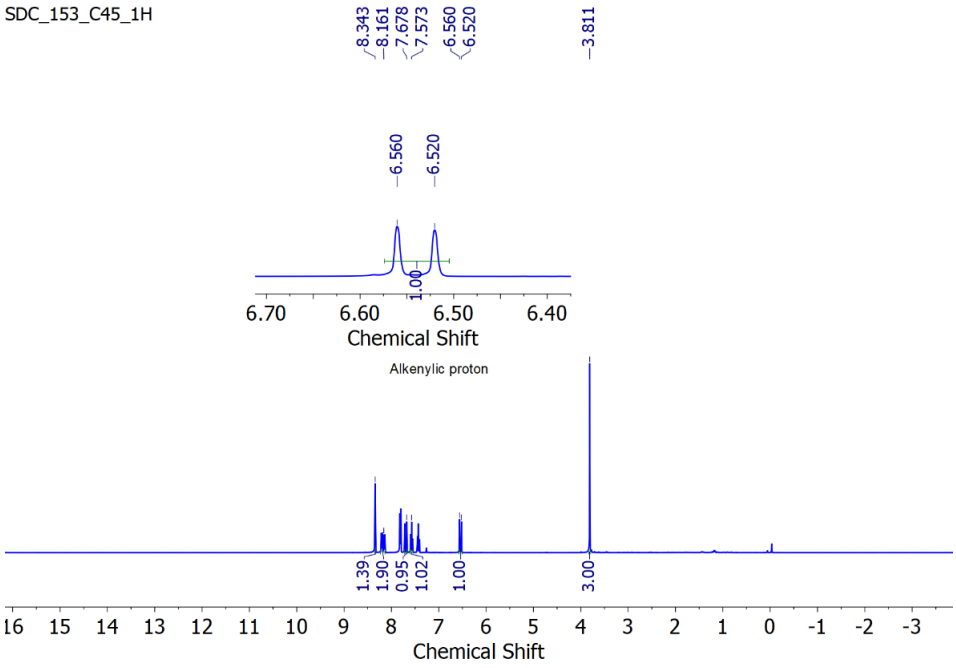

Fig. S11 ^{1}H NMR spectrum of **1f** (400 MHz, $CDCl_3$).

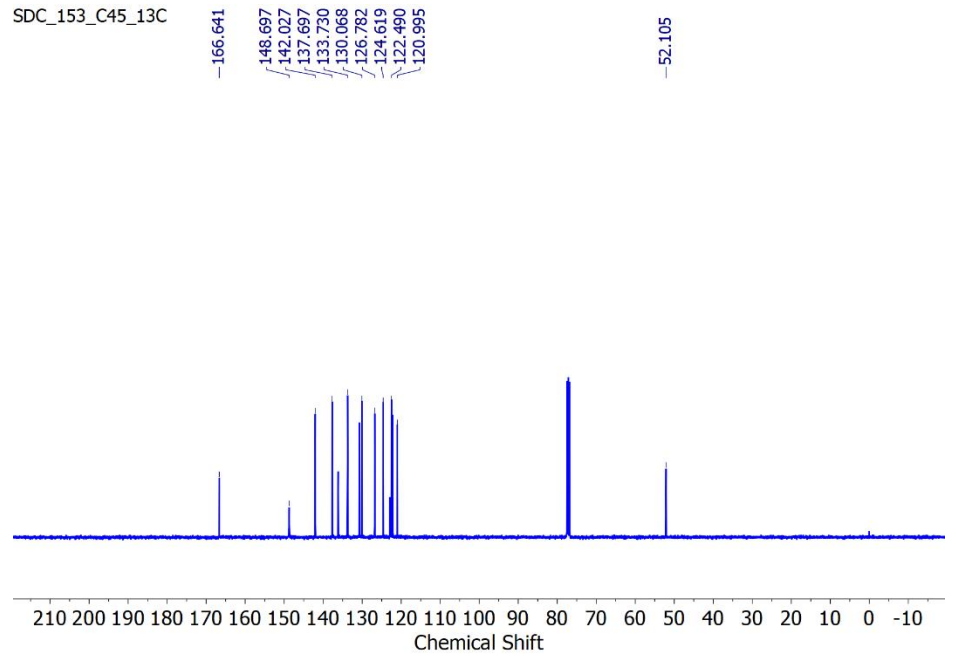

Fig. S12 ^{13}C NMR spectrum of **1f** (100 MHz, $CDCl_3$).

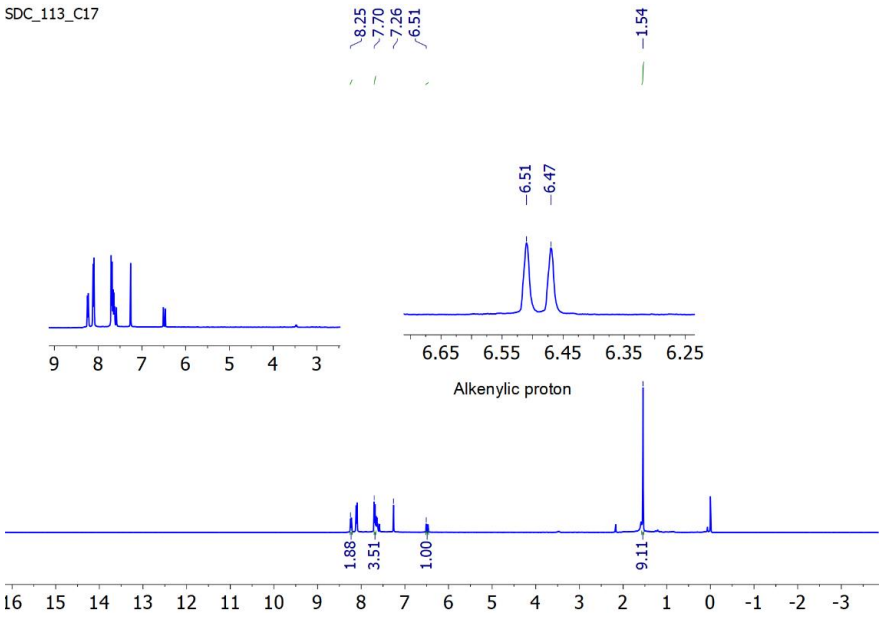

Fig. S13 ^{1}H NMR spectrum of **2a** (400 MHz, $CDCl_3$).

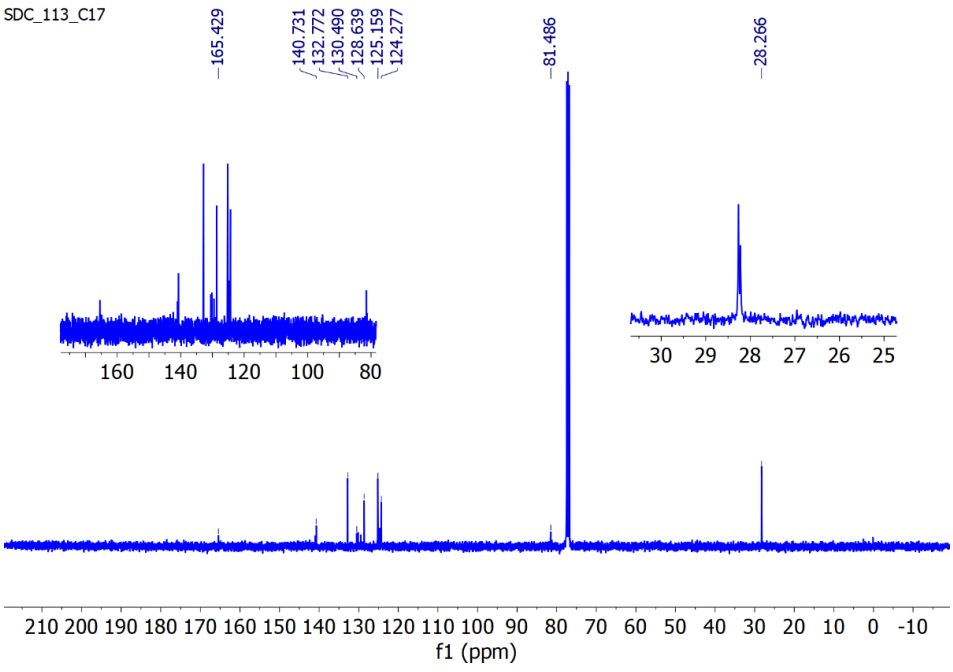

Fig. S14 ^{13}C NMR spectrum of **2a** (100 MHz, $CDCl_3$).

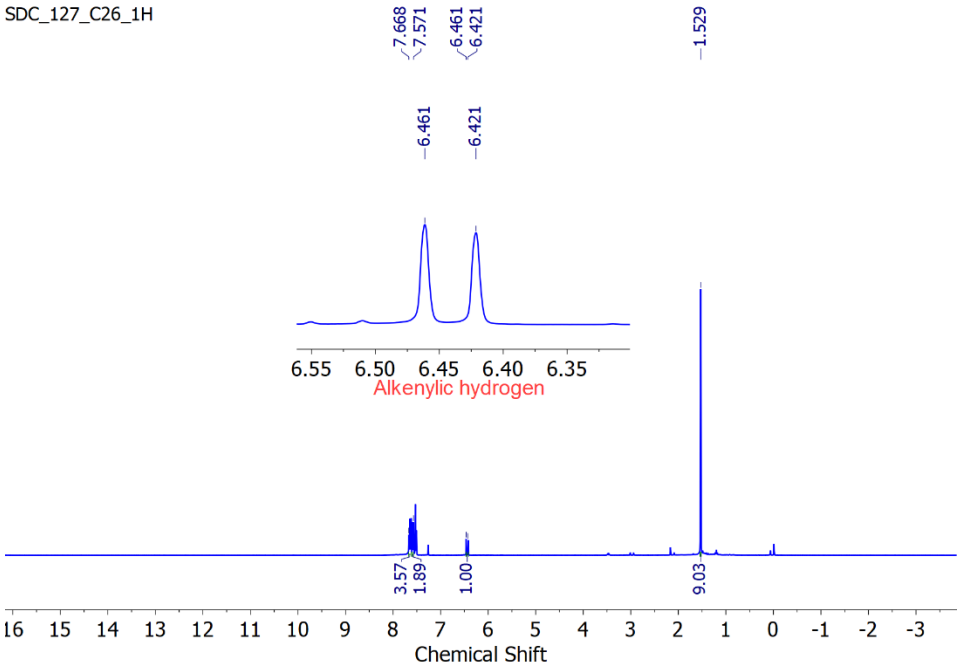

Fig. S15 ^{1}H NMR spectrum of **2b** (400 MHz, $CDCl_3$).

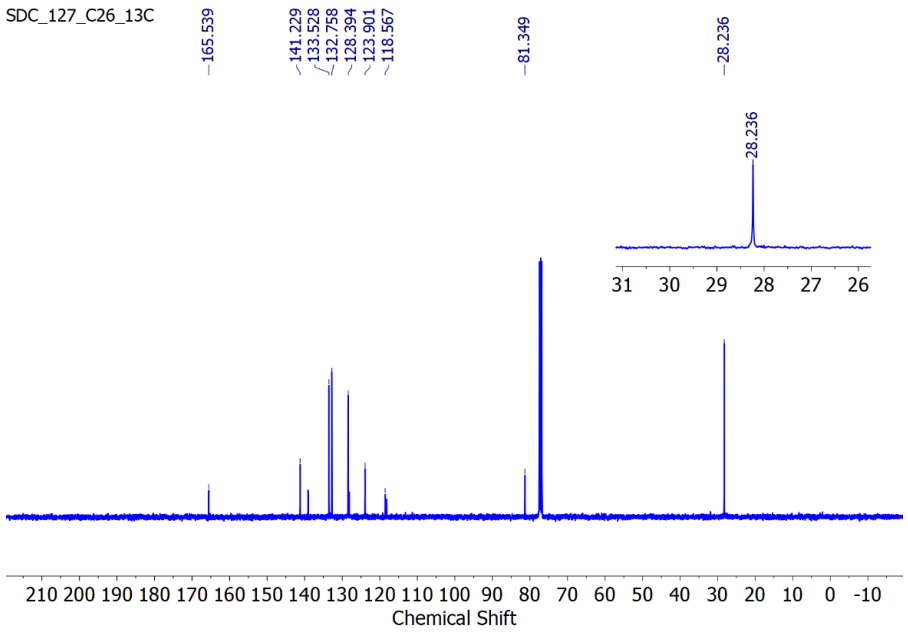

Fig. S16 ^{13}C NMR spectrum of **2b** (100 MHz, $CDCl_3$).

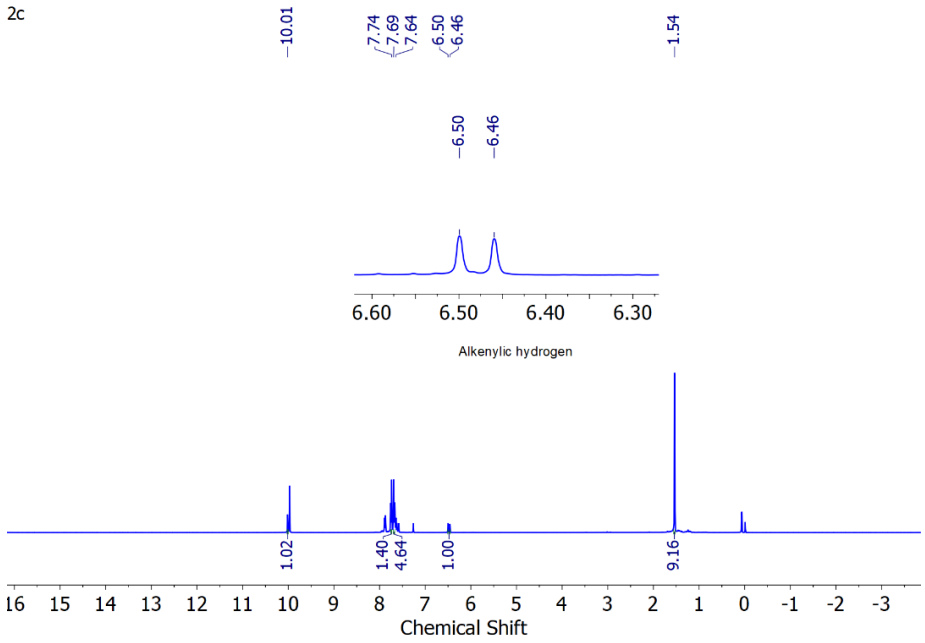

Fig. S17 ^{1}H NMR spectrum of **2c** (400 MHz, $CDCl_3$).

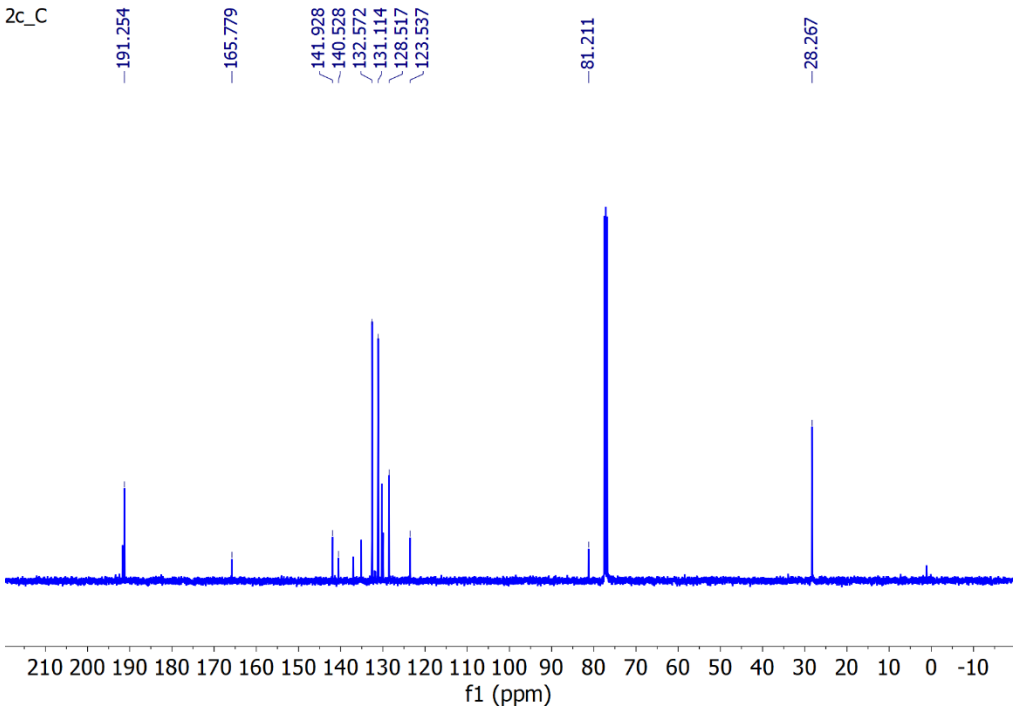

Fig. S18 ^{13}C NMR spectrum of **2c** (100 MHz, $CDCl_3$).

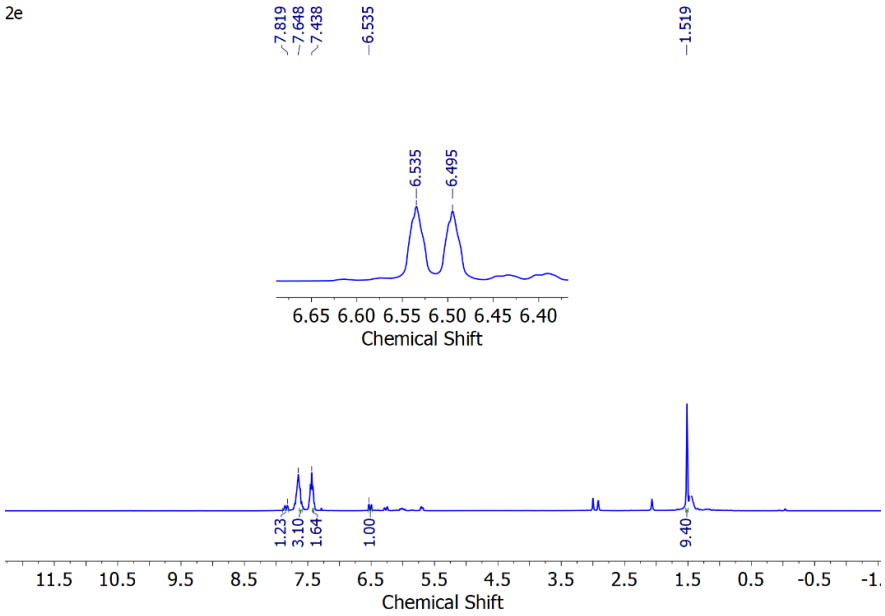

Fig. S19 ^{1}H NMR spectrum of **2d** (400 MHz, $CDCl_3$).

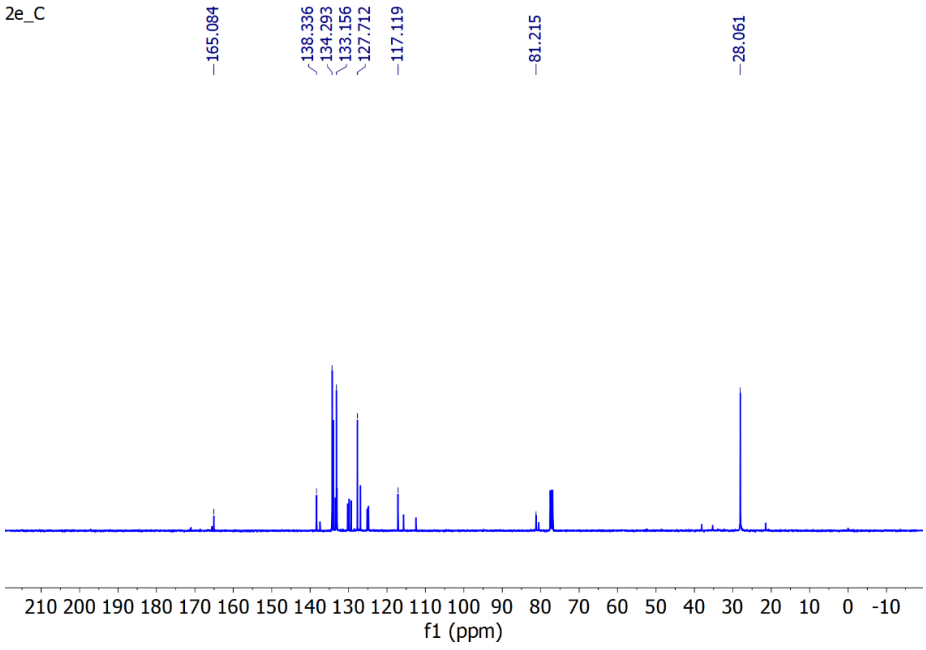

Fig. S20 ^{13}C NMR spectrum of **2d** (100 MHz, $CDCl_3$).

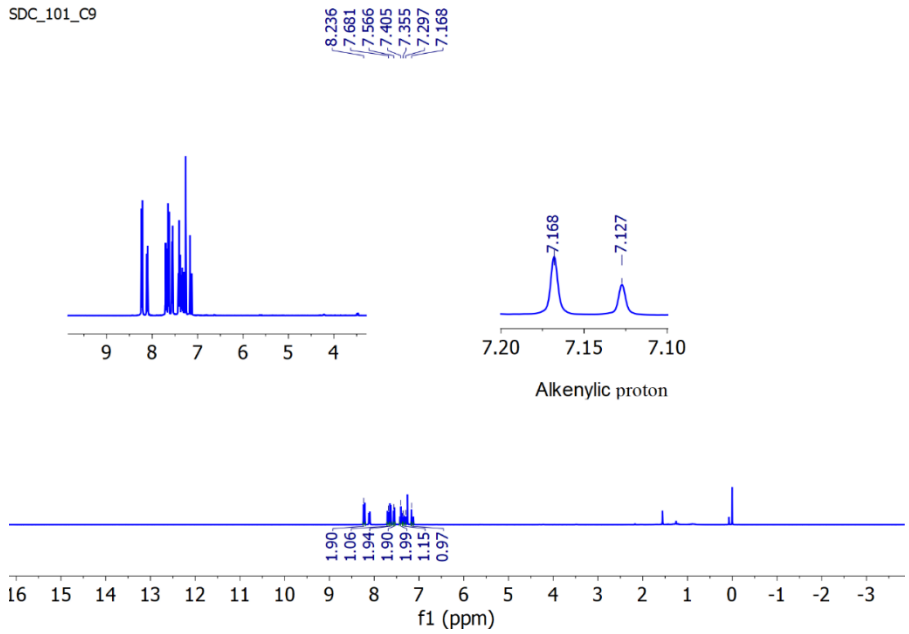

Fig. S21 ^{1}H NMR spectrum of **3a** (400 MHz, $CDCl_3$).

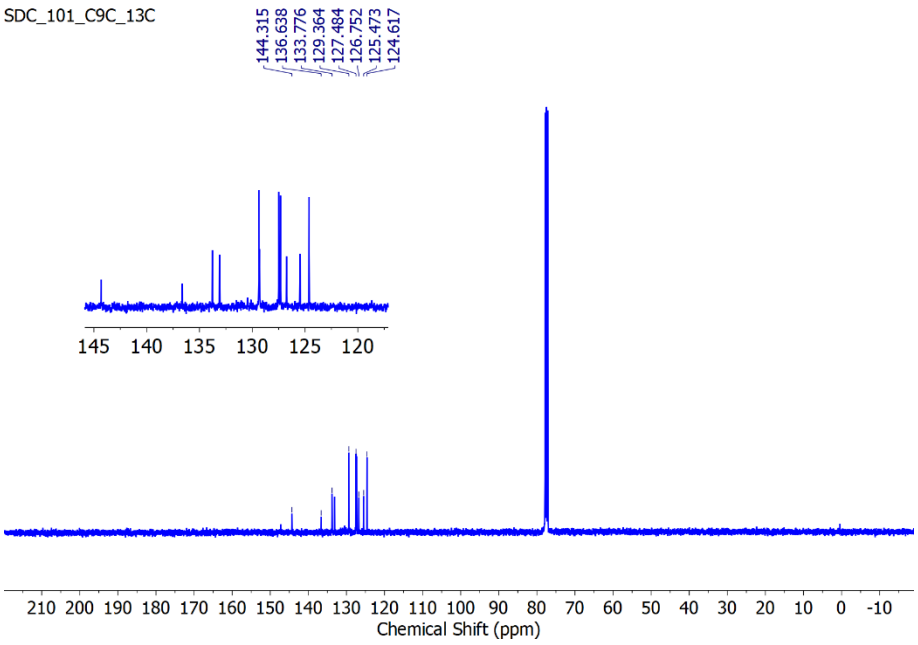

Fig. S22 ^{13}C NMR spectrum of **3a** (100 MHz, $CDCl_3$).

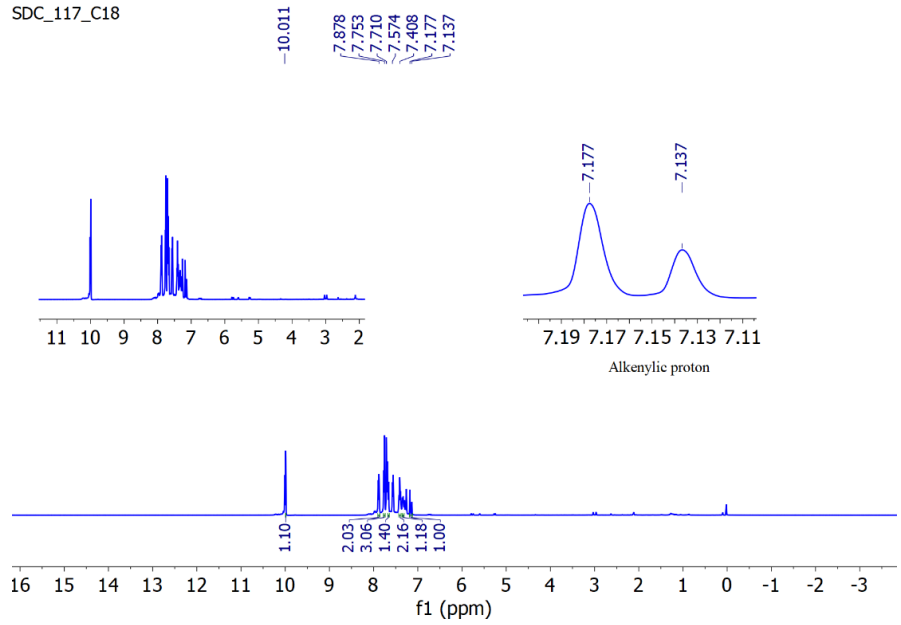

Fig. S23 ^{1}H NMR spectrum of **3b** (400 MHz, $CDCl_3$).

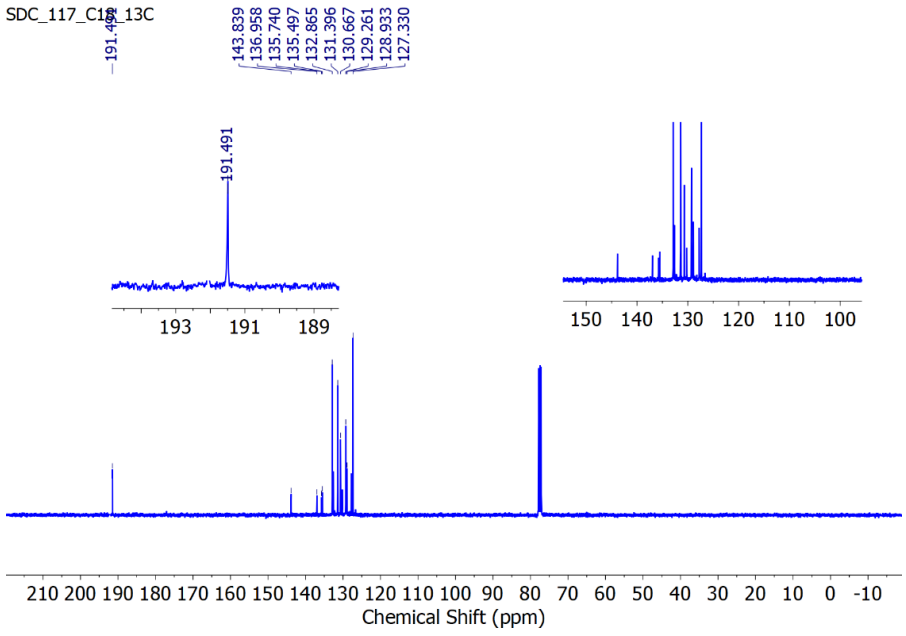

Fig. S24 ^{13}C NMR spectrum of **3b** (100 MHz, $CDCl_3$).

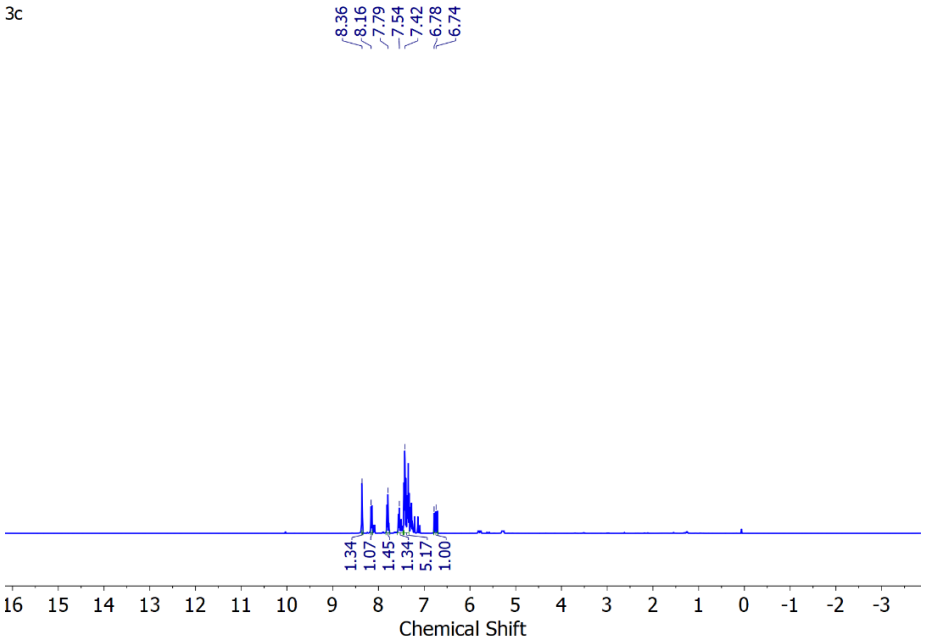

Fig. S25 ^{1}H NMR spectrum of **3c** (400 MHz, $CDCl_3$).

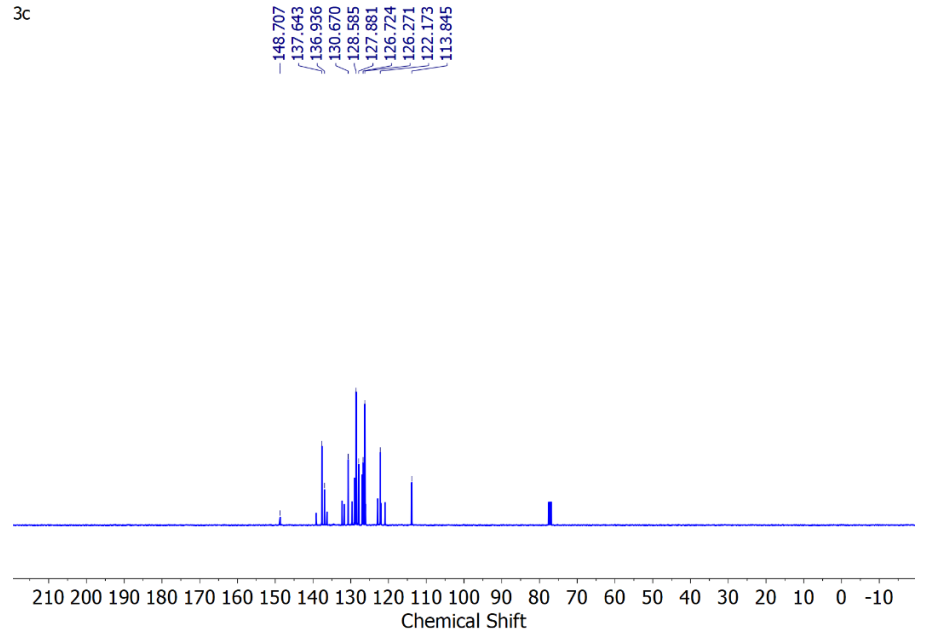

Fig. S26 ^{13}C NMR spectrum of **3c** (100 MHz, $CDCl_3$).

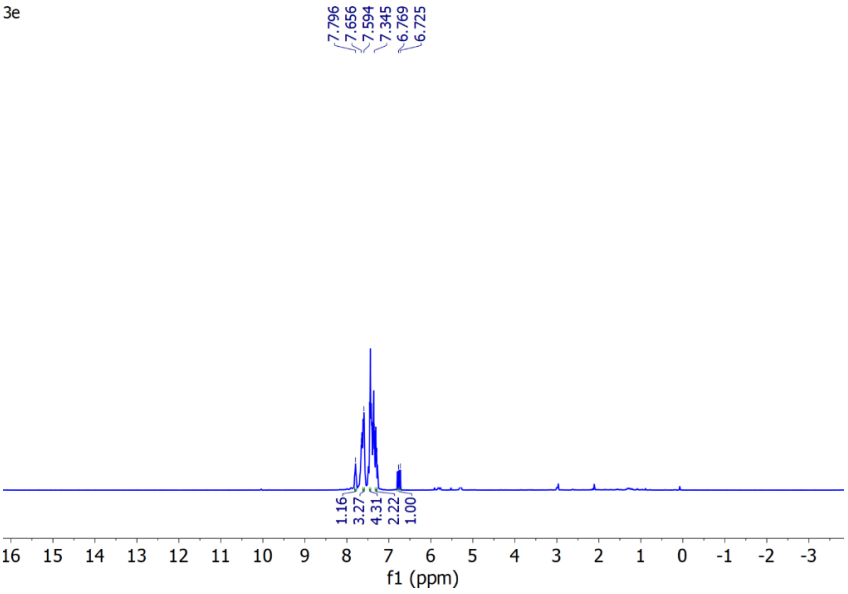

Fig. S27 ^{1}H NMR spectrum of **3d** (400 MHz, $CDCl_3$).

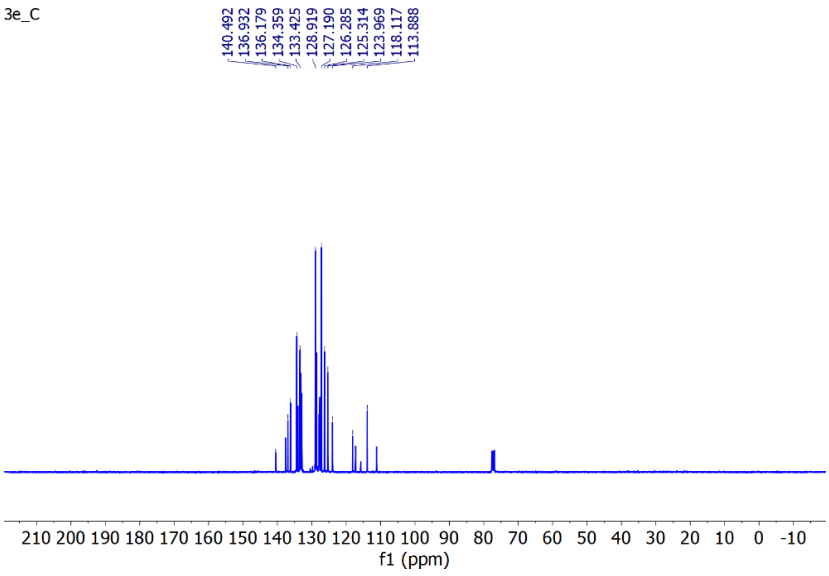

Fig. S28 ^{13}C NMR spectrum of **3d** (100 MHz, $CDCl_3$).

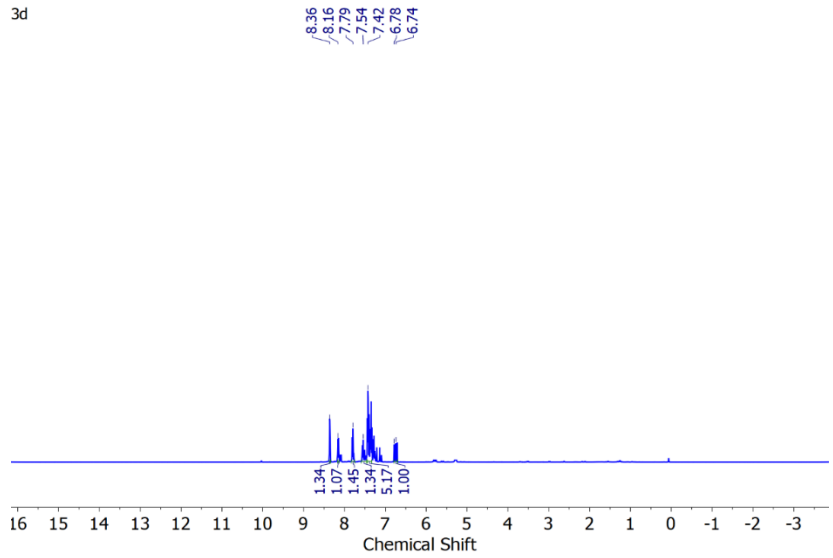

Fig. S29 ^{1}H NMR spectrum of **3e** (400 MHz, $CDCl_3$).

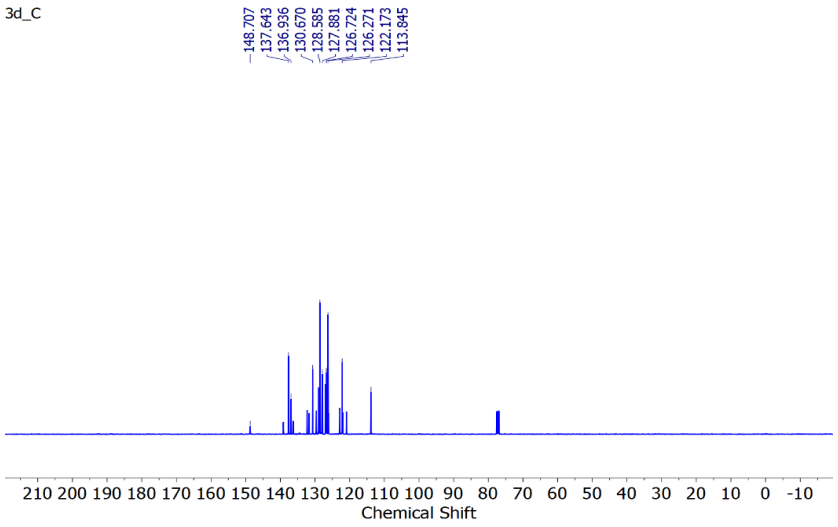

Fig. S30 ^{13}C NMR spectrum of **3e** (100 MHz, $CDCl_3$).

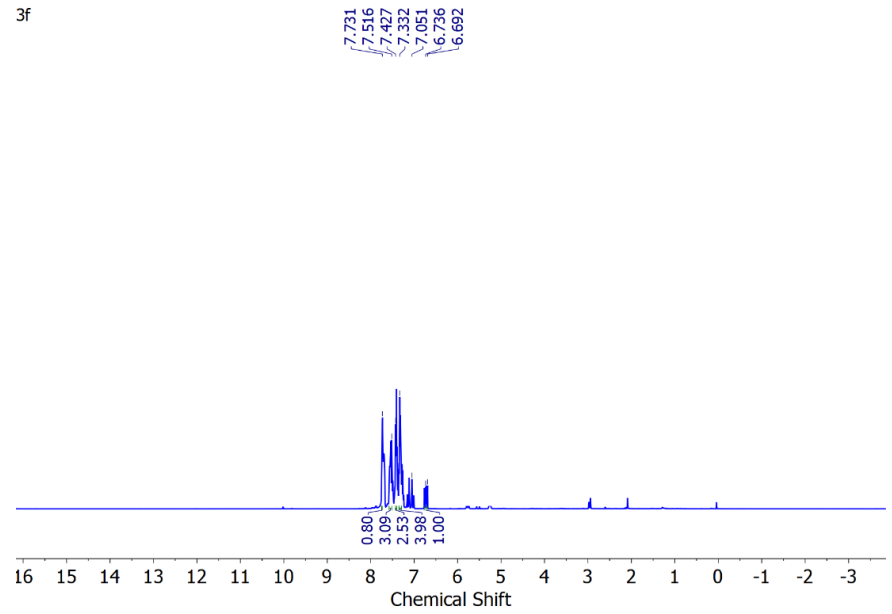

Fig. S31 ^{1}H NMR spectrum of **3f** (400 MHz, $CDCl_3$).

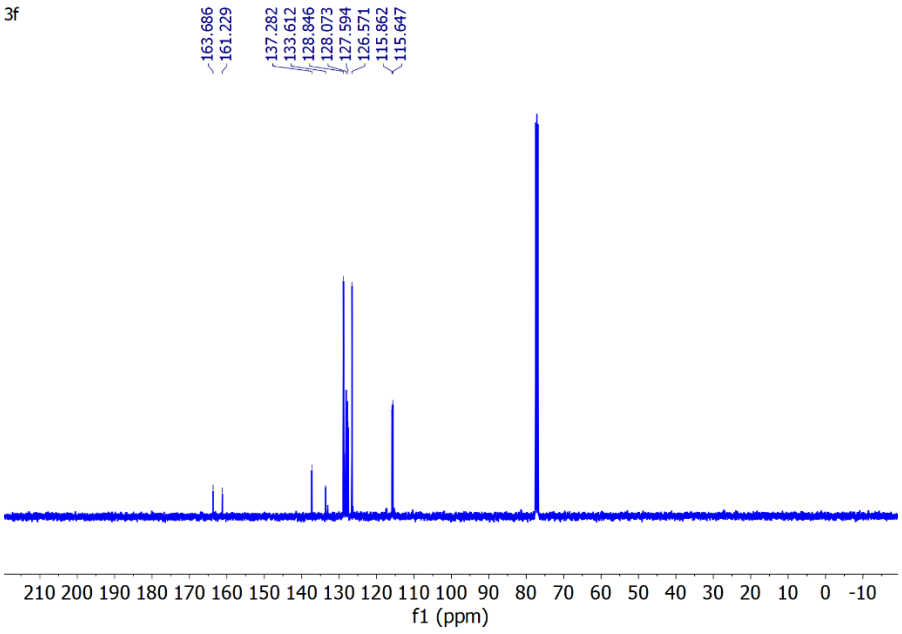

Fig. S32 ^{13}C NMR spectrum of **3f** (100 MHz, $CDCl_3$).

2. Suzuki-Miyaura reaction

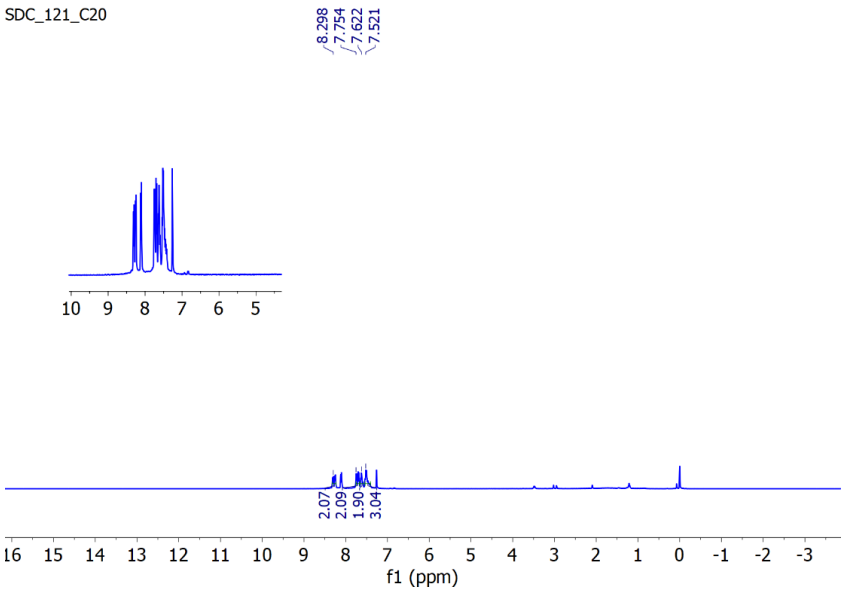

Fig. S33 ^{1}H NMR spectrum of **4a** (400 MHz, $CDCl_3$).

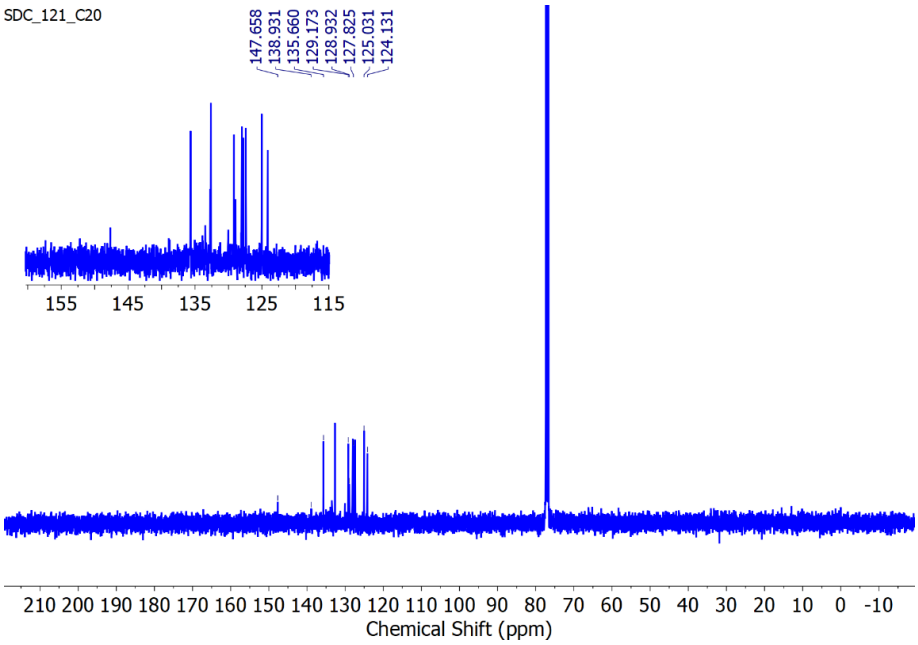

Fig. S34 ^{13}C NMR spectrum of **4a** (100 MHz, $CDCl_3$).

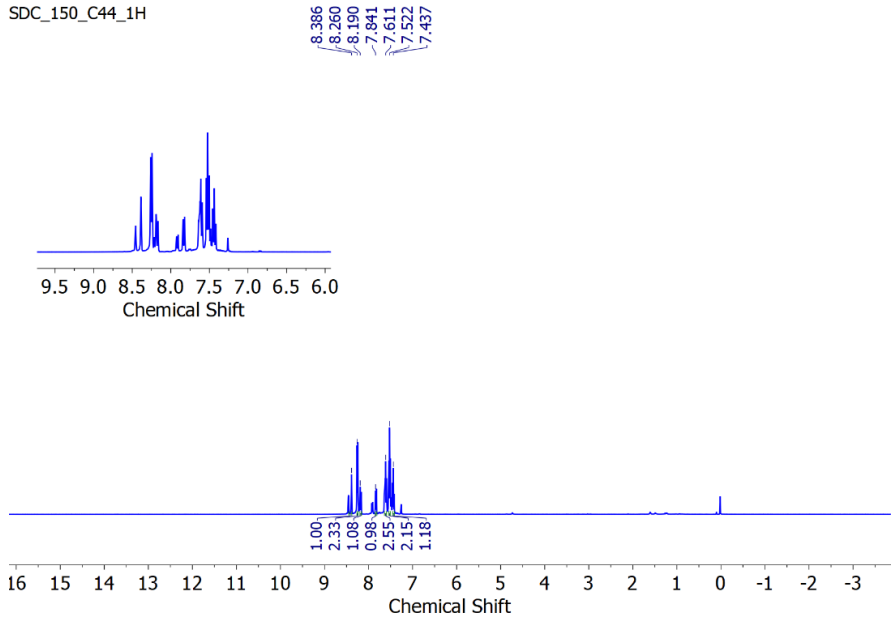

Fig. S35 ^{1}H NMR spectrum of **4b** (400 MHz, $CDCl_3$).

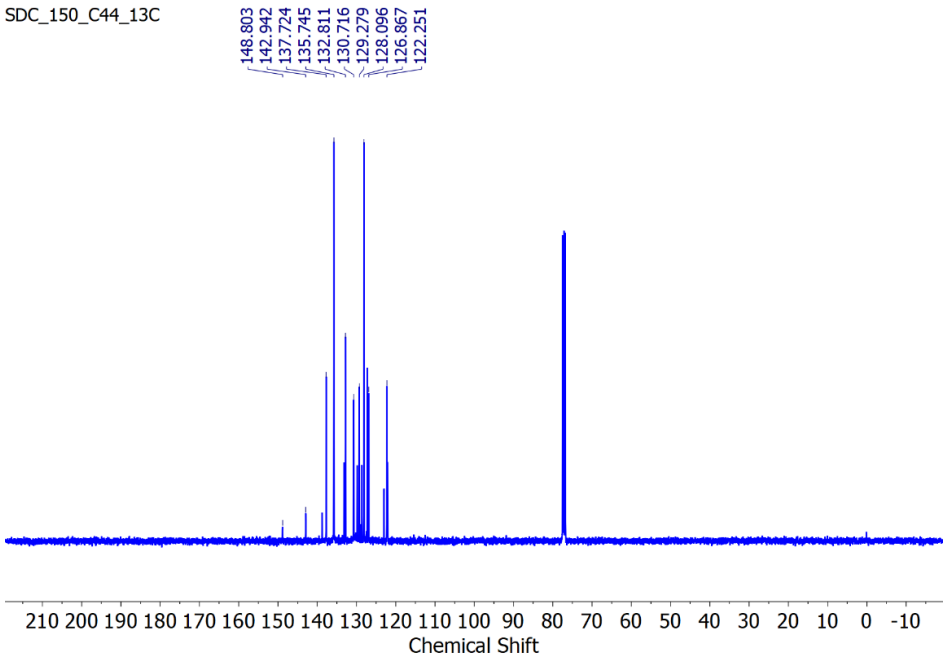

Fig. S36 ^{13}C NMR spectrum of **4b** (100 MHz, $CDCl_3$).

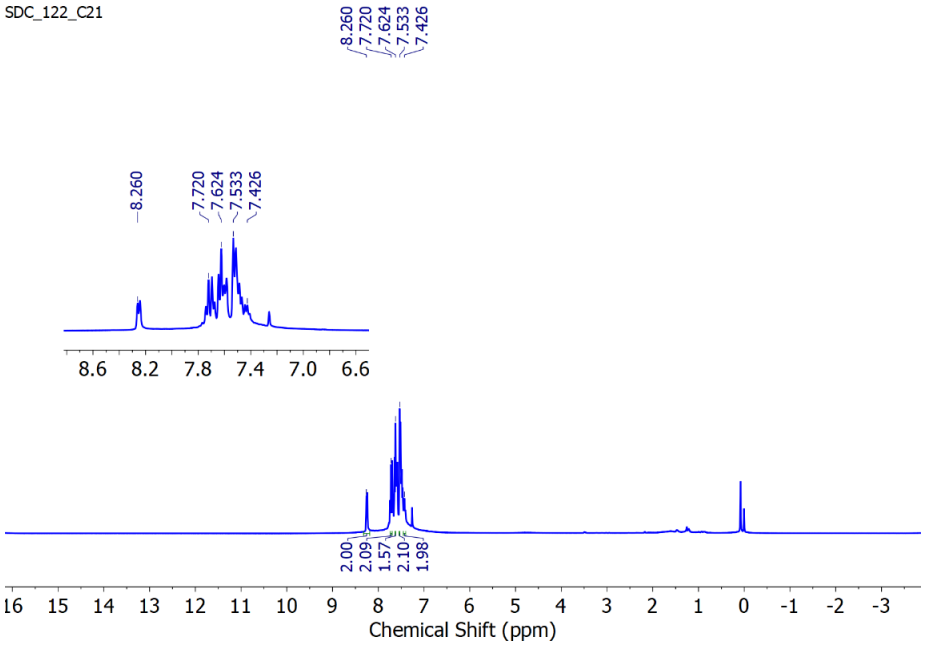

Fig. S37 ^{1}H NMR spectrum of **4c** (400 MHz, $CDCl_3$).

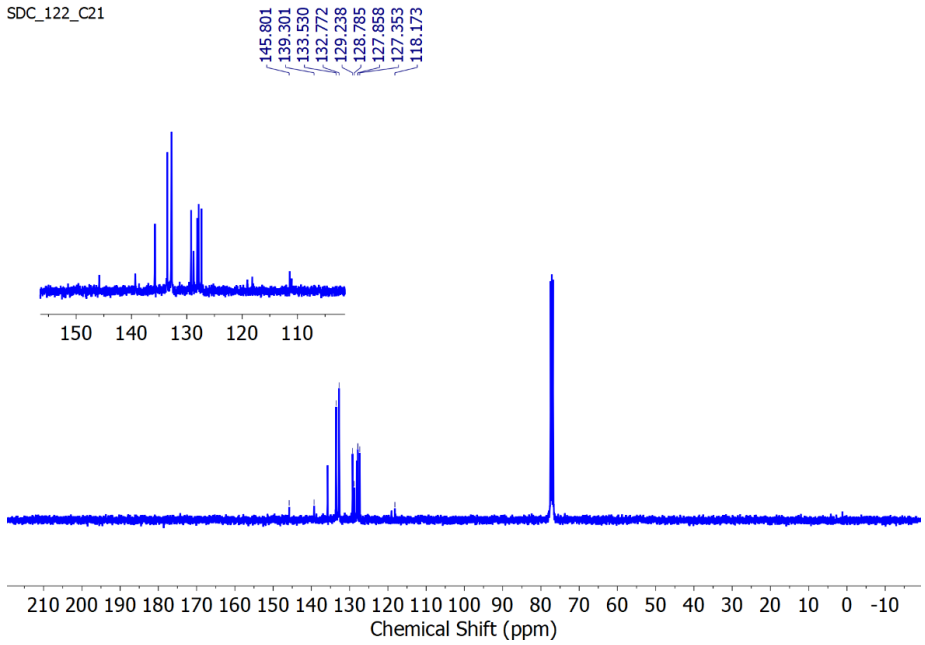

Fig. S38 ^{13}C NMR spectrum of **4c** (100 MHz, $CDCl_3$).

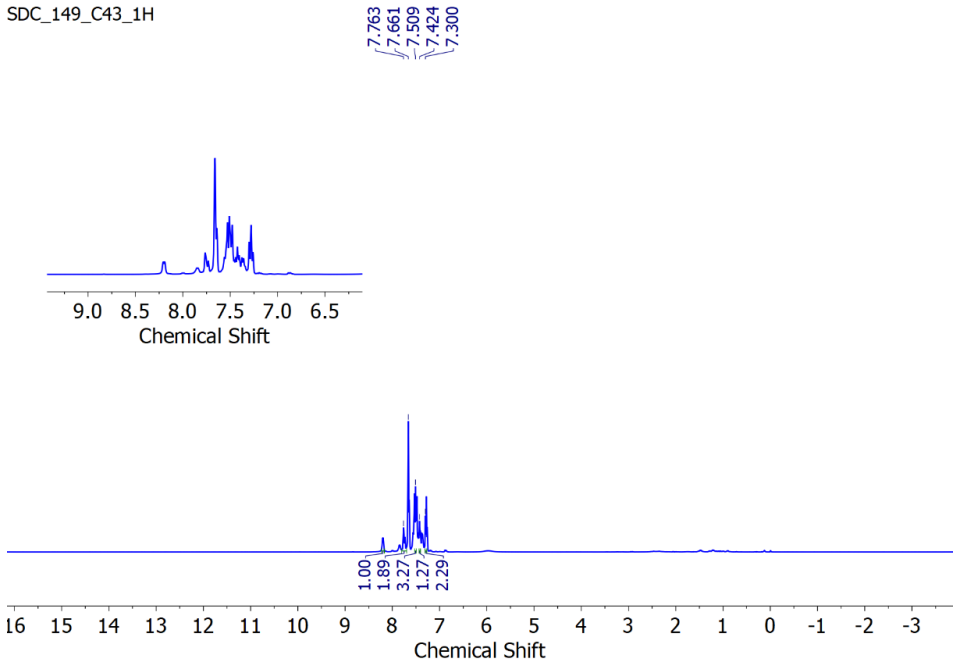

Fig. S39 ^{1}H NMR spectrum of **4d** (400 MHz, $CDCl_3$).

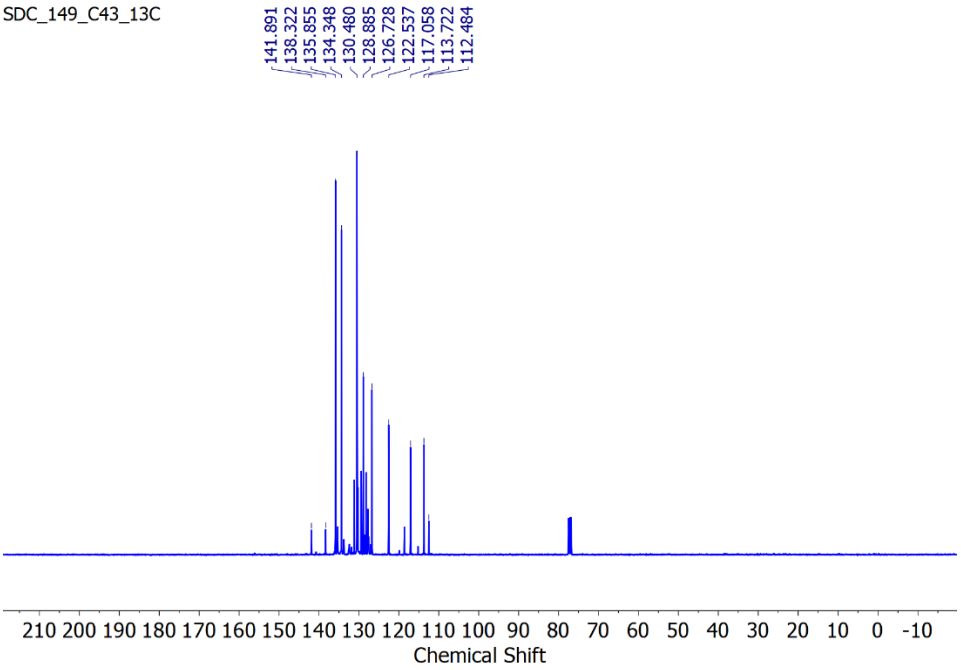

Fig. S40 ^{13}C NMR spectrum of **4d** (100 MHz, $CDCl_3$).

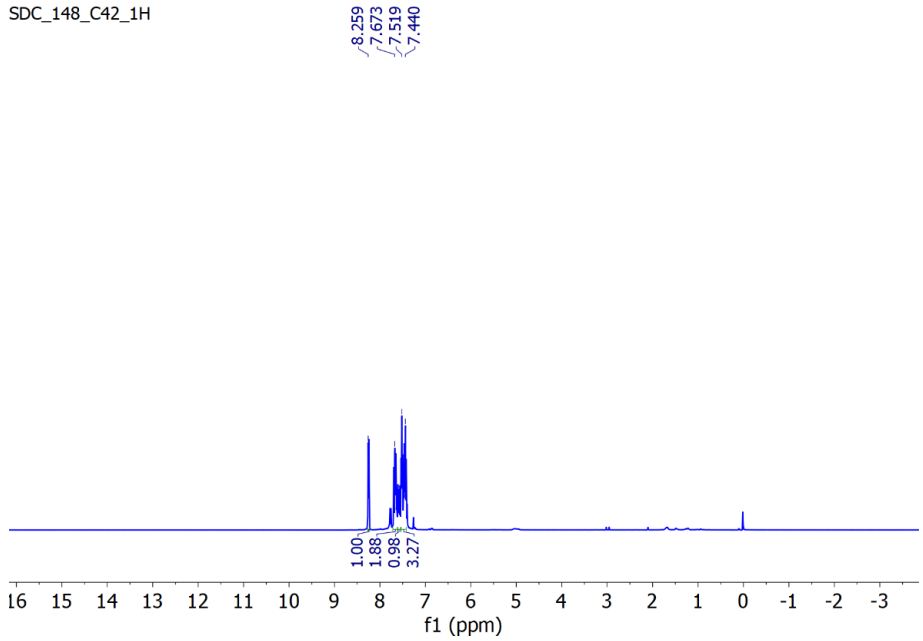

Fig. S41 ^{1}H NMR spectrum of **4e** (400 MHz, $CDCl_3$).

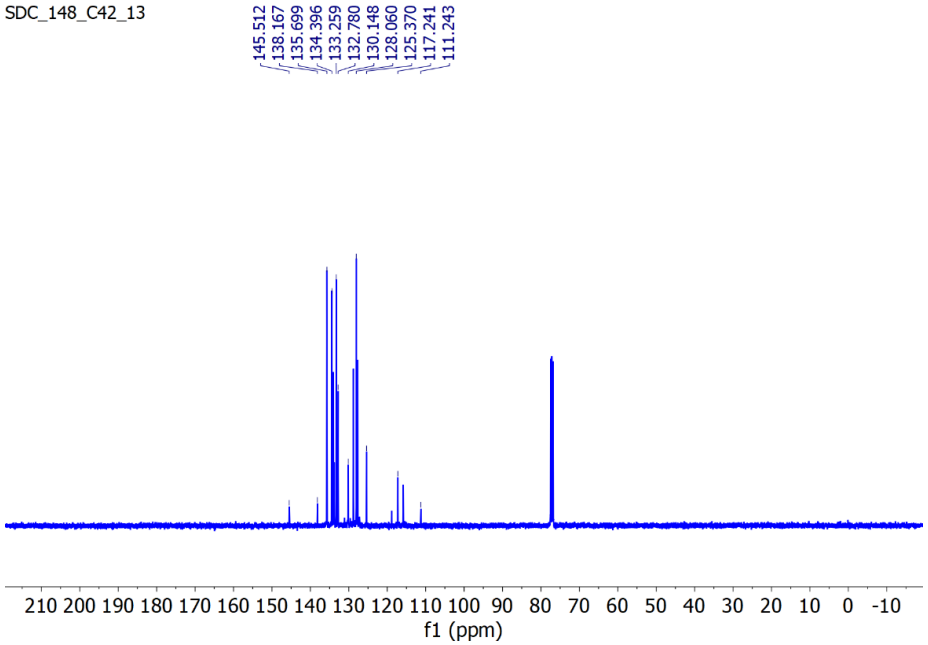

Fig. S42 ^{13}C NMR spectrum of **4e** (100 MHz, $CDCl_3$).

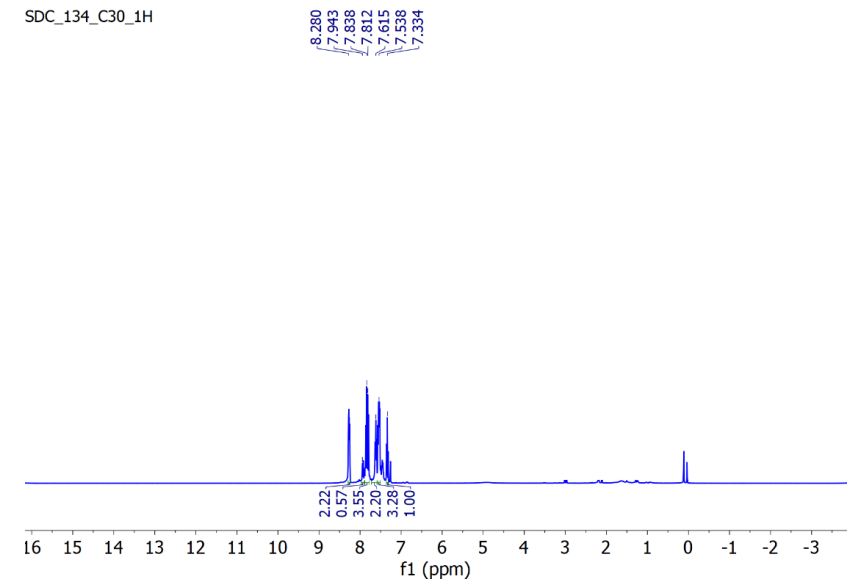

Fig. S43 ^{1}H NMR spectrum of **4f** (400 MHz, $CDCl_3$).

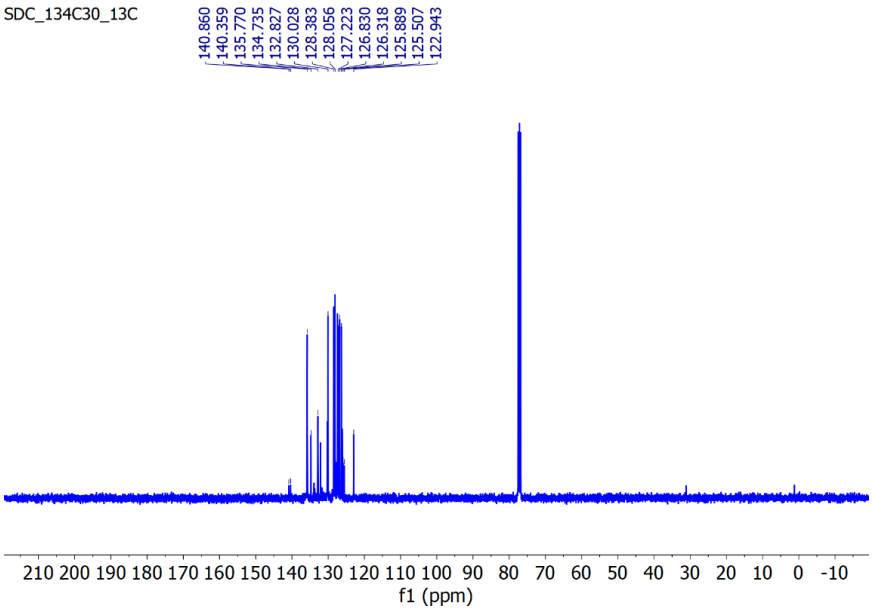

Fig. S44 ^{13}C NMR spectrum of **4f** (100 MHz, $CDCl_3$).